Functions of human DNA topoisomerases in cell proliferation and effects of anti-cancer drugs and natural compounds on the type II enzymes

Inaugural-Dissertation

zur Erlangung des Doktorgrades
der Mathematisch-Naturwissenschaftlichen Fakultät
der Heinrich-Heine-Universität Düsseldorf

vorgelegt von

Faiza Kalfalah
aus Tripoli, Libyen

Düsseldorf, Dezember 2009

aus dem Institut für Klinische Chemie und Laboratoriumsdiagnostik
der Heinrich-Heine Universität Düsseldorf

Gedruckt mit der Genehmigung der
Mathematisch-Naturwissenschaftlichen Fakultät der
Heinrich-Heine-Universität Düsseldorf

Referent: Prof. Dr. Fritz Boege

Koreferent: Prof. Dr. Peter Proksch

Tag der mündlichen Prüfung:

Contents

Summary

Human DNA topoisomerases are ubiquitous enzymes that remove topological constraints like superhelical tension, knots or tangles from the cellular DNA, and are thus essentially required for DNA metabolism. They are divided into type I and type II enzymes, which transiently cleave one or both strands of DNA, respectively. Although the strand breaks generated by these enzymes are transient in nature, they could be converted into permanent breaks when the topoisomerase catalytical cycle is inhibited. Several identified topoisomerase-inhibitory drugs are in wide clinical use as anticancer therapeutics since they represent some of the most successful drugs used for the treatment of human malignancies. On the other hand, the DNA-damaging and recombinogenic potential of topoisomerases is detrimental, since it eventually leads to the development of secondary leukemias by inducing translocations of the MLL locus in patients treated with regimens including topoisomerase-directed drugs. Yet, a source of environmental topoisomerase toxication could be the diverse group of bioflavonoids, which are not only an integral component of the human diet but are also probably the most abundant source of natural antioxidants. However, these polyphenols are also known to be potent topoisomerase inhibitors. Therefore, they are suspected to have profound genotoxic potential.

It is now well established that DNA topoisomerases play essential roles in all DNA metabolic processes like replication, transcription, chromosome segregation and DNA repair. A number of questions, however, are still open such as to what extent these functions are partitioned between the major players topoisomerase I, IIα and IIβ. In addition, it is unclear, in which cell cycle phase topoisomerase-targeted anti-cancer drugs most efficiently exert their effect, and whether certain food components such as polyphenols, that were shown to inhibit topoisomerases *in vitro*, have indeed the same effect in a living cell, where e.g. limited permeation and cellular metabolism could have counteracting consequences.

Thus, this work aimed at characterizing the activity and mechanism of action of bioflavonoids against topoisomerases in comparison to standard topoisomerase toxins, which have been widely applied in cancer therapy. Firstly, biomarkers were established to allow distinction between mitosis and interphase, as well as between sub-stages of interphase in a given cell. For this purpose, proliferating cell nuclear antigen (PCNA) and the replication-initiating factor Cdc6 were chosen as biomarkers and tagged with a fluorescent protein CFP or YFP, respectively. These proteins were stably expressed in two different human cell lines.

Co-expression of these markers in a cell yielded a number of unexpected, so far unknown features of Cdc6 in mitosis, and, thus provided new insights into the still discussed regulation of Cdc6 during the initiation of replication. Co-expression of PCNA or Cdc6 with topoisomerases I, IIα and IIβ, respectively, as differently coloured bio-fluorescent proteins allowed the detailed microscopic analysis of the cell cycle-specific behaviour of the topoisomerases and their response to drug-inhibition of their catalytic cycle. Observed effects could then be correlated to *in vitro*-effects by means of conventional relaxation and cleavage assays.

Zusammenfassung

Humane DNA Topoisomerasen sind ubiquitär vorkommende Enzyme, die essentielle Funktionen im DNA Metabolismus erfüllen. Topoisomerasen haben die Aufgabe topologische Barrieren, wie beispielsweise Torsionspannungen und Verdrillungen zellulärer DNA zu entfernen. Man unterscheidet Topoisomerasen vom Typ1 und Typ2, welche entsprechend einzel- oder doppelsträngige DNA schneiden und religieren können. Die DNA-Strangbrüche, die von den Enzymen induziert werden, sind normalerweise nur transient und kurzlebig. Jedoch können bei Inhibition des katalytischen Reaktionsmechanismus permanente Brüche entstehen. Viele Topoisomeraseinhibitoren, die diesen Mechanismus bekanntermaßen induzieren, sind in der klinischen Anwendung als Krebstherapeutika weit verbreitet. Sie bilden die weltweit erfolgreichste Wirkstoffgruppe gegen bösartige Tumoren. Jedoch haben Topoisomerasen ein hohes genotoxisches und mutagenes Potential, das gravierende Nebenwirkungen dieser Medikamente hervorbringt. Eine Therapie mit Topoisomeraseinhibitoren induziert häufig Translokationen des MLL Lokus von denen sekundäre, therapieinduzierte Leukämie hervorgerufen werden. Eine natürliche Quelle von Topoisomeraseinhibitoren sind pflanzliche Polyphenole, insbesondere Bioflavonoide. Sie bilden einen integralen Bestandteil der menschlichen Ernährung und sind wahrscheinlich die wichtigste Quelle natürlicher Antioxidantien. Daneben sind einige dieser Polyphenole in der Lage Topoisomerase effektiv zu hemmen und besitzen somit vielleicht ein genotoxisches Potential. Es ist bekannt, dass DNA Topoisomerase eine essentielle Rolle in allen metabolischen Prozessen der DNA, wie Replikation, Transkription, Trennung der Chromosomen und DNA Reparatur, spielt. Unklar ist, wie diese Funktionen zwischen Enzymtyp 1 und 2 und weiterhin zwischen den beiden Isoformen (α und β) des Typ 2 aufgeteilt sind. Außerdem ist es unklar in welcher Phase des Zell Zyklus Topoisomerase-hemmende Krebstherapeutika ihre größte Wirkung erzielen. Die dritte und vielleicht entscheidende Frage ist, ob bestimmte Ernährungskomponenten, wie Polyphenole, welche in vitro eine inhibitorische Wirkung auf Topoisomerase zeigten, den selben Effekt auch in lebenden Zellen haben, wo unter anderem verschlechterte Permeation und der zelluläre Metabolismus kompensierend wirken können. Demzufolge war das Ziel dieser Arbeit die Aktivität und den Wirkmechanismus von Bioflavonoiden auf Topoisomerase zu untersuchen und mit herkömmlichen Topoisomerase Toxinen, die bisher in der Krebstherapie eingesetzt werden zu vergleichen. Zuerst wurden Biomarker etabliert, um sowohl eine Unterscheidung

zwischen Mitose und Interphase, als auch zwischen verschiedenen Stadien der Interphase zu ermöglichen. Dafür wurden PCNA und CDC6 entweder mit YFP oder CFP markiert und in zwei verschiedenen humanen Zelllinien stabil exprimiert. Durch Koexpression dieser Marker in der Zelle konnten unerwartete, bisher unbekannte Funktionen von Cdc6 bei der Initiation der Replikation aufgedeckt werden. Koexpression von PCNA und Cdc6 mit Topoisomerase 1, IIα und IIβ als farblich unterschiedliche biofluoreszierende Proteine erlaubt eine detaillierte mikroskopische Analyse des Zellzyklus abhängigen Verhaltens der Topoisomerasen. Zusätzlich wurde untersucht wie sich die Hemmung des Katalytischen Zyklus durch Toxine auswirkt. Diese Beobachtungen konnten dann mit den in vitro erhaltenden Daten, aus Relaxations- und Spaltungsassays, korreliert werden.

1. Introduction

The DNA of mammalian chromosome is an extremely long double-stranded helix, which is organized in a highly packaged structure in the cell nucleus called chromatin Fig. 1.1. One of the most striking features of the DNA double helix is the intertwining of the two complementary strands (Watson and Crick, 1953b). The discovery of this DNA structure led to the immediate recognition that biological processes, such as replication and transcription, would be severely affected by the topological state of the genetic material (Watson and Crick, 1953a). DNA in all species ranging from bacteria to humans is globally underwound (negatively supercoiled) (Cozzarelli et al., 2006; McClendon et al., 2005; Schvartzman and Stasiak, 2004; Wang, 2002), and the maintanance of this topological state is essential for DNA metabolism (Liu et al., 2009). DNA underwinding makes it easier to separate complementary DNA strands from one another, thus greatly facilitating initiation of transcription, replication and the assembly of replication forks. Once the fork begins to scan the DNA template, topological constrains are produced: Fork progression results in acute overwinding (positive supercoiling) and underwinding (negative supercoiling) of the DNA ahead and behind the tracking systems, respectively (Schvartzman and Stasiak, 2004; Wang, 1996; Wang, 2002). Overwinding dramatically increases the difficulty of opening the double helix and represents a block to all DNA processes requiring strand separation. Moreover, when diffusing across the replication fork, it leads to intertwining between newly replicated daughter molecules (see 1.4).

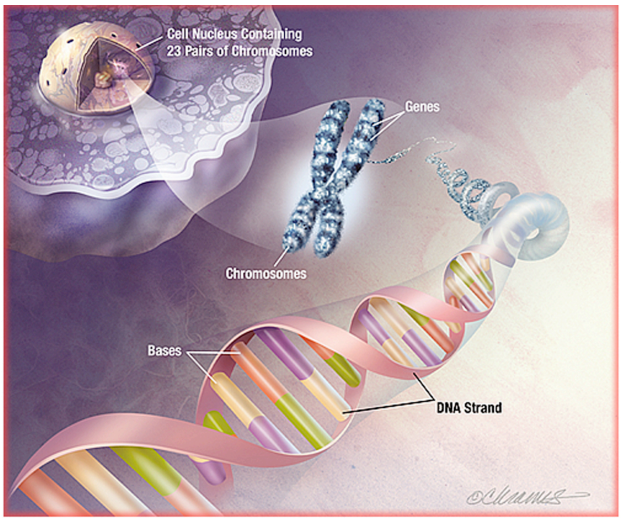

Fig. 1.1: **Condensation of DNA in the nucleus**

Additional topological problems are posed by the extreme length of the double helix. The genetic material from a single human cell, which approaches two meters in length, exists in a nucleus that is only five to ten microns in diameter. Consequently, the double helix is subjected to the same forces and constraints as a rope tightly packed from floor to ceiling in a room.

Nuclear processes such as recombination and replication naturally generate knots and tangles in DNA, respectively (Sherratt et al., 2004; Zechiedrich et al., 1997). If knots accumulate in the genome, DNA tracking systems are unable to separate the two strands of the double helix (Schvartzman and Stasiak, 2004; Wang, 2002; Zechiedrich et al., 1997). Moreover, if tangled (*i.e.*, catenated) daughter chromosomes are not separated prior to cell division, cells will die due to mitotic failure (Champoux, 2001; Nitiss, 1998; Wang, 2002). The topological state of DNA, including DNA under- and overwinding, and tangling, cannot be altered without breaking one or both strands of the double helix (Fig. 1.2).

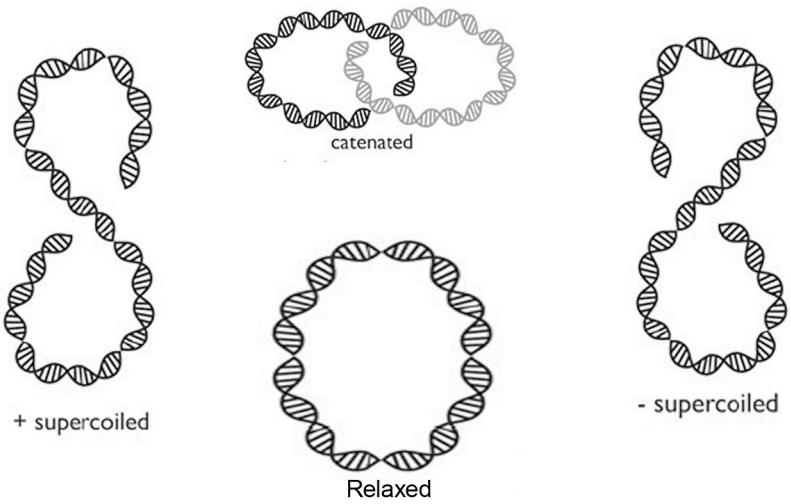

Fig. 1.2: **Topological forms of circular DNA.** This figure adapted from (Schoeffler and Berger, 2008).

Nature's tool for solving these topological problems are DNA topoisomerases (Topos), enzymes that catalyse the breakage and rejoining of DNA strands and the passage of other, intact DNA strands through these transient gaps (Champoux, 2001; Nitiss, 2009a; Wang, 1991; Wang, 2002).

In this section, I will briefly introduce DNA Topos in general, followed by a detailed description of human Topo I and II and a review of the current knowledge about drugs targeting these enzymes, which are currently used in cancer chemotherapy.

1.1 DNA topoisomerases

DNA topoisomerases are molecular "magicians" that are absolutely essential for solving the various topological problems arising from the double-helical structure of DNA (Champoux, 2001; Wang, 1996). Since the discovery of the first member of this enzyme family in 1971 by James Wang, efforts have been made to solve the mystery of how these enzymes function (Wang, 1969; Wang, 1971; Wang, 2009; Wang and Davidson, 1968). Topos were first classified according to their mechanistic features: Type I Topos produce transient single strand breaks in the DNA molecule through which another (in most cases the complementary) single DNA strand is passed. In contrast, type II Topos introduce transient double strand breaks, through which another double helical DNA element is passed (Forterre and Gadelle, 2009). A more detailed classification has recently been agreed upon which takes also into account sequence- and structural data now available for all variants of Topos. Type I Topos are thus divided into three subfamilies (IA, IB, IC) whereas type II Topos are divided into two subfamilies (IIA and IIB). The new classification summarized in Table 1.1 has unified and rationalized older nomenclature, where enzymes were either numbered according to catalytic type (eukaryotic Topos) or in the sequence of their discovery (bacterial Topos) and in addition sometimes given generic names (ω protein, gyrase, reverse gyrase) (Forterre and Gadelle, 2009; Wang, 2002).

Type	Structure	Catalysis	Members
IA	monomers	Single strand break, 5'-P-attached	•Bacteria: Topo I (ω), III, and reverse gyrase •Yeast: Topo III •Higher eukaryotes: Topo IIIα and IIIβ
IB	monomers	Single strand break 3'-P-attached	• Eukaryotes: Topo I •Vertebrates: mitochondrial Topo I (Topo Imt)
IC	monomer	Single strand break 5'-P-attached	• *Methanopyrus* Topo V
IIA	dimers	Double strand break 5'-P-attached	•Bacteria: DNA gyrase and Topo IV •Yeast: Topo II •Higher eukaryotes: Topo IIα and IIβ
IIB	tetramer	Double strand break 5'-P-attached	•*Sulfolobus shibatae* Topo VI

Table 1.1

A common feature of all Topos is their catalytic mechanism, which encompasses the formation of a DNA phosphodiester bond between a tyrosine in the active centre of the enzyme and a phosphate at one end of the transient DNA strand break. Type IB Topos are thus covalently attaching themselves to the 3'-end of the broken DNA strand, whereas all other Topos are getting attached to the 5'-end Fig. 1.3. Mammals have seven distict genes coding for Topos: TOP1 and TOP1mt (coding for nuclear Topo I and mitochondrial Topo Imt), TOP2A and TOP2B (coding for Topo IIα and Topo IIβ), TOP3A and TOP3B (coding for Topo IIIα and Topo IIIβ), and Spo 11 (Champoux, 2001; Pommier, 2009; Wang, 2002). Of these, Topo IIIα, Topo IIIβ, and Spo 11 are assigned to highly specialized tasks (repair and recombination of DNA), whereas Topo I, Topo IIα and IIβ are involved in most if not all processes of DNA-metabolism. Targeting of these more generalistic Topos by cancer drugs, xenobiotics and nutritional compounds is the subject of my thesis. Therefore, I will now discuss the human variety of these enzymes in more detail.

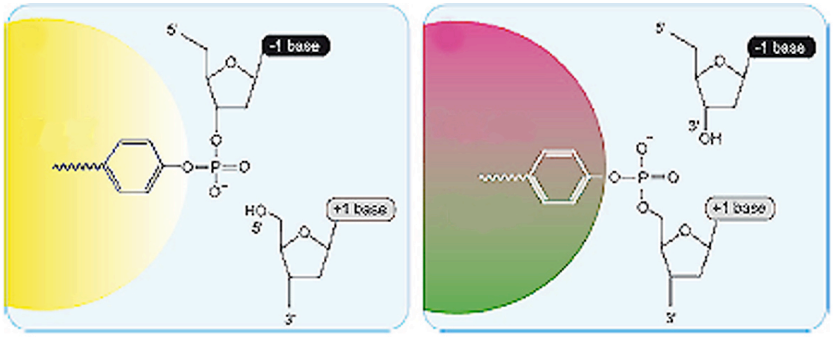

Fig. 1.3: **Formtion of transient breakage of DNA by topoisomerase.** Transesterification between a topoisomerase tyrosil group and a DNA phosphate group leads to the breakage of the DNA backbone and formation of a covalent enzyme–DNA intermediate (covalent complex). In type IA or type II topoisomerases the protein is covalently bound to the DNA 5´phosphate whereas members of the type IB subfamily are attached to the 3´phosphate. Figure adapted from (Pommier, 2009).

1.1.1 Human nuclear topoisomerase I

Vertebrates possess two different members of the Topo IB family: Topo I and Topo Imt that localize in the nucleus and in the mitochondria, respectively. These enzymes have almost identical biochemical activities and play a major role in resolving topological stress generated during transcription of nuclear and mitochondrial genomes (Dalla Rosa et al., 2009; Forterre and Gadelle, 2009; Leppard and Champoux, 2005; Pommier et al., 1998; Zhang et al., 2001). Only the nuclear variant of topoisomerase I (Topo I) will be considered in this work.

1.1.1.1 Human topoisomerase I domain structure

Topo I consists of a single polypeptide of 765 amino acids (~91 kDa) and functions as a monomer (Champoux, 2001; Leppard and Champoux, 2005; Pommier et al., 1998). The enzyme is divided into four domains based on sequence homology between proteins of various species and sensitivity to proteolysis. The N-terminal domain (amino acids 1-214) is highly variable and dispensable for activity *in vitro*. It contains nuclear localization sequences and sites for interaction with other proteins (Alsner et al., 1992; Leppard and Champoux, 2005; Mo et al., 2000). The core domain of Topo I (amino acids 215-635) is highly conserved and contains residues for enzyme catalysis, as well as DNA substrate recognition and binding (Champoux, 2001; Redinbo et al., 2000; Stewart et al., 1997). A dispensable linker domain (amino acids 636-712) is positioned between the core region and C-terminal domain of the enzyme. This linker domain is poorly conserved and interacts with the DNA substrate (Leppard and Champoux, 2005; Stewart et al., 1999). Finally, the C-terminal domain of Topo I (amino acids 713-765) is conserved and contains the active site tyrosine required for DNA cleavage and religation (Champoux, 2001; Leppard and Champoux, 2005; Redinbo et al., 2000; Stewart et al., 1997). The most complete crystal structure of Topo I comprises residues 201-765 and shows a protein that clamps completely around DNA (Fig. 1.4.).

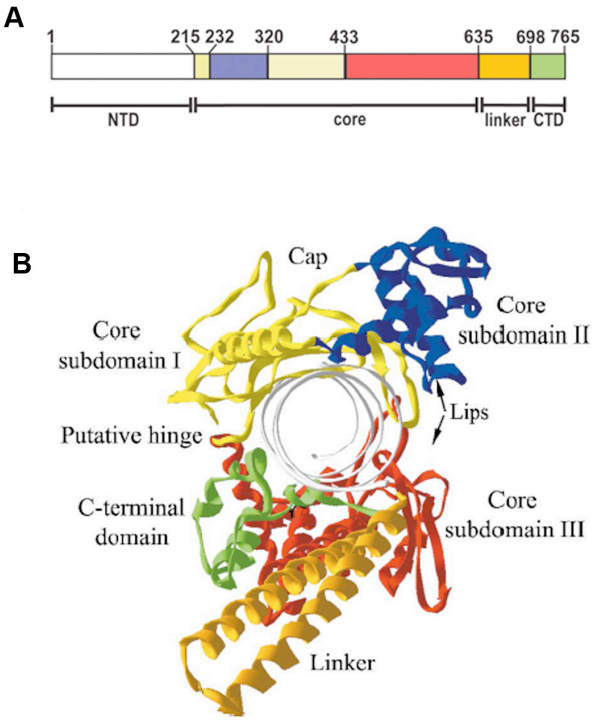

(**A**) Topo I divided into four domains: the N-terminal domain (NTD, open box), the core domain, the linker (orange), and the C-terminal domain (CTD, green). The core domain can further be divided into subdomain I (yellow), subdomain II (blue) and subdomain III (red). (**B**) Crystal structure of Topo I in complex with DNA: Topo I various domains are labelled as in A. Figure adapted from (Champoux, 2001).

Fig. 1.4: **Structure of human Topo I**

The core domain of the enzyme can further be divided into subdomains I, II and III. Subdomain I and II fold tightly together forming the top half or "cap" of the enzyme. The cap is characterized by two long "nose-cone" that come together in a "V" away from the body of the enzyme. Subdomain III together with the C terminal domain, forms the lower lobe of Topo I; it extents from the cap of the enzyme downward bearing two long α helices. C terminal domain is connected to core subdomain III through the linker, a flexible coiled-coil structure that protrudes from the base of the enzyme. The C terminal domain is positioned such that the active site tyrosine is embedded within the base of the protein near the surface of the central cavity created by the tight clamping of the enzyme around duplex DNA.

1.1.1.2 Topoisomerase I catalytic cycle

Topo I activity occurs independently of ATP or a divalent cations (Champoux, 2001; Pommier et al., 1998). The most attractive model for DNA relaxation by Topo I proposes that relaxation proceeds by a "controlled rotation" mechanism where, after cleavage, the tension in the DNA drives its rotation (Stewart et al., 1998). Rotation occurs in the closed clamp conformation and the rate of rotation is not severely impeded when the enzyme is locked in this closed conformation (Carey et al., 2003). The catalytic cycle of Topo I can therefore be summarized in five steps (Champoux, 2001; Pommier et al., 1998; Wang, 2002): 1.) site-specific, noncovalent binding of a DNA substrate; 2.) generation of a single-stranded DNA break and covalent linkage to the 3' terminus of the break, creating the "cleavage complex"; 3.) controlled rotation of the double-helix around the single-stranded DNA break; 4.) Religation of the cleaved DNA strand, regenerating the active site tyrosine residue and reestablishing noncovalent binding; 5.) and enzyme dissociation or initiation of a new round of catalysis.

1.1.2 Human topoisomerases II

Type II enzymes are dimers and act by generating transient double strand breaks in one DNA double helix, followed by the passage of a second double helical DNA segment through the broken DNA molecule (Champoux, 2001; Wang, 1996). Consequently, these enzymes are able to remove superhelical twists from DNA and resolve knotted or tangled duplex molecules. Type II Topos are required for transcription, replication, recombination, chromosome segregation, and proper chromosome condensation and decondensation (Champoux, 2001; Nitiss, 2009a; Wang, 2002).

1.1.2.1 Topoisomerase II isoforms

While non vertebrates such as yeasts and flies encode only one type II Topo (Goto and Wang, 1984), vertebrate species express two isoforms of the enzyme denominated α and β (Champoux, 2001; Drake et al., 1989). Topo IIα and IIβ display a high degree of amino acid sequence identity (~70%) and similar biochemical characteristics, but differ in their molecular masses (170 vs. 180 kDa, respectively) and are encoded by separate genes located on chromosomes 17q21-22 and 3p24, respectively (Austin and Marsh, 1998; Champoux, 2001; Liu et al., 2009). Gene structure analysis shows that the genes of Topo IIα and IIβ contain 35 and 36 exons, respectively (Lang et al., 1998; Sng et al., 1999). The intron/exon boundaries are highly conserved between the two genes suggesting that they have arisen from duplication of a single ancestor gene relatively recent in evolution (Coutts et al., 1993). The only intron/exon boundaries not conserved are within the regions encoding the N- and C terminal domains of the two enzymes, which are also in their exon sequences much more divergent form each other than the rest of the two genes.

Both human isoforms of Topo II are able to complement the loss of the only Topo II enzyme in yeast (Meczes et al., 1997; Wasserman et al., 1993), and can thus be considered as functional equivalents in this system. This suggests that they possess very similar basic enzymatic activities and biological capabilities. However, already early on, it was observed that they are functionally distinguished by their sensitivity to specific inhibitors (Drake et al., 1989). Moreover, in vertebrate cells, they have distinct expression patterns. Topo IIα is expressed only in proliferating cells, whereas expression of Topo IIβ is independent of the proliferation state (Heck et al., 1988; Woessner et al., 1991). Only Topo IIα associates with mitotic chromosomes (Christensen et al., 2002c; Meyer et al., 1997) and, consistent with this, seems essential for cell division and the growth (Carpenter and Porter, 2004; Linka et al., 2007). While proliferating cells can survive the absence of Topo IIβ, this isoform cannot compensate for the loss of Topo IIα (Carpenter and Porter, 2004; Grue et al., 1998; Linka et al., 2007). Thus, Topo IIα is believed to be the isoform that functions in growth-dependent processes, such as DNA replication and chromosome segregation (Nitiss, 2009a; Wang, 2002). The β isoform, on the other hand, is ubiquitously expressed in all cell types. It is clearly not capable of supporting cell proliferation (Linka et al., 2007) but seems to play a role in DNA transcription and to be essential for the embryonal development of neurons (Lyu and Wang, 2003; Yang et al., 2000). It should finally be noted that functional specialization of Topo IIα and IIβ appears to be determined by their non-conserved C-terminal domains (Linka

et al., 2007). It is unknown how theese domains determine the unique behaviour of Topo IIα and IIβ in the living vertebrate cell, since they are dispensable for enzyme activity per se.

1.1.2.2 Topoisomerase II domain structure

The model for most structural studies of eukaryotic type II Topos has been the enzyme of S. cerevisiae. Since eukaryotic type II Topos are highly conserved the structure obtained from the yeast enzyme (Fig. 1.5) is likely also applicable for the two human enzymes.

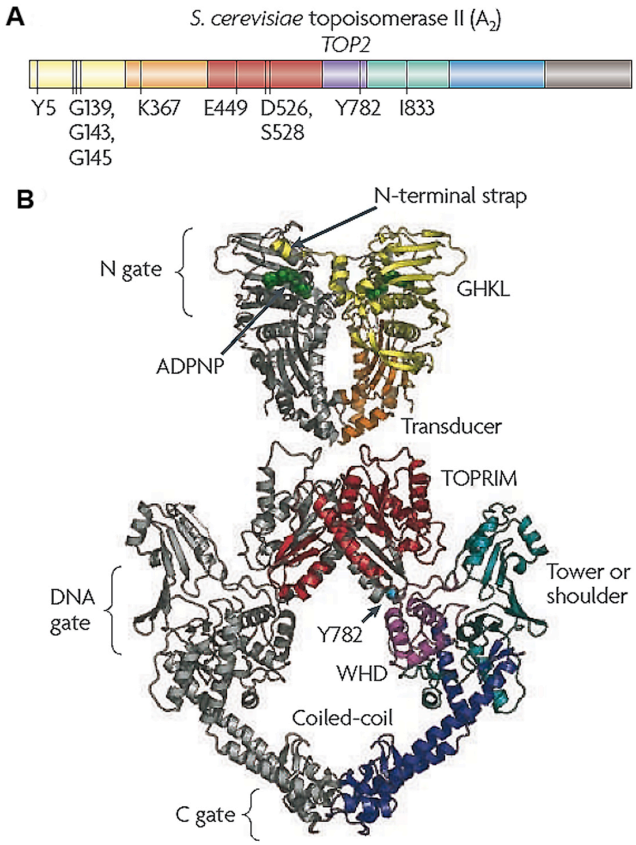

(**A**) The figure show domain structure of eukaryotic Topo II, indicated in different colour the residues marked include G139, G143, and G145 in the ATP binding domain; K367- ATpase domain; E449, D526, and D528 involved in binding a divalent cation; Y782 active site; 1833 involved in DNA interaction. (**B**) Crystal structure of yeast Topo II: Topo II various domains are labelled as in A. Figure adapted from (Nitiss, 2009a).

Fig. 1.5: **Structure of yeast Topo II.**

The primary structure of Topo IIα and β is very similar and can be divided into three domains (Austin and Marsh, 1998; Berger and Wang, 1996; Champoux, 2001; Schoeffler and Berger, 2008; Wang, 1996):

N terminal domain: This portion of the enzyme composes the domain for ATP binding and hydrolysis (Berger, 1998; Schoeffler and Berger, 2008). Crystal structures of this domain were solved for yeast Topo II and human Topo IIα (Classen et al., 2003; Wei et al., 2005).

Central domain: The central domain of Topo II includes a TOPRIM domain followed by breakage reunion domain, which carries the active site tyrosine (amino acid 805 for Topo

IIα and 821 for Topo IIβ). A crystal structure for this domain in the absence of a DNA substrate was solved for yeast Topo II (Berger et al., 1996).

C terminal domain: The C terminal domain is highly variable among species and between the two human isoforms. This domain contains both nuclear localization sequences and sites of phosphorylation and is dispensable for catalytic activity *in vitro* (Dong and Berger, 2007; Shiozaki and Yanagida, 1992). While crystal structures have been solved for both the N-terminal and central domains of a eukaryotic Topo II, a structure for the C-terminal domain of the enzyme has yet to be solved.

1.2 Topoisomerase II catalytic cycle

The recognition of DNA by Topo II is mainly determined by the topological structure of the DNA and Topo II does not have any preferred cleavage sequence (Sander et al., 1987). The lack of choice for a specific DNA sequence may have an important physiological role, since it permits the enzyme to act all over the genome. The recognition of topological forms of the DNA is exemplified by the preferential binding of the enzyme to supercoiled over relaxed DNA (Osheroff, 1986) and the enzyme's interaction with curved DNA and DNA crossovers (Zechiedrich and Osheroff, 1990). In this way the enzyme can discriminate between the substrates and products of its catalytic reaction. Human Topo IIα and β function as homodimers, and their catalytic activities are dependent on the presence of a divalent cation (such as magnesium) and ATP (Berger and Wang, 1996; Burden and Osheroff, 1998). Their catalytic cycles are virtually identical and can be divided into six discrete steps (Fig. 1.6).

Step 1: (DNA binding) To initiate catalysis, the enzyme non-covalently binds a DNA double helix termed the G-segment (the double helix that is cleaved by the enzyme and is opened as a "gate") and a second helix the T-segment (the double helix that is "transported" through the open DNA gate) (Wang, 2002). There is no cofactor requirement for this initial step (Osheroff, 1987).

Step 2: (DNA cleavage) In the presence of a divalent cation, a pre-strand passage cleavage/religation equilibrium is established (Gellert, 1981; Liu et al., 1983; Osheroff, 1987). While magnesium is thought to be the physiologically relevant divalent cation for this process, others such as calcium can substitute it *in vitro* (Baldwin et al., 2004). The two monomers of Topo II each cleave one strand in the G segment, resulting in a transient double-stranded break in the DNA. Sites of cleavage within the homodimer are four bases apart,

generating a 4-base 5' overhang on either side of the double-stranded break. In order to maintain genomic integrity, the active site tyrosyl residue of each monomer forms a covalent attachment to the 5' termini of the cleaved DNA strands. This transient intermediate is called "cleavage complex". While essential for maintaining the integrity of the genetic material, high concentrations of these complexes are potentially harmful for cells (Fortune and Osheroff, 2000; Kaufmann et al., 1998). Unlike a traditional ligase, which requires base pairing to correctly position DNA ends for rejoining (Lehman, 1974), Topo II can religate cleaved DNA strands in the absence of base pairing interactions.

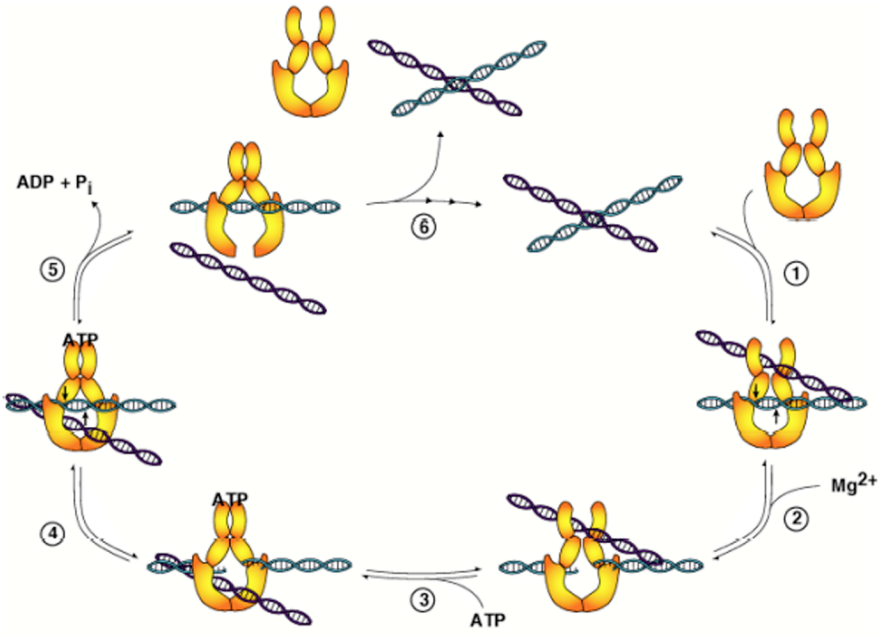

Fig. 1.6: **Catalytic cycle of Topo II.** 1) Topo II binds to DNA. 2) In order to prevent breaks in the DNA from becoming permanent double strand breaks, the enzyme covalently attaches to DNA at the active site tyrosine residue in the presence of a divalent cation. The covalent enzyme-DNA intermediate is known as the "cleavage complex". 3) Once a cleavage complex is formed Topo II binds ATP and undergoes a conformational change. This change in confirmation allows the enzyme to pass an intact strand of DNA through the cleaved DNA strand. 4) After Topo II passes the intact DNA strand it religates the cleaved strand. 5) It hydrolyzes ATP to complete the catalytic cycle. 6) It releases the DNA substrate. Figure adapted from (Baldwin and Osheroff, 2005).

Step 3: (ATP-binding) Each protein monomer binds a molecule of ATP, resulting in a conformational change and passage of the intact T-segment DNA through the cleaved G-segment (Lindsley and Wang, 1993). Hydrolysis of one ATP molecule appears to stimulate the passage event (Baird et al., 1999). Translocation of the T-segment DNA through the N

terminal gate of Topo II and closure of this gate forms what is termed a "protein clamp" (Roca and Wang, 1992).

Step 4: (DNA strand passage) Following DNA strand passage, the enzyme religates the cleaved double helix and establishes post strand passage cleavage/religation equilibrium. This conformation topologically links the enzyme to the DNA, allowing it to diffuse along the double helix without dissociation.

Step 5: (ATP hydrolysis) Upon hydrolysis of a second molecule of ATP, Topo II undergoes another conformational change that results in the opening of the C terminal gate (Lindsley and Wang, 1993). The T-segment DNA strand is released through this gate (Roca and Wang, 1992).

Step 6: (enzyme turnover) Finally, the enzyme returns to its original conformation and can either remain associated with the DNA substrate for a new round of catalysis, or it can dissociate and begin catalysis on a new substrate (Osheroff, 1986).

1.3 Subnuclear distribution of human topoisomerases

1.3.1 Topoisomerase I

Indirect immunofluorescence studies have shown that during interphase Topo I is located in the nucleoplasm and in the nucleoli (Meyer et al., 1997; Muller et al., 1985). After that, this observation has been initially confirmed by transient expression of GFP Topo I fusion proteins (Mo et al., 2000). Interestingly, a number of studies have shown that the N - terminal domain of Topo I is important for correct cellular targeting of Topo I. It targets Topo I to the nucleoli in human cells (Mao et al., 2002; Mo et al., 2000). During interphase Topo I locates in the nucleus and concentrates in the nucleoli and plays an important role in rDNA transcription. In fact, Topo I colocalizes with RNA polymerase I in the nucleoli at fibrillar centers (Christensen et al., 2002a; Christensen et al., 2004). During mitosis, Topo I associates with chromosomes (Christensen et al., 2002a; Meyer et al., 1997; Mo et al., 2000).

1.3.2 Topoisomerase II

The precise localization of Topo IIα and IIβ at the subnuclear level in living cells is a subject still open to discussion and to some extent investigated in the current study. Indirect immunofluorescence studies have shown that Topo IIα and Topo IIβ have a nuclear

localization during interphase. Both enzymes are found in the nucleoplasm and the nucleoli (Meyer et al., 1997). The staining of the nucleoplasm has been reported to be either homogeneous (Chaly and Brown, 1996; Sugimoto et al., 1998) or with some speckle formation (Meyer et al., 1997). Most studies support a nucleolar localization of Topo IIα (Meyer et al., 1997; Sugimoto et al., 1998) although some data also indicate an exclusion of this isofrom from nucleoli (Chaly and Brown, 1996). A localization study in living cells using GFP-tagged Topo II demonstrated an almost identical distribution pattern of both Topo II isoforms in the interphase nucleus with a distinctive concentration in nucleoli (Christensen et al., 2002c). In contrast, a different localization of Topo IIα and β was observed during metaphase, where Topo IIα strongly accumulates on the chromosome, while the β enzyme only weakly binds to the chromosomes. Only in anaphase during chromosome segregation, Topo IIβ also shows a significant association with chromosomes, so that at this point the distribution pattern of both isoforms becomes similar again (Christensen et al., 2002c). Recently, it was discovered that it is the divergent C terminal domain of human Topo II that determines these isoform-specific localization differences (Linka et al., 2007).

1.4 Biological functions of human topoisomerases I and II

Due to their catalytic properties Topo I and II are likely to be involved in most DNA-metabolic processes. Many of the biological roles of Topos in the cell are possibly shared among the different types, although the unique ability of Topo II to decatenate interlinked DNA makes it likely that this type has in addition unique biological functions. The putative roles of Topo I and II in meiosis, recombination, DNA damage/repair and apoptosis are not well understood. However, it is by now quite clear that Topo II is required in mitosis for chromosome condensation and segregation (Carpenter and Porter, 2004; Linka et al., 2007), and that Topo I and II play a crucial role in transcription and replication, as will subsequently be summarized in more detail.

1.4.1 Role of topoisomerases in replication

The movement of the replication and transcription machinery on DNA results in the accumulation of positive superhelical twists ahead of the machinery and negative superhelical twists behind it. In addition, precatenanes evolve during replication behind the replication fork (Fig. 1.7) (Liu and Wang, 1987). Although the torsional stress of DNA overwinding can be removed by the actions of an enzyme that generates single-stranded breaks in the double

helix, the untangling of daughter chromosomes can only be accomplished by an enzyme that creates double-stranded breaks (Champoux, 2001; Osheroff, 1986; Wang, 1996; Wang, 2002). Thus, it has been assumed that Topo I functions ahead of the replication fork, while Topo II acts behind it. However, several lines of evidence suggest that type II Topos can also function ahead of DNA tracking systems like the replication fork. Yeast Topo II can compensate for the loss of Topo I in *S. cerevisiae*, but loss of both enzymes abruptly halts DNA synthesis (Kim and Wang, 1989). This finding indicates that the type II enzyme can assume the role of Topo I ahead of the replication machinery.

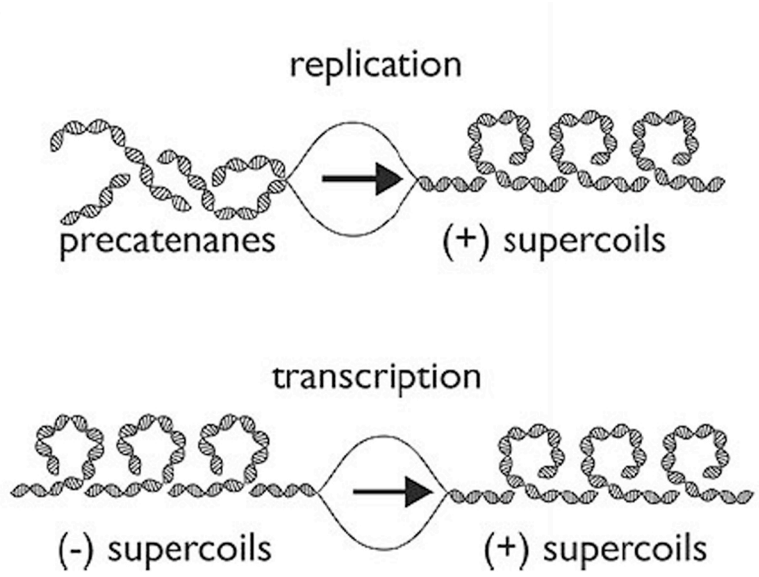

Fig. 1.7: **Topological problems during replication and transcription.** During DNA replication, positive supercoils accumulate ahead of the replication fork. As the fork advances, the positive supercoils further accumulate which could lead to diffusion of supercoiling across the fork. These interwindings are known as precatenanes, and would remain interlinked if left unresolved. During DNA transcription, positive supercoils accumulate ahead of the progressing fork, whereas negative supercoils accumulate behind it. Arrows indicate the direction of fork progression. Figure adapted from (Schoeffler and Berger, 2008).

In the absence of a Topo activity the unwinding of the DNA leads to the accumulation of positively supercoiled DNA in front of the replication fork. In addition, when the replication machinery is permitted to rotate around its axis the positive supercoils ahead of replication would be redistributed behind the replication fork thus leading to an intertwining of the pair of replicated DNA (precatenane formation) (Fig 1.8). This structure is a substrate for Topo II-mediated DNA decatenation and may represent a unique mechanism of action for Topo II during replication elongation. In the latter stages of replication, when two replication forks converge, there is no longer place for Topo I to relax positive supercoils, because its action requires binding to a short strech of double-stranded DNA. Completion of replication thus

leads to two interlinked catenanes (Wang, 2002), which again requires Topo II for its resolution.

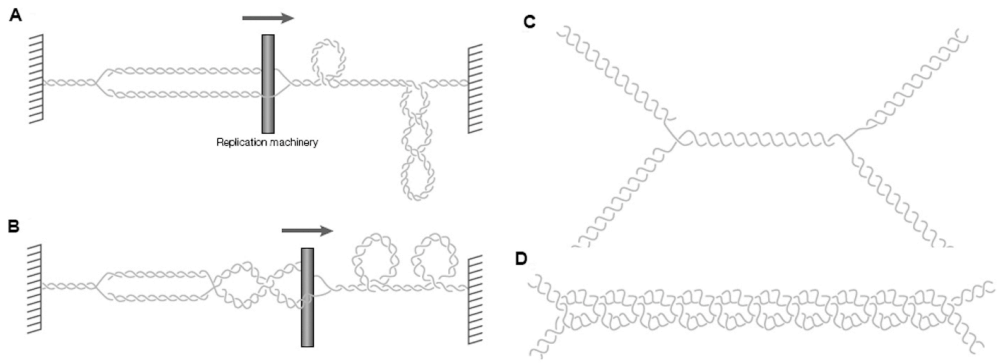

Fig. 1.8**: Problems evolving from the elongation of replication forks.** (**A**) and (**B**) The replication machinery moves along chromosomal DNA (rod). Due to the enormous size of a chromosome, the ends of a replication unit cannot freely rotate around the DNA axis and can thus be considered as being attached to an immobile structure. (**A**) Progression of the replication fork builds up positive supercoils ahead of the fork. (**B**) In case the replication machinery is free to rotate around its axis, this positive supercolis can be redistributed into the region behind the fork, thereby intertwining the newly replicated helixes. (**C**) When the unreplicated segment becomes very short, a four-way branched DNA intermediate is formed. This structure can arise from the converging of two replication forks and also from the pairing of two gapped DNA molecules to form a recombination intermediate. **D**) The residual intertwines between the parental strands can be converted to intertwines between newely replicated daughter molecules.

The importance of Topo II in DNA replication was first observed in yeast: Yeast cells lacking Topo I are viable, and undergo normal DNA replication (Brill et al., 1987; Kim and Wang, 1989) without activation of any S phase dependent checkpoints (Bermejo et al., 2007), which demonstrates that Topo II alone can fully support replication. In the absence of Topo II, however, cells also complete DNA replication but they die when they enter mitosis (Holm et al., 1985). In addition, the expression of a catalytically inactive protein failed to complete replication at sites where two replication forks meet (Nitiss, 2009a).

In mammalian cells, Topo I and Topo IIα are essential for cell proliferation (Carpenter and Porter, 2004), whereas Topo IIβ is dispensable for replication, as cell lines from various tissues could be isolated from homozygous Topo IIβ knockout mice (Yang et al., 2000). Biochemical analysis of human Topo IIα has shown that the protein is much more active in relaxing positively supercoiled substrates than in relaxing negatively supercoiled substrates, a property not found in Topo IIβ (McClendon et al., 2005). As positive supercoiling is expected to be generated in front of a replication fork, it has been suggested that at some point in replication Topo IIα could also play a role ahead of the replication fork. In contrast, Topo IIβ has been proposed to serve a regulatory role on gene transcription (see below).

1.4.2 Role of topoisomerases in transcription

The topological problems encountered during transcription resemble those of replication. However, during transcription positive and negative supercoils are produced ahead and behind the transcription machinery, respectively, with no intertwining. These toplogical problems require intervention of different Topos (Fig 1.9). Topo I and Topo IIβ are constitutively expressed throughout the cell cycle (Austin and Marsh, 1998; Baker et al., 1995), and are thus the most likely candidates to resolve the topological problems during the transcription process. The presence of eukaryotic Topo I in actively transcribed regions is well documented (Christensen et al., 2004; Nitiss, 1998; Wang, 1996).

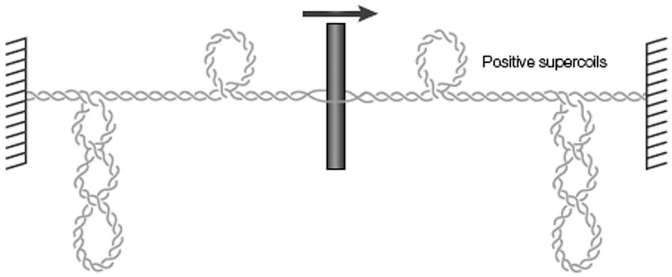

Fig. 1.9: **Topological problems associated with transcription.** Progression of the transcription machinery generates positive supercoils ahead the transcription machinery and negative supercoils behind it.

Depletion of yeast Topo I has no effect on cell growth (Thrash et al., 1985; Wang, 2002), indicating that Topo II can substitute all roles of Topo I during transcription. There is also evidence suggesting a role for Topo I in transcription initiation independent of the catalytic activity of the enzyme (Nitiss, 2009a; Pommier et al., 1998). Although both yeast and mammalian cells lacking Topo I are viable, the enzyme is required for embryogenesis in higher organisms, suggesting an additional essential role in early development.

Localization studies show a colocalisation of Topo I with transcribed regions (Shaiu and Hsieh, 1998). In interphase nuclei, Topo I accumulates in the nucleoli, which are nuclear structures involved in the ribosome biogenesis (Christensen et al., 2004). According to the high transcription activity that occurs on rDNA (Hannan et al., 1998), it is suggested that Topo I enrichment in the nucleolar compartment is due to its role in rDNA transcription, and, accordingly, Topo I was shown later on to colocalise with RNA polymerase I in the transcriptionally active sub-comportant of a nucleolus, the fibrillar centers (Christensen et al., 2004).

The effects on replication differ between yeast cells completely lacking any Topo II proteins and cells carrying enzymatic inactive protein (Brill et al., 1987; Gartenberg and

Wang, 1992; Kim and Wang, 1989; Nitiss, 2009a). Type I and II are essential in transcripton It (Kretzschmar et al., 1993; Merino et al., 1993; Mondal and Parvin, 2001; Shykind et al., 1997). Recent work has also provided evidence for a specific role for mammalian Topo IIβ in transcription initiation (Ju et al., 2006). Using chromatin immunoprecipitation technique, the authors showed that Topo IIβ associates with signal-dependent promoters as part of a complex that includes many proteins important in DNA repair. The presence of repair proteins does not seem to be required to repair the Topo IIβ-induced break. Rather, Topo IIβ is recruited to a subset of promoters, in a complex that includes DNA repair proteins (Ju et al., 2006; Ju and Rosenfeld, 2006). Further support for the specific role of Topo IIβ in transcription regulation stems from the observation that Topo IIβ plays a key role in neural development, because it has been suggested that the loss of function of Topo IIβ might lead to alterations in gene expression in neural tissue (Lyu et al., 2006; Lyu and Wang, 2003; Tsutsui et al., 2001).

1.5 Topoisomerase inhibitors

Substances interacting with the catalytical cycle of Topos are mostly associated with cancer therapy and are in this context considered the strongest pharmocological radiomimetics available. Malignant cells are frequently characterized by rapid growth coupled with an impaired ability to activate cell cycle checkpoints and DNA repair pathways (Nakanishi et al., 2006). Consequently, DNA in cancerous tissues often sustains elevated rates of replication and transcription, despite a decreased competence to restore genomic integrity following damage. This dual property of cancer cells displaying a high DNA metabolism but low genetic stability makes the double helix an attractive target for cancer chemotherapy. Indeed, several classes of widely utilized anticancer drugs act by damaging DNA, either directly or indirectly. Multiple therapeutic strategies are used to damage DNA. Ultimately, these strategies block DNA replication or other essential nucleic acid processes, generate mutations, create DNA strand breaks, or induce chromosomal abnormalities. For example, methotrexate, which inhibits the cellular enzyme dihydrofolate reductase, decreases cellular thymine pools and promotes incorporation of deoxyuridine into chromosomes (Schilsky, 1996). Mechlorethamine (nitrogen mustard) (Povirk and Shuker, 1994) and cisplatin (Zorbas and Keppler, 2005) alkylate bases or crosslink the two strands of the double helix. Other agents like bleomycin (Povirk, 1996) generate DNA strand breaks by a chemical mechanism.

One of the most effective mechanisms for generating DNA strand breaks is interference with the catalytic cycle of Topos. The initial suggestion that Topos could be a target for potent cancer drugs came from the laboratory of Kurt Kohn in the late 1970s, who found that protein-associated DNA breaks were formed in cells treated with DNA-intercalative compounds (Ross et al., 1979; Ross et al., 1978). Few years later, Leroy Liu and co-workers demonstrated that certain anticancer drugs specifically stimulate Topo II-mediated DNA cleavage both *in vitro* and *in vivo* (Chen et al., 1984; Nelson et al., 1984; Tewey et al., 1984a). Topo-directed cancer drugs thus enhance the intinsic property of all Topos to cleave DNA. Although the strand breaks generated by Topos are transient in nature, they are potentially deleterious to the cell. Topo II generates transient, enzyme coupled DNA double strand breaks, whereas Topo I creates enzyme coupled DNA nicks, which are presumably converted to permanent double-stranded breaks, when encountered by a replication fork (Nitiss, 1998; Nitiss, 2009a; Wang, 1996). Strand breakage as well as the inhibition of essential DNA metabolic processes initiates cellular stress responses and recombination/repair pathways (Baldwin and Osheroff, 2005; Ju et al., 2006; Pommier, 2006). By stabilizing the Topo DNA cleavage complex Topo-directed cancer drugs convert Topos from essential enzymes to potent cellular toxins that fragment the genome (Kaufmann et al., 1998; Nitiss, 2009b; Pommier, 2006). Consequently, these drugs have been termed Topo poisons. If the accumulation of breaks thus induced overwhelms a cell, apoptotic pathways are triggered. However, if the level of DNA strand breaks produced by Topo poisons is not lethal, repair of these breaks generates chromosomal translocations and/or other aberrations (Li and Liu, 2001) that can lead to specific types of leukemia (Kaufmann et al., 1998; Nitiss, 2009b; Pommier, 2006).

Cellular sensitivity to Topo II poisons is stringently correlated to the physiological level and activity of the target enzyme (Nitiss et al., 1992). Cells that contain increased amounts of Topo II display a hypersensitivity to these drugs. This is due to a higher level of Topo II-mediated DNA strand breaks incucable by the drugs. In contrast, cells that contain decreased amounts of the enzyme display enhanced resistance to Topo II poisons. This is due to a lower level of Topo II-mediated DNA cleavage, which is less toxic to cells. Finally, mutant type II Topos that are hypersensitive or resistant to an anticancer drug *in vitro* confer a similar degree of hypersensitivity or resistance to cells (Danks et al., 1988; Zwelling et al., 1989).

1.5.1 Topoisomerase I poins as cancer drugs

Topo I is the target for an emerging class of drugs based on camptothecin, a natural product derived from the bark of the Chinese yew tree, *Camptotheca acuminata* (Wall and Wani, 1995). All Topo I drugs stabilize the cleavage complex and therefore are Topo poisons. These drugs represent some of the most active new agents in the clinic and show promise against malignancies that respond poorly to existing therapies, such as non-small cell lung cancer, metastatic ovarian cancer, and colorectal cancer (Leppard and Champoux, 2005; Pommier, 2006; Pommier, 2009). Two water-soluble camptothecin derivatives are approved by the FDA for intravenous administration in patients: topotecan and irinotecan (Fig. 1.10). Topotecan is used to treat ovarian cancers and small cell lung carcinoma, whereas irinotecan is a prodrug used against colorectal tumors. Other drugs that target Topo I, including the indenoisoquinolines, indolocarbazoles, and the phenanthridines, are currently under clinical development (Pommier, 2009).

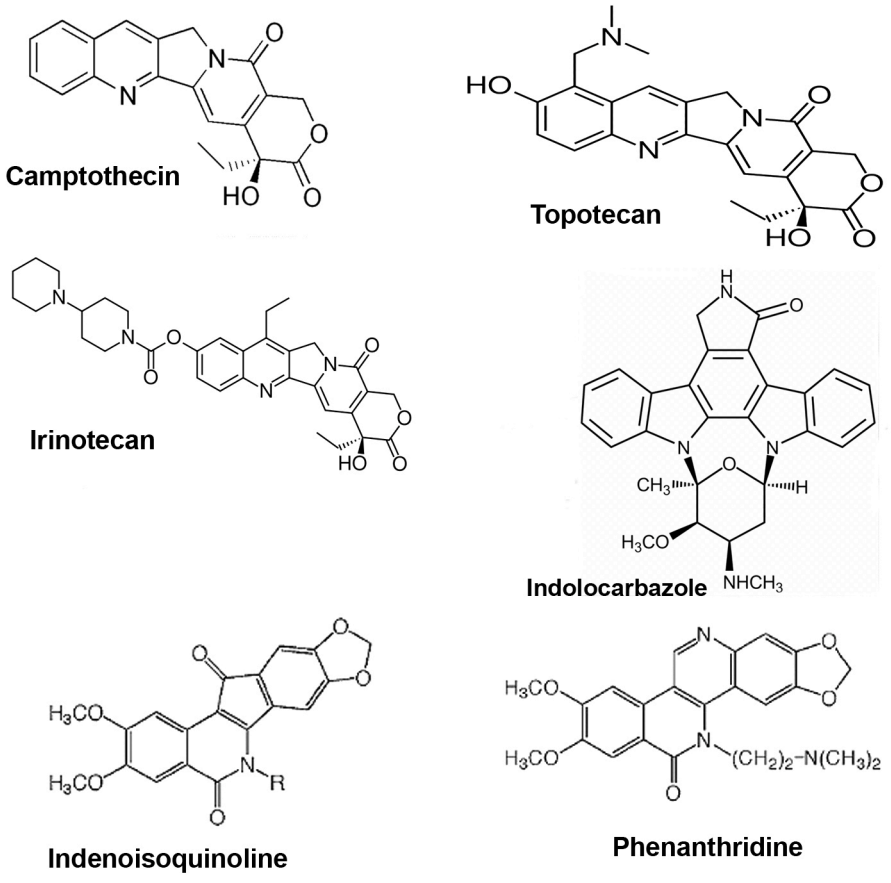

Fig. 1.10: **Chemical structure of Topo I poisons.**

1.5.2 Inhibitors of topoisomerase II

Topo II is the target for a large and diverse group of substances that interfere with the catalytic cyle at various positions. Roughly, they can be divided into two types: poisons and catalytic inhibitors. **Topo II poisons** enhance DNA cleavage by Topo II. This group comprises (i) cancer drugs, (ii) mutagenic metabolites of xenobiotics and therapeutics, (iii) plant polyphenols and alkaloids constituting a significant portion of human food intake, and (iv) DNA base modifications induced by radiation or oxidative stress (Kingma et al., 1995; Kingma and Osheroff, 1997a; Kingma and Osheroff, 1997b). **Topo II catalytic inhibitors** decrease DNA cleavage by Topo II, and thus, antagonise poisoning. This group comprises (i) DNA intercalating Topo II poisons that at high concentrations inhibit Topo II DNA binding and (ii) a variety of synthetic and semi-synthetic substances that inhibit DNA cleavage by interrupting the catalytic cycle before or after the sequence of DNA-cleavage/-strandpassage/-religation. The latter substances have some anti proliferative potential of their own but are currently only used in the clinic as antidotes and ameliorators of undesired effects of Topo II poisoning cancer drugs (Nitiss, 2009b).

1.5.2.1 Topoisomerase II poisons in cancer therapy

Agents that increase the levels of Topo II DNA cleavage complexes have been denominated “poisons”, because they convert these enzymes into potent DNA damaging agents (Baldwin and Osheroff, 2005; Pommier, 2006). Some Topo II poisons act by enhancing the forward rate of cleavage complex formation through an unknown mechanism (Nitiss, 2009b). Others inhibit the ability of Topo to ligate cleaved DNA intermediates, but have little effect on the rate of enzyme-mediated DNA cleavage (Baldwin and Osheroff, 2005). Clinically relevant Topo II poisons appear to belong mostly to the second group (Baldwin and Osheroff, 2005; Kaufmann et al., 1998; Li and Liu, 2001; Pommier, 2006). They are among the most important anticancer drugs currently used for treating human malignancies worldwide. They are front-line therapeutics for a variety of systemic cancers and solid tumors, including leukemias, lymphomas, sarcomas, and breast, lung, and germ line cancers. In fact, every form of cancer considered to be curable by systemic chemotherapy is currently subjected to treatment regimens utilizing these drugs (Burden and Osheroff, 1998), and it is estimated that one half of all chemotherapy regimens include these agents (Baldwin et al., 2004; Hande, 1998; Pommier et al., 1998). These important cancer therapeutics

represent a structurally diverse group of synthetic and semi-synthetic compounds (Fig.1.11), which can be divided into DNA-intercalative and non-intercalative Topo II poisons.

Non-intercalative Topo II poisons are believed to bind specifically to Topo II, thereby rendering the enzyme incapable of performing DNA-ligation during a subsequent catalytic cycle. All cancer drugs of this type are derived from podophyllotoxin (Baldwin and Osheroff, 2005; Hande, 1998), a natural toxin of *Podophyllum peltatum* (may apple), which has been used as a folk remedy for more than a thousand years. Podophyllotoxin is a Topo II poison as well as an inhibitior of tubulin polymerization (Baldwin and Osheroff, 2005; Hande, 1998). Two synthetic analogs etoposide (VP16) and teniposide (VM26) with increased antineoplastic activity and decreased toxicity are much stronger Topo II poisons than podophyllotoxin, but do not inhibit tubulin polymerization (Chen et al., 1984). VP16 and VM26 are approved for clinical use against cancer since 1980 (Baldwin and Osheroff, 2005; Hande, 1998) and are still the most highly prescribed anticancer drugs in the world (Bandele and Osheroff, 2008; Burden and Osheroff, 1998; Hande, 1998).

DNA-intercatalytive Topo II poisons currently in clinical use are a structurally divergent group, comprising aminoacridines, anthracyclines and anthracenediones (Fig.1.11).

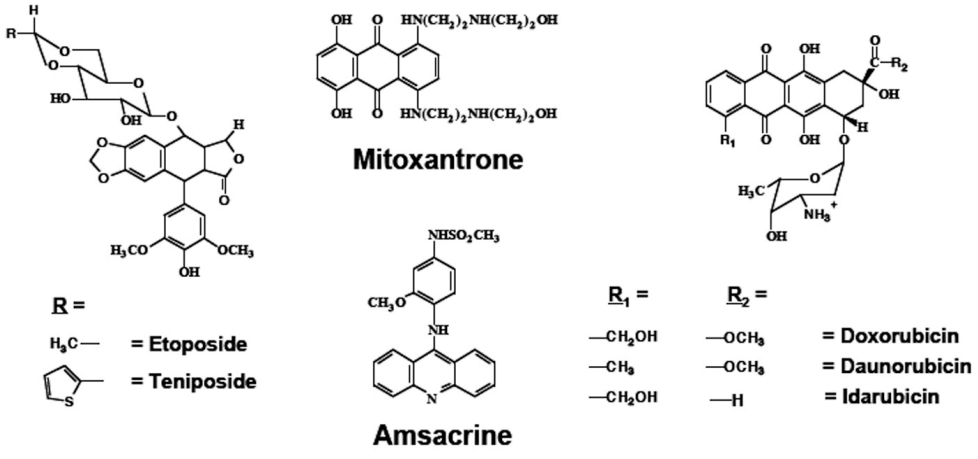

Fig. 1.11: **Structures of Topo II poisons in clinical use**

The lead compounds m-amsacrine (m-AMSA), doxorubicine (DOX) and mitoxantrone (MITOX) have all been reported to stimulate Topo II mediated DNA cleavage (Pommier et al., 1983). Current belief holds that these effects are due to intercalation at the DNA-cleavage site of Topo II, which induces a shift of the cleavage/reliagtion equilibrium towards the

cleaved state or even makes ligation entirely impossible. Therefore, these drugs are thought to exert their effect by first intercalating into DNA and then form a ternary complex with DNA and Topo II (Nitiss, 2009b). Formation of this ternary complex is insofar specific as it does not occur with most other DNA intercalating substances lacking antitumor activity (e.g. ethidium bromide) (Liu, 1989; Tewey et al., 1984b). The most significant difference between intercalating and non-intercalating Topo II poisons is, that the intercalators have additional effects that impact on the levels of Topo II mediated cleavage in a geometry-specific manner. As they intercalate, these compounds locally underwind the DNA double helix, thereby inducing compensatory unconstrained positive superhelical twists in DNA segments that are not free to rotate (e.g. circular plasmids or chromatin domains). Thus, a DNA domain that is normally negatively supercoiled would appear to contain positive superhelical twists when absorbing these drugs at higher concentrations. This has two consequnences: Firstly, the torsional stress induced in the double helix will eventually limit the capacity for absorbing more of these compounds. In other words, dose response relationships of these compounds are to some extent governed by overall DNA topology (Chen et al., 1984; Liu, 1989). Secondly, the distorsions of the helix induced by drug intercalation inhibit DNA binding of Topo II. Therefore, with increasing concentrations, these compounds will inhibit Topo II mediated DNA cleavage and thus delimit their own efficacy as stimulators of cleavage (Pommier et al., 1983). For the intercalative acridine derivative m-AMSA and the intercalating anthracenedione derivative MITOX potent antitumor activity has been stringently correlated to the specific formation of Topo II linked DNA strand breaks both *in vitro* and in mammal cells (Bailly et al., 1997; Crespi et al., 1986; D'Arpa and Liu, 1989; Errington et al., 2004; Liu, 1989; Nelson et al., 1984; Shenkenberg and Von Hoff, 1986). Such a mechanistic correlation failed for the anthracyclins (e.g. DOX) because *in vitro* anaylsis of DNA cleavage is not possible with these drugs due to their strong DNA intercalation (Liu, 1989). Moreover, the quinone ring, common to all anthracyclines can be oxidized generating reactive oxygen species (ROS), which lead to a wide array of genomic and cellular damage unrelated to Topo II (Froelich-Ammon and Osheroff, 1995; Lothstein et al., 2001). Therefore, it is still controversial, whether antracyclins indeed act through Topo II poisoning and not through the generation of ROS or some other mechanims (Nitiss, 2009b). All three types of intercalating Topo II poisons discussed have an established activity against a variety of human neoplasias and are widely employed in frontline chemotherapy (Baldwin et al., 2004; Hande, 1998; Pommier et al., 1998). MITOX is in addition used as an immunosuppressant in the treatment of multiple sclerosis (Komori et al., 2009).

Isoform selectivity of Topo II poisons is an issue of considerable clinical ramifications. Most of the cancer drugs in clinical use have been demonstrated to target Topo IIα and β *in vitro*. But is not clear at present, whether this also holds true in the living cell, and what are the relative contributions of the isoforms to therapeutic outcomes. Since Topo IIα is upregulated in many cancer cells and the isoform essential for DNA proliferation (Carpenter and Porter, 2004; Grue et al., 1998; Linka et al., 2007), it has been suggested that it is also the more important drug target. Moreover, it has been suggested that poisoning of the "housekeeping enzyme" Topo IIβ in non-proliferative compartments and tissues, such as the heart or the skin, could mostly contribute to the dose-limiting toxicity of some of these agents (Austin and Marsh, 1998; Azarova et al., 2007; Gatto and Leo, 2003). Conversely, it has been argued that simultaneous formation of DNA cleavage complexes by Topo IIα and Topo IIβ is more likely to induce permanent DNA strand breaks in a a given cell nucleus, since the two isoforms are involved in different DNA-metabolic processes (Austin and Marsh, 1998; Gatto and Leo, 2003). Thus, it would be of interest to chracterize the relative impact of known and used Topo II poisons on the two isoforms, and to identify and characterize new potential Topo II poisons that act selectively on only one of them. Currently, there are two substances published that believed to act as a selective poison of Topo IIα (Fehr et al., 2008; Toyoda et al., 2008), and two substances suggested to target selectively the β-isoform (Barthelmes et al., 2001; Gao et al., 1999).

1.5.2.2 Topoisomerase II catalytic inhibitors

These drugs do not increase the level of enzyme-mediated DNA cleavage complexes. Rather, they block specific other steps in the catalytic cycle of Topo II leading to a decrease in Topo II activity (Andoh and Ishida, 1998; Pommier et al., 1998). The best characterized compounds of this class are merbarone and the bisdioxopiperazines ICRF-193 and ICRF-187 (Fig. 1.12), which were all shown to block DNA cleavage mediated by Topo II (Fortune and Osheroff, 1998). Bisdioxopiperazines inhibit yeast DNA Topo II by trapping the enzyme in the form of a closed protein clamp (Roca et al., 1994). While Topo II poisons kill cells by fragmenting the genome, catalytic inhibitors are thought to kill by depriving cells of the essential activity of Topo II. Consequently, increased expression of Topo II confers resistance to catalytic inhibitors (Kusumoto et al., 1996), whereas it confers hypersensitivity to poisons (Nitiss et al., 1992). Cells treated with catalytic inhibitors display elongated and entangled chromosomes and ultimately die from mitotic failure (Larsen et al., 2003) similar to cells lacking Topo IIα (Carpenter and Porter, 2004; Grue et al., 1998; Linka et al., 2007). Despite

these anti neoplastic activities, the only catalytic inhibitor so far in clinical use (Dexrazoxane) is employed as an antidote for Topo II poisons that ameliorates undesired effects of antracyclins in the heart and thus allows for a dose escalation of these drugs (Andoh and Ishida, 1998; Larsen et al., 2003; Lyu et al., 2007). Some other catalytic inhibitors of Topo II displaying anticancer activity in model organisms and are currently tested in clinical trials (Attia et al., 2009).

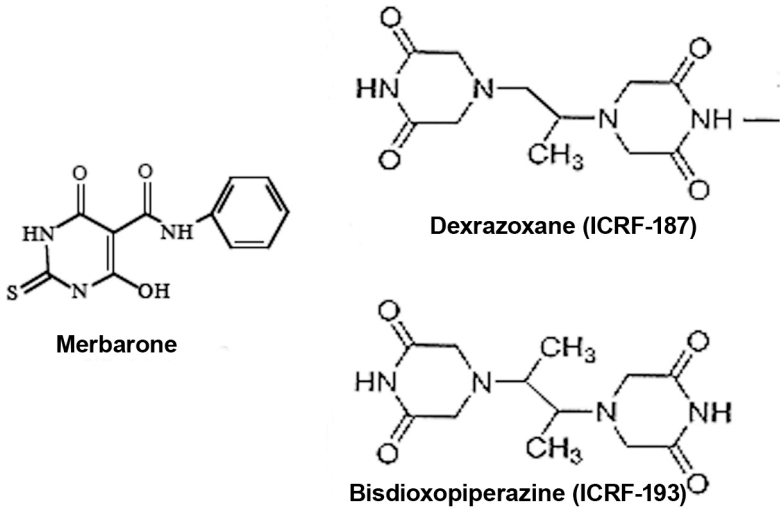

Fig. 1.12: **Structures of Topo II catalytic inhibitors**

1.5.3 Natural and xenobiotic topoisomerase poisons

In addition to the synthetically derived Topo II poisons that are used to treat cancer and the antibacterial quinolones that target the prokaryotic type II enzymes (DNA gyrase and topoisomerase IV), three other categories of Topo poisons have been identified. These include natural products that are normal dietary components (bioflavonoids and alkaloids), toxic metabolites of therapeutic or industrial chemicals (quinones), and damaged DNA bases that are generated by a wide variety of genotoxic agents (Fig. 1.13). Thus far, compounds in the first two categories have been found to affect primarily the type II enzyme. Damaged DNA bases however affect the cleavage equilibrium of type I and II Topos.

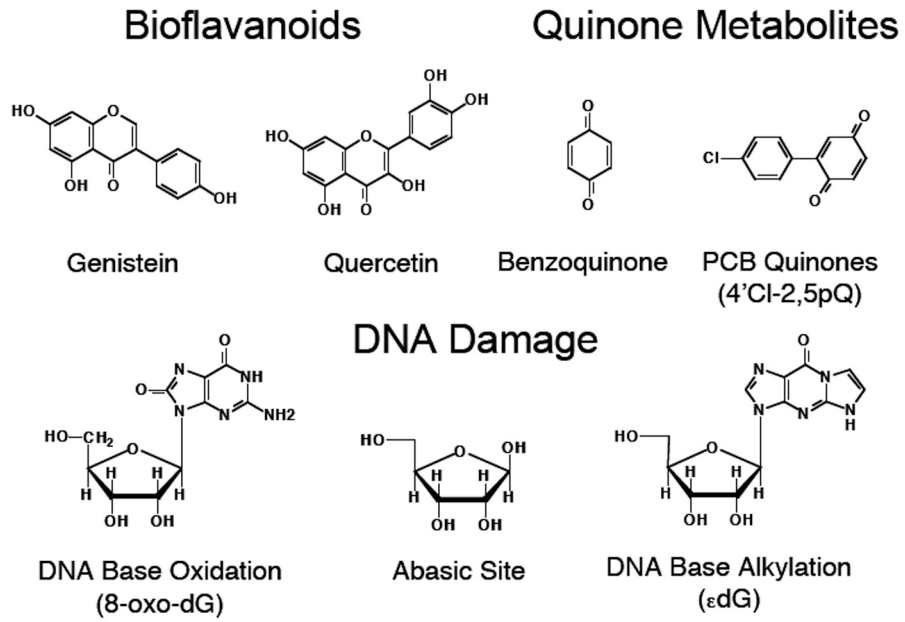

Fig. 1.13: **Structures of environmental Topo II poisons**

1.5.3.1 Topoisomerase II poisoning by bioflavonoids

Polyphenols are the most abundant antioxidants in our diet (Ross and Kasum, 2002). They are potent inhibitors of tyrosine kinases, act either as agonists or antagonists of estrogen receptor or alter sex hormone production and metabolism (Kandaswami et al., 2005). Furthermore, they display antiproliferative and proapoptotic effects, decrease the expression or function of several proteins that are involved in cell-cycle progression (Taylor et al., 2009). Epidemiological studies have suggested associations between the consumption of polyphenol rich foods or beverages and the prevention of diseases (Scalbert and Williamson, 2000). Commonly referred to as antioxidants, they may prevent various diseases associated with oxidative stress, such as cancers, cardiovascular diseases, inflammation and others.

Flavonoids (i.e., phytoestrogens) comprise the most common group of plant polyphenols. They are components of many fruits, vegetables, and plant leaves fulfilling diverse functions like pigmentation in flowers and protection from attack by microbes and insects. (Ross and Kasum, 2002; Siddiqui et al., 2006). These compounds are a significant component of human food and some of them affect human cells through a variety of pathways; they are strong antioxidants and efficient inhibitors of growth factor receptor tyrosine kinases (Ross and Kasum, 2002; Scalbert and Williamson, 2000). Most importantly, some flavonoids are potent poisons of Topo I and II (Bandele and Osheroff, 2007; Boege et al., 1996).

The flavonoid with the strongest potential to poison Topo II known to date is genistein. Previous studies have shown that genistein enhances DNA cleavage by Topo IIα and IIβ *in vitro* almost as strongly as etoposide (Bandele and Osheroff, 2007; Bandele and Osheroff, 2008; Lopez-Lazaro et al., 2007; Markovits et al., 1995; Taylor et al., 2009). Genistein has been shown to cause apoptosis in cultured cancer cells and to protect against the development of carcinomas in animal models (Taylor et al., 2009). As a consequence, the National Cancer Institute is currently sponsoring several clinical trials investigating genistein as a therapeutic for treating prostate, bladder, and kidney cancer and for its chemoprevent effects in breast and endometrial cancer (Taylor et al., 2009). Genistein is a frequent component of asian dietary items, in particular soy. Epidemiological evidence links regular ingestion of soy to a low incidence of breast and colorectal cancers observed in the pacific rim (Bandele and Osheroff, 2007; Ross and Kasum, 2002; Siddiqui et al., 2006). However, there is also evidence associating soy consumption during pregnancy to the development of infant leukemias (Ross et al., 1994; Spector et al., 2005; Taylor et al., 2009). Some authors attribute these putative anticancer as well as mutagenic effects to Topo II poisoning by genistein (Bandele and Osheroff, 2007; Bandele and Osheroff, 2008). Given this assumption, the daily genistein uptake in an asian diet should subject humans to the equivalent of a continuous cancer chemotherapy (e.g. with etoposide), without giving rise to the severe side effects obligatory in such a therapy (nausea, lack of appetite, myelodepression, loss of hair, etc.). These paradoxical situation holds true also for the flavonoids most prominent in western diets (e.g. quercetin) (Neukam et al., 2008) and raises the question of whether genistein and related flavone compounds indeed act as strong Topo II poisons *in vivo*. Most recently, alternariol, a mutagenic toxin formed by the mold fungus alternaria alternata has been reported to act as a selective poison of Topo IIα (Fehr et al., 2008).

1.5.3.2 Alkaloids

Alkaloids are naturally occurring chemical compounds containing basic nitrogen atoms. The name derives from the word alkaline and was used to describe any nitrogen-containing base. Alkaloids are produced by a large variety of organisms, including bacteria, fungi, plants, and animals. The phenanthridine alkaloid lycobetaine is a minor constituent of plants from the family Amaryllidaceae and was found to act as a selective Topo IIβ poison (Barthelmes et al., 2001). Ellipticine is another plant alkaloid with DNA-intercalating property showing a high degree of activity against Topo II (Tewey et al., 1984a).

1.5.3.3 Quinones

Quinones are highly reactive compounds that are often produced in the body as a result of detoxification or other metabolic pathways. Quinones damage cells by generating oxygen radicals and by covalently modifying proteins and (to a lesser extent) nucleic acids (Shen et al., 1996). Exposure to benzene (metabolized to benzoquinone) has been linked to the development of malignancies in rodents and of leukemia in humans. Recent studies demonstrate that benzoquinone is a strong Topo II poison *in vitro* and in cultured human cells (Lindsey et al., 2005a; Lindsey et al., 2005b). It is presumed that benzoquinone requires attachment to the enzyme to inhibit function. However, the mechanism by which quinone adduction enhances enzyme-mediate DNA cleavage is largely unknown. In addition to benzoquinone other quinones, including Menadione (known as vitamin K3), also display activity against Topo II (Wang et al., 2001). Finally, various metabolites of paracetamol (N-acetyl *p*-benzoquinone imine) are established Topo II poisons thought to play a role in the generation of chromosomal aberrations (Bender et al., 2004). It should be noted that in western society the genistein paradox to some extent also applies to the intake of paracetamol.

1.5.3.4 Topoisomerase inhibition by DNA base modifications

Certain DNA lesions are potent enhancers of DNA cleavage mediated by type I and II enzymes. Topo I is most sensitive to abasic sites, oxidative lesions, and alkylated bases (Pommier et al., 2003). It was recently shown that Topo I and Topo II accumulate at UVA-induced damage on DNA in living cells (Mielke et al., 2004; Mielke et al., 2007). Topo II is particularly sensitive to lesions that interrupt the double helix, in partricular abasic sites and alkylated bases that contain exocyclic rings (Khan et al., 2003). DNA damage increases cleavage at naturally occurring sites of Topo I or Topo II action. In all cases, lesions must be located proximal to the sites of cleavage in order to act as enzyme poisons. Topo I is generally sensitive to lesions immediately upstream or downstream from the scissile bond (Sordet et al., 2004), whereas Topo II requires that damage be localized within the four-base stagger that separates the two scissile bonds on the opposite strands of the double helix (Frankenberg-Schwager et al., 2008; Khan et al., 2003). Although DNA damage increases levels of Topo I and Topo II cleavage complexes, the mechanisms by which lesions alter the activity of these enzymes differ. DNA damage increases the concentration of Topo I-DNA cleavage complexes primarily by inhibiting rates of enzyme-mediated DNA ligation (Pommier et al., 2003). In contrast, damage has no obvious effects on rates of Topo II-mediated DNA ligation

and appears to act primarily by enhancing the forward rate of cleavage (Cline and Osheroff, 1999). The physiological impact made by the action of DNA lesions on Topo is unclear. However, it is notable that Topo I and Topo II both appear to play roles in fragmenting genomic DNA during apoptosis (Pourquier and Pommier, 2001; Sordet et al., 2004). It has been suggested that DNA lesions that are generated following the release of oxygen radicals from permeable mitochondria in apoptotic cells could enhance the apoptotic activities of Topos (Pourquier and Pommier, 2001; Sordet et al., 2004).

1.5.4 Topoisomerase II-initiated chromosome translocations and leukemia

In addition to its role as an essential cellular protein and target for anticancer drugs, clinical studies suggest that Topo II-initiated DNA breaks can lead to chromosomal translocations that trigger specific types of leukemia. For example, a small percentage of patients treated with regimens that include etoposide ultimately develop acute myelocytic leukemia (Felix, 2001). Along the same lines, correlations between the rising use of the Topo II poison mitoxantrone to treat breast cancer and the development of secondary leukemias have been noted (Martinez et al., 2007). The common feature in half of these leukemias is the presence of translocations within an 8.3 kb breakpoint cluster region in the *MLL* (mixed lineage leukemia) gene at chromosome band 11q23. The basis for the development of Topo II-initiated leukemias is unclear, but it appears to be related to interactions of the enzyme with certain sequences in the *MLL* gene locus. In correlation with clinical data, etoposide was found to induce Topo II-mediated DNA cleavage proximal to the chromosomal breakpoint region (Libura et al., 2005). Analogous links seem to exist between Topo II and the initiation of acute myeloid leukemias (AMLs) in infants (Libura et al., 2005; Rowley, 1998) that also involves chromosomal translocations in the *MLL* gene. Moreover, it has been shown that prolonged exposure to very low doses of MITOX (such as used in immunosupressive therapy of multiple sclerosis) induces similar chromosome translocations in hematopoietic stem cells (Hasan et al., 2008). Epidemiological studies have established that maternal consumption during pregnancy of foods that are high in naturally occurring Topo II poisons increases the risk of infant AMLs ~10-fold (Ross et al., 1984). A similar connection is also postulated for the mycotoxin alternariol (Fehr et al., 2008), and enhancement of Topo II mediated cleavage in the MLL breakpoint region has also been demonstrated *in vitro* for various flavonoids regularly ingested with a western diet (Ross, 2000). These correlations seem to suggest that

Topo II-induced DNA breaks may be initiating these translocations. AMLs, along with non-lymphocytic leukemias, also have been linked to exposure to chemicals, such as benzene (Irons, 2000). The mechanism by which benzene induces leukemias has not been fully elucidated, but it is thought to be caused by one of benzene's metabolites, 1,4-benzoquinione. Exposure of mammalian cells to 1,4-benzoquinone generates DNA mutations, insertions, deletions, and strand breaks (Wallace, 1989). In addition, 1,4-benzoquinone was recently demonstrated to be a Topo II poison (Lindsey et al., 2005a; Lindsey et al., 2005b). The ability of Topo II to cause rather than cure cancer is most likely related to the level of enzyme activity in a particular cell. If the concentration of Topo II-mediated DNA cleavage in a cell is high, then recombination and repair pathways will be overwhelmed and cells will initiate apoptosis (Kaufmann et al., 1998). However, if the concentration of Topo II-mediated DNA cleavage is too low to initiate cell death, chromosomal breaks and translocations can result from normal cell survival pathways (Burden and Osheroff, 1998). Another factor suggested to play a role in this is the stability and reversibility of the cleavable complexes induced by the drugs (Felix et al., 2006).

1.6 Scope of the dissertation

Inhibitors of Topo I and II are widely applied in clinical cancer treatment. In addition, interference with the catalytical activity of these enzymes is thought to contribute to environmental and food toxicity in a paradoxical manner. Polyphenols, the most abundant antioxidants in our diet, benzene, an important industrial solvent and precursor in the production of drugs, plastics, synthetic rubber, and dyes, and metabolites of the the widely used "over the counter" pain killer paracetamol, are all considered as Topo targeting agents (Bender et al., 2004; Fehr et al., 2008; Lindsey et al., 2005a; Lindsey et al., 2005b). Due to the wide distribution of Topo targeting substances in nature, they should be equivalent to a daily dose of cancer chemotherapy. However, this is apparently not the case because side effects typical for Topo cancer drugs are not observed in normal life. This paradox could be due to *in vivo* factors like the bioavailability or the metabolic processing of these agents. Therefore, one aim of this dissertation was to resolve the paradox by comparing in living cells the inhibitory efficiency of established, clinically relevant Topo-targeted compounds with that of xenobiotics and natural food constituents shown by *in vitro* assays to inhibit Topo activity. This was done by expressing fluorescently tagged Topos in cell culture thus enabling measurement of Topo-inhibition in living cells in a non-destructive manner, by measuring the relative redistribution of the enzymes in the cell nucleus and their retardation or immobilization on the nuclear DNA in response to Topo targeted drugs (Christensen et al., 2004; Christensen et al., 2002c). By this approach it was also possible to address the iso-form selectivity of Topo II poisons, which is an issue of considerable relevance for cancer therapy.
On the other hand, it is to be expected that the pleiotropic involvement of Topo I, IIα, and IIβ in the processes of transcription or replication influences the nuclear distribution and availability of these enzymes at different stages of the mitotic cell cycle. This could have a profound influence on the effectiveness of Topo-targeted compounds and may account for discrepancies between nuritional, xenobiotic and therapeutical Topo poisoning. To address this issue, it was necessary to establish a cell model that allows discriminating between the different cell cycle stages of interphase without interference of external factors. I have chosen to use proliferating cell nuclear antigen (PCNA) and the replication-initiating factor Cdc6 as cell cycle marker coexpressing them with Topo I, IIα, and IIβ as fusion proteins with YFP and/or CFP. While PCNA is an established marker for the different stages of S phase, Cdc6 was expected to distinguish between G1 and G2. In the course of etstablishing this system, I

discovered several unexpected features of Cdc6 so far unknown, which forced me to also include a more detailed investigation of Cdc6 localization and -dynamics in this work.

2. Materials

2.1 Vectors and cDNAs

2.1.1 Expression of bicistronic vectors

The expression of fluorescent chimera of a definite protein in mammalian cells was enabled by the bicistronic vectors pMC-GFP-P and pMC-CFP-H (Christensen et al., 2002a; Mielke et al., 2000). In which the puromycin resistance gene (pyromycin-N-acetyltransferase, pac) or the hygromycin resistance gene (hygromycin B phosphotransferase) constitutes the second cistron, followed by the simian virus 40 (SV40) polyadenylation signal. The first cistron carried green fluorescent protein (GFP) tagged protein, where the GFP was attached to the N-terminal or the C-terminal domain of the protein, depending on the presumed minimal interference with the protein. An IRES (Internal Ribosomal Entry Site) element from the polio virus is between the two cistrons, which permits the translation of both the gene of interest and the selection marker from a single mRNA. A cytomegalovirus promoter (CMV) fused to the myeloproliferative sarcomvirus (MPSV) LTR enhancer repeat ensures a high transcription level of the bicistronic message in various mammalian cells, while the transcriptional linkage ensures a fixed simultaneous expression of the selection marker and the gene of interest (Fig 2.1).

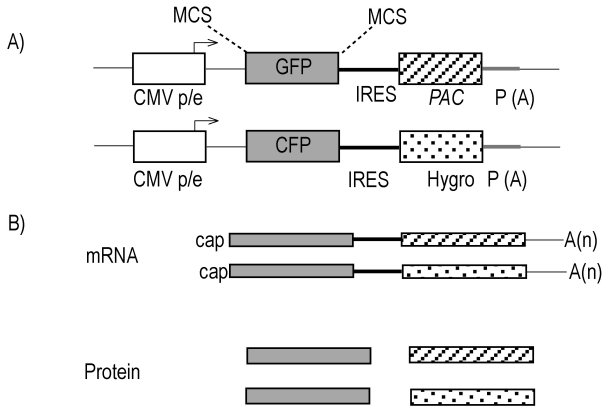

Fig. 2.1: **The Construction scheme of bicistronic plasmid. (A)** CMV promotor (open box), GFP or CFP (grey box), an IRES element (black bar), *pac* (diagonally striped box), Hygro (doted box), and SV40 P(A) site (grey bar). **(B)** Expression of bicistronic mRNA, inwhich the first cistron was translated by normal CAP dependent translation, and IRES element was responsible for translation of the second cistron.

The use of two different selection markers allowed the coexpression of two different proteins as differently coloured bio-fluorescent protein chimera. In addition, the plasmids were used as basic constructs for cloning of all fusion proteins described in this work, where the multiple cloning sites were inserted infront or behind the fluorophor. GFP or one of its

various forms CFP (cyan fluorescent protein), or YFP (yellow fluorescent protein) was subcloned in the basic construct.

2.1.2 Expression of tricistronic vectors

The tricistronic expression vectors were constructed for the simultaneous and coordinated expression of three independent genes in mammalian cells. One single promoter (CMV) fused to LTR enhancer (MPSV) allows a high transcription of all three cistrons. The tricistronic plasmid contains two IRES that allowed an efficient translation of the internal cistrons. The *ClaI*/*NotI* fragment of the plasmids pMC-GFP-P and pMC-CFP-H were combined to give tricistronic expression vectors with puromycin resistance activity as shown in (Fig. 2.2).

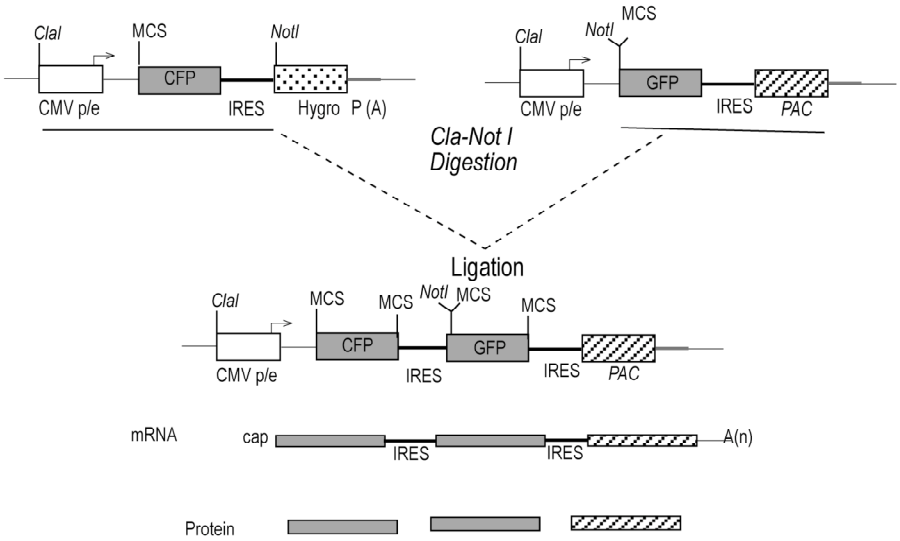

Fig. 2.2: **Construction scheme of tricistronic plasmid.** The cDNA sequences are inserted into multiple cloning sites (MCS) of plasmids pMC-GFP-P and pMC-CFP-H, respectively. Both plasmids contain unique *ClaI* and *NotI* restriction sites, which enable the fusion of two cDNA containing fragment. This constuct mediate the trannscription of one tricistroic mRNA which is translated into three proteins

2.1.3 cDNA

The cDNA of human Cdc6 (cell division cycle 6) was kindly gifted from Dr. Friedrich Grummt (University of Würzburg, Germany). Human PCNA (proliferating cell nuclear antigen) cDNA was obtained from Dr. Wilhelm G. Dirks (DSMZ, Braunschweig, Germany),

where *MluI/ ApaI* restriction sites were inserted in the gene by means of linker PCR, facilitating its cloning in the basic construct.

2.1.4 DNA oligonucleotides

All nucleotides used for PCR amplification, oligohybridization and DNA sequencing were purchased in HPLC grade from IBA (Göttingen,Germany).

2.2 Bacterial strains and growth media

2.2.1 *E. coli* strains

DH5α	Genotype: supE44 ΔlacU169 (Φ80lacZΔM15) hsdR17 recA1 endA1 gyrA96 thi-1 relA1 (Hanahan, 1983)
Top10	Genotype: mcr A Δ (mrr-hsdRMS-mcrBC) Φ80lacZΔM15 ΔlacX74 recA1 araD139 Δ (ara-leu)7697 galU galK rpsL (StrR) endA1 nupG, (Invitrogen, Carlsbad, USA)
SURE	Genotype: e14-(McrA-) Δ(mcrCB-hsdSMR-mrr)171 endA1 supE44 thi-1 gyrA96 relA1 lac recB recJ sbcC umuC:Tn5 (Kanr) uvrC [F´proAB lacIqZΔM15 Tn10 (Tetr)], Stratagene, (La Jolla, USA)

2.2.2 Bacterial growth media

LB-medium (1 l)	10 g Trypton, 5 g yeast extract, 10 g NaCl, adjusted to pH 7.5 by (NaOH)
LB-agar	10 g agar in 1000 ml LB medium
TB-medium (1 l)	12 g Trypton, 24 g yeast extract, 4 ml Glycerol, dissolved in 900 ml H_2O and autoclaved. 100 ml of sterile phosphate-buffer (0.17 M KH_2PO_4, 0.72 M K_2HPO_4) was added after autoclaving

SOB-medium (1 l) 20 g Trypton, 5 g yeast extract, 0.5 g NaCl, 0.184 g KCl were dissolved in 1 l H_2O, adjusted to pH 7.0 (NaOH) and autoclaved. Just before use, 5 ml of 2 M $MgCl_2$ and 20 ml of 1 M $MgSO_4$ were added.

For selection 50 μg/ml ampicillin was added to the media.

2.3 Cell culture

2.3.1 Cell lines

HT-1080 Human fibrosarcoma cell line established from the biopsy from a 35-year-old man (Rasheed et al., 1974) # DSM ACC 315 (DSMZ, Braunschweig, Germany).

HEK 293 Human primary embryonal kidney cell (Graham et al., 1977), #DSM ACC 305, (DSMZ, Braunschweig, Germany)

2.3.2 Supplements and Antibiotics

When not otherwise specified, listed products were provided by Gibco/Invitrogen, Carlsbad, USA.

Dulbecco's Modified Eagle's Medium (DMEM) high glucose
CO_2 Independent Medium (without L-glutamine)
PBS (Ca^2, Mg^{2+} free),
Foetal Bovine Serum (FCS)
Penicillin (10.000 U/ml) and Streptomycin (100 μg/ml) solution
Trypsin-EDTA solution
GlutaMAX-I Supplement, 200 mM
Puromycin (Sigma, St. Louis, USA)
Hygromycin (Sigma, St. Louis, USA)
DMSO (Sigma, St. Louis, USA)

2.3.3 Media

Growth medium	DMEM high glucose, 10% FCS, 100 U/ml penicillin, 100 µg/ml streptomycin
Selection medium I	DMEM high glucose, 10% FCS, 100 U/ml penicillin, 100 µg/ml streptomycin, 0.4 µg/ml puromycin
Selection medium II	DMEM high glucose, 10% FCS, 100 U/ml penicillin, 100 µg/ml streptomycin, 100 µg/ml hygromycin
Selection medium III	DMEM high glucose, 10% FCS, 100 U/ml penicillin, 100 µg/ml streptomycin, 0.4 μg/ml100 µg/ml hygromycin.
CO_2-independent medium	CO_2-independent medium, 20% FCS, 100 U/ml penicillin, 100 µg/ml streptomycin, 1% GlutaMAX-I

2.4 Buffers and Stock Solutions

6X Agarose loading buffer	15 % Ficoll type 400, 40 mM Tris-HCl (pH 8.5), 40 mM glacial acetic acid, 2 mM EDTA, 0.25 % bromphenol blue
2X HPEM buffer	60 mM Hepes, 130 mM Pipes, 20 mM EGTA, 4 mM $MgCl_2$
5X Laemmli buffer	156.25 mM Tris-HCl (pH 6.8), 25 % glycerine, 5 % SDS, 0.2 % bromphenol blue
20X NuPAGE MOPS SDS Running Buffer	Supplied by Invitrogen, Carlsbad, USA
10X PBS	1.4 M NaCl, 27 mM KCl, 100 mM $Na_2HPO_42H_2O$, 18 mM KH_2PO_4
50X TAE buffer	2 M Tris-HCl (pH 8.5), 2 M acetic acid, 0.1 M EDTA

TE buffer	10 mM Tris-HCl (pH 8.0), 0.1 mM EDTA
10X TGS buffer	2.5 M Tris, 1.92 M glycin, 0.1% SDS

2.5 Enzymes

Expand High Fidelity PCR system	Roche, Mannheim, Germany
DNase I free RNase	Roche, Basel, Switzerland
Quick Ligation Kit	NEB, Ipswich, USA
Restriction Enzyme	
1) Apa I, Mlu I	Amersham, Little Chalfont,USA
2) Bam H1, Mss I, Pst I	Fermentas, St Leon-Roth, Ger
3) Bsu 36I, Eco RI, Hind III, Not I, PspOM I, Spe I	NEB, Ipswich, USA
RNase A	Qiagen, Hilden, Ger

2.6 Chemicals

2´-Deoxycytidine hydrochloride	Sigma, St. Louis, USA
Ethidium bromide solution (1%) (EtBr)	Roth, Karlsruhe, Ger
Leptomycine B	Sigma
Mevinolin (Lovastatin)	Sigma
Nocodazole	Sigma
Propodium iodide	Sigma
Thymidine	Sigma
X-gal	Calbiochem, Darmstadt, Ger
Z-Leu-Leu-Leu-al (MG132)	Sigma
Taxol	Sigma

2.7 Topoisomerase toxins and inhibitors

Name	Stock / DMSO	Working dilution	Clinical use	Class	Source
Alternariol (AOH)	10mM	≤ 100 μM	No	TopoIIα poison	Fehr et al 2008
Amsacrine (m-AMSA)	20mM	≤ 200 μM	Yes	Intercalating Topo II poison	Sigma, USA
Camptothecin (CPT)	20mM	≤ 10 μM	Yes	TopoI poison	Sigma, USA
Dexrazoxane (ICRF-187)	50mM	≤ 100 μM	No	TopoII inhibitor	Zinecard Pharmacia & Upjohn, USA
Doxorubicin (DOX)	20mM	≤ 200 μM	Yes	Intercalating Topo II poison	Sigma, USA
Epicatechin	50 mM	≤ 200 μM	No	Bioflavonoids	Sigma, USA
Etoposide (VP16)	50mM	≤ 100 μM	Yes	TopoII poison	Bristol- Germany
Genistein	20mM	≤ 200 μM	No	TopoII poison	Sigma, USA
Lycobetaine (E701a)	10mM	≤ 100 μM	No	TopoIIβ poison	Dr. Doris Marko (Uni of Karlsruhe, Germany)
Mitoxantrone (MITOX)	20 mM	≤ 100 μM	Yes	TopoII poison	Sigma
Quercetin	100mM	≤ 100 μM	No	Topo poison	Sigma
Xk469	100mM	≤ 20 mM	No	Topo IIβ inhibitor	Sigma

Table 2.1 Topo toxins and inhibitors used in this dissertation

2.8 Antibodies

2.8.1 Primary antibodies

Antibody	Antigen	Origin	WB	Source
JL-8	GFP	mouse	1:4000	#632381, Clontech, Mountain View, USA
1DCS-180	Cdc6	mouse	1:200	#DM3050, Acris GmbH,Hiddenhausen Germany
180.2	Cdc6	mouse	1:1000	#sc-9964, Santa Cruz Biotechnology, INC Heidelberg, Germany
PC10	PCNA	mouse	1:200	#sc-56, Santa Cruz Biotechnology,
H-300	Cdt1	rabbit	1:200	# sc-28262, Santa Cruz Biotechnology,
H-231	Topo II α	rabbit	1:10000	#sc-13058, Santa Cruz Biotechnology,
AS 1586-1621	Topo II β	rabbit	1:10000	(Boege et al., 1995)
B-5-1-2	α-Tubulin	mouse	1:10000	#T6074, Sigma, St. Louis, USA

Table 2.2 Primary antibodies used in this dissertation

2.8.2 Secondary antibodies

Name	Origin	Dilution	Source
ECL Mouse IgG, HRP-Linked Whole Ab	sheep	1:40000	Amersham, Little Chalfont, England
ECL Rabbit IgG, HRP-Linked Whole Ab	donkey	1:10000	Amersham,
Cy3™ Conjugated goat anti mouse	goat	1:4000	Jackson Immune Research, Europe Ltd, UK

Table 2.3 Secondary antibodies used in this dissertation

2.9 Consumed items

Immobilon-P (PVDF) Transfer Membrane	Millipore, Bedford, USA
NuPAGE Novex 4-12% Bis-Tris Gel	Invitrogen, Carlsbad, USA
Gel cassette Novex, 1 mm	Invitrogen,
1 Kb plus DNA Ladder	Invitrogen,

Peq Gold Protein marker II	PeQlab, Erlangen, Germany
PeqGold Protein marker IV (prestain)	PeQlab,

2.10 Kits

TOPO TA Cloning Kit	Invitrogen
QIAquick Gel Extraction Kit	Qiagen, Hilden Germany
QIAGEN Plasmid Maxi Kit	Qiagen
DNeasy Mini Kit	Qiagen
Effectene Transfection Reagent	Qiagen,
BCA Protein Assay Reagent	Pierce, Rockford, USA
ECL Plus Western Blotting Reagents	Amersham, Little Chalfont, UK
ECL Direct Labeling and Detection System	Amersham

2.11 Instruments

Horizontal Gel Electrophoresis Apparatus Horizon 11.14	Whatman/ Biometra, Göttingen, Germany
Vertical polyacrilamid gel electrophoresis system Novex Mini-Cell Electrophoresis	Invitrogen, Carlsbad, USA
Semi-dry blot chamber multiphor II novablot	Amersham, Little Chalfont, UK
PCR Cycler Mastercycler	Eppendorf, Hamburg, Germany
Photometer Biophotometer	Eppendorf
PH meter Calimatic 766	Knick, Berlin, Germany
Ultrasound Homogeniser Sonopuls	Bandelin, Berlin, Germany
Flow cytometer FACSCalibur	BD Bioscience, Heidelberg, Germany
Incubator	Heraeus, Hanau Germany

Luminscent image analyzer LAS-4000	Fujifilm, Tokyo, Japan
Epifluorescent Inverse Microscope Axiovert 100	Carl Zeiss, Göttingen, Germany
Delta TC3 Culture Dish System	Bioptechs Inc., Butler, USA
Digital Camera Spot-RT SE Monochrom	Diagnostic Instruments, Sterling Heights, USA
Confocal Laser Scanning Microscope (LSM 510 Meta)	Carl Zeiss
Centrifuge Centrikon H-401	Kontron, Heraeus, Hanau, Germany
Centrifuge 5417R	Eppendorf
Centrifuge Rotixa / P	Hettich, Tuttlingen, Germany

3. Methods

3.1 Cloning

3.1.1 Construction of bicistronic vectors

The plasmids pMC-TopoIIα-YFP-P, pMC-TopoIIβ-YFP-P and pMC-YFP-TopoI-P, which contained the gene for the fluorescent chimera TopoIIα, Topo IIβ and TopoI, respectively, were described previously (Christensen et al., 2002a; Linka et al., 2007)

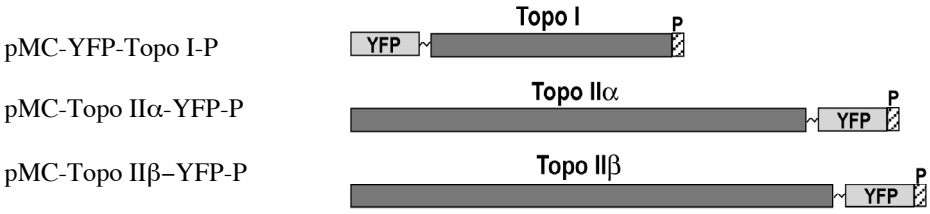

Fig. 3.1: **Schematic construction of the plasmids encode TopoI, IIα and IIβ with YFP** on a vector carrying puromycin resistance (diagonally striped box).

3.1.1.1 Generation of the fluorescent chimera of Cdc6

The full-length sequence of human Cdc6 (RefSeq BC025232) was fused C-terminally to YFP in the puromycin-containing vector or C-terminally to CFP in the hygromycin-containing vector. Thus, the first cistron of the transcribed messenger encoded Cdc6-YFP or Cdc6-CFP and the second cistron encoded puromycin or hygromycin resistance activity, respectively.

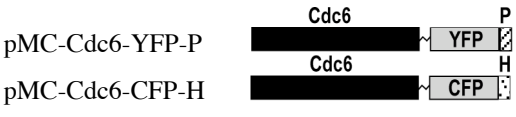

Fig. 3.2: **Human Cdc6 variant.** Schematic construction of the plasmids encode Cdc6 protein with YFP or CFP on Puromycin and Hygromycin vectors respectivly.

MluI-ApaI restriction sites were introduced to cDNA by mean of linker PCR with the primers as listed in Table 3.1. Cdc6 was then subcloned in pMC-CFP-H and pMC-YFP-P using *MluI-ApaI* restriction to produce pMC-Cdc6-CFP-H and pMC-Cdc6-YFP-P.

Construct	Primer	Sequence
pMC-Cdc6-YFP-P	1) 5`-MluI-Cdc6	5´-GGG CGG ACG CGT GCC ACC ATG CCT CAA ACC CGA TCC CAG GCA C-3´
	2) 3´-Cdc6-ApaI	5´-GGG CGG GCC CCC AGG CAA TCC AGT AGC TAA GAT ATT TCC-3´

Table 3.1 Primers with *MluI* and *ApaI* restriction sites for Cdc6

3.1.1.2 Generation of the fluorescent chimera of PCNA

The coding sequence of human PCNA (RefSeq NM_002592) was fused N-terminally to YFP in the puromycin-containing vector or N-terminally to CFP in the hygromycin-containing vector.

pMC-YFP-PCNA-P
pMC-CFP-PCNA-H

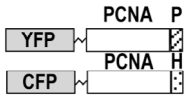

Fig. 3.3: **Human PCNA variant.** Schematic construction of human PCNA with YFP or CFP on puromycin and hygromycine vectors.

MluI-ApaI restriction sites were introduced to cDNA by mean of linker PCR with the primers as listed in Table 3.2. pMC-YFP-PCNA-P was then produced. pMC-CFP-PCNA-H was produced by subcloning of PCNA into pMC-CFP-HN by *MluI-ApaI* restriction.

Construct	Primer	Sequence
pMC-YFP-PCNA-P	1) 5`-MluI-PCNA	5´ACGCGTATGTTCGAGGCGCGCTG GT-3´
	2) 3´-ApaI-PCNA	5´GGGCCCCTAAGATCCTTCTTCAT CCTCGATCTT -3´

Table 3.2 Primers with *MluI* and *ApaI* restriction sites for PCNA

3.1.2 Construction of tricistronic vector

The need of coexpressing different types of Topoisomerases and Cdc6 or PCNA as differently colored protein chimera is the reason for the use of tricistronic vectors. Tricistronic vectors were generated by ligation of two bicistronic vectors, of which one carried the

puromycin resistance gene and the other one carried the hygromycin resistance gene after restriction with *ClaI-NotI*.

3.1.2.1 Generation of yellow colored Topo with blue colored Cdc6

pMC-YFP-TopoI-P, pMC-TopoIIα-YFP-P and pMC-TopoIIβ-YFP-P were digested by (*ClaI-NotI*), and were then ligated to *ClaI-NotI* digestion of pMC-Cdc6-CFP-H in order to produce the plasmids shown in Fig 3.4.

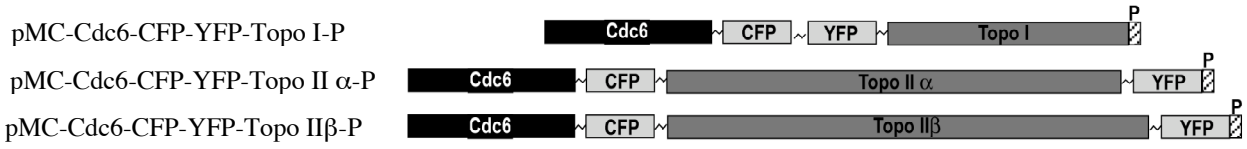

Fig 3.4: **Human Topo I, IIα, IIβ, variant with Cdc6**. Several variants of Topos (dark grey) taged to YFP (grey) together with Cdc6 (black) taged with CFP on puromycine resistant (striped) vector.

3.1.2.2 Generation of yellow colored Topo with blue colored PCNA

pMC-YFP-TopoI-P, pMC-TopoIIα-YFP-P and pMC-TopoIIβ-YFP-P were digested by (*ClaI-NotI*), and were then ligated *ClaI-NotI* digestion of pMC-CFP-PCNA-H in order to produe the plasmids shown in Fig. 3.5.

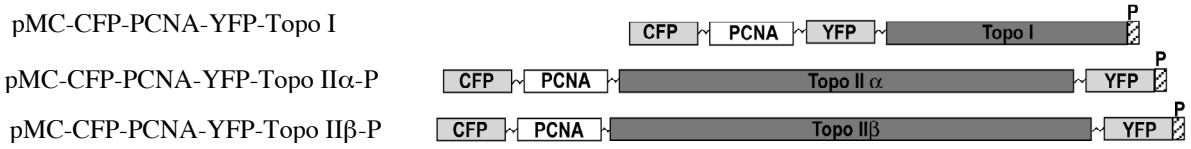

Fig. 3.4: **Human Topo I, IIα, IIβ variants with PCNA.** Several variants of Topos (dark grey) taged to YFP (grey) together with PCNA (white) taged to CFP (grey) on puromycine resistant (striped) vector.

3.1.3 Standard PCR

PCR was performed using the Expand high fidelity PCR Kit (Roche). To reduce a non-specific amplification and increase the target yield, Hot Start PCR was used under the following conditions:

Denaturation	2’ 96°C	
Addition of polymerase		
Denaturation	30” 94°C	25 cycles
Anealing	30” 55°C	
Elongation	1-3’ * 72°C	
Final elongation	12’ 72°C	

*: Depending on the length of the expected PCR product

3.1.4 Purification of PCR products

The PCR products were purified from primers and nucleotides before restriction digestion. Purification was performed using the Qiaquick PCR purification Kit according to the manufacturer’s protocol. The purified fragments were finally dissolved in 30 μl Tris buffer.

3.1.5 Gel electrophoresis and recovery of DNA from agarose gels

DNA fragments can be separated in an electric field according to their size by agarose gel electrophoresis. The used concentration of the agarose is dependent on the size of the DNA fragments. The agarose was melted by boiling in 1x TAE buffer. After cooling to 60°C, EtBr was added to a final concentration of 1 μg/ml. The solution was poured into a horizontal casting tray and was allowed to harden. For electrophoresis, the gel was placed in a gel chamber and was covered with 1x TAE buffer. The samples mixed with 6x DNA loading buffer were loaded together with DNA size marker onto the gel. Electrophoresis was run at 90-120 V. After the run, the separated DNA bands were visualized using a transilluminator at 280 nm.

3.1.6 Restriction digestion

3.1.6.1 Analytical restriction digestion

Analytical restriction digestion was used to check for the correct orientation and length of the inserted DNA fragment into the plasmid vector. 1-2 μg of plasmid DNA was digested

with 5 units of restriction enzyme. Buffer was used as recommended by the manufacturer. Digests were normally incubated for 1 hr at 37°C. The DNA fragments were analyzed by agarose gel electrophoresis.

3.1.6.2 Preparative restriction digestion

The preparative restriction digestion was used to isolate specific DNA fragments. 2-4 μg of plasmid DNA was digested with 5-10 units of restriction enzyme in the appropriate buffer for 1 hr at 37°C. DNA was separated by agarose gel electrophoresis. The DNA bands were cut from the gel with a disposable scalpel as precise as possible on a transilluminator at 280 nm and put into a reaction tube. DNA was extracted from the gel using a gel extraction kit according to the manufacturer's instruction.

3.1.6.3 Partial restriction digestion

4-5 μg of plasmid DNA was digested with 5-10 units of the single cutting enzyme at 37°C in a final volume of 100 μl. After 1 hr, 2, 0.57, 0.163, 0.046 units of the multi cutting enzyme were added and the final volume was adjusted to 35 μl. The digestion was carried out at 37°C for 15 min, after which time the samples were subjected to agarose gel electrophoresis.

3.1.7 Ligation

To insert restriction fragments into vectors, the Quick Ligation kit (NEB) was used according to manufacturer's protocol. Ligation was performed in a final volume of 10-20 µl for 10 min at RT and transferred to ice.

3.1.8 Transformation and isolation of plasmid DNA

3.1.8.1 Generation of competent *E. coli* cells

E. coli was grown in 1 L SOB medium at 18°C and harvested by centrifuging at 4000 x g and 4°C for 20 min, when the OD600 of the culture reached a value of 0.5-0.8. Cells were gently resuspended in 40 ml ice-cold TB buffer (10 mM Pipes, 55 mM $MnCl_2$, 15 mM $CaCl_2$, 250 mM KCl), incubated on ice for 20 min and again centrifuged at 4000 x g and 4°C for 20min. Cells were then gently resuspended in 20 ml ice-cold TB buffer and DMSO was added

with gentle swirling to a final concentration of 7%. After 10 min incubation on ice, cells were divided into 0.5 ml aliquots, frozen in liquid nitrogen and stored at - 80 °C.

3.1.8.2 Transformation of *E. coli*

An aliquot of 0.5 ml competent cells was mixed with 2 µl ligation reaction mixture, incubated on ice for 30 min, shocked at 42°C for 30 sec and immediately re- transferred to ice. 0.5 ml of pre-warmed LB-media was added to the cells and the mixture was incubated for 1 hr at 37°C with vigorous shaking at 250 rpm. Thereafter, transformed cells were transferred to LB-agar plates containing 50 µg/ml ampicillin.

3.1.8.3 Plasmid preparation at a small scale (Minipreps)

Several single colonies from a selective plate were picked and inoculated in 2.5 ml TB medium containing 50 µg/ml ampicillin and incubated overnight at 37°C with vigorous shaking at 250 rpm. After approximately 14 hrs of incubation, 2 ml of the culture were pelleted by centrifugation at 6800 x g and 4°C for 2 min. The cell pellet was mixed with 400 µl lysis solution (0.2 N NaOH, 1% SDS) and immediately neutralized with 300 µl of 7.5 M NH4OAc, kept on ice for 10 min, to precipitate genomic DNA and proteins, followed by centrifugation at 14000 x g and 4°C for 10 min. The DNA was precipitated from the supernatant in the presence of 500 µl 2-propanol and by centrifugation at 14000 g and 4°C for 30 min. DNA pellet was washed with 70% EtOH, dried and resuspended in 50 µl TE supplemented with 50 µg/ml RNaseA. The plasmids sequence was finally confirmed by restriction digestions and sequencing.

3.1.8.4 Plasmid preparation at a large scale (Maxipreps)

A single colony from a selective plate was picked and inoculated in a primary culture of 3 ml selective TB medium containing 50 µg/ml ampicillin and incubated for 8 hrs at 37°C with vigorous shaking at 250 rpm. Thereafter, the starter culture was diluted in 250 ml selective TB medium and grown overnight under the above-mentioned conditions. Bacterial cells were harvested by centrifugation at 6000 x g and 4°C for 15 min and the purification of plasmid DNA was performed using the QIAGEN Plasmid Maxi kit according to the manufacturer's protocol. DNA concentration was determined spectrophotometric at 260 nm.

3.1.8.5 Sequencing of plasmids

Sequencing of the constructs was performed by the BMFZ (Biologisch-Medizinisches Forschungszentrum) of the Heinrich-Heine-University Düsseldorf (Germany).

3.2 Cell culture

3.2.1 Maintenance of mammalian cells

HT-1080 and HEK-293 cells were maintained as subconfluent monolayer cultures in growth medium (see 2.3.3) at 37°C in a humidified atmosphere containing 5% CO_2. For passage, cells layers were washed once with PBS, detached by a short treatment with Trypsin-EDTA for HT-1080 cells or only EDTA for HEK-293 cells and reseeded upon dilution with culture medium (1:6).

3.2.2 Freezing and thawing of cells

After trypsinization, the cells were resuspended in DMEM and centrifuged at 300 xg for 3 mins. The cell pellet was resuspended in 1.5 ml FCS containing 10% DMSO and transferred to 1.8 ml cryo tubes, which were then transferred to isopropanol freezing boxes. After incubation for 24 hr at -80°C, the tubes were then transferred to liquid nitrogen.

For thawing procedure, cryo tubes were thawed in a 37°C water bath. Cells were immediately transferred in a Falcon tube with 5 ml pre-warmed (37°C) culture medium and centrifuged at 300 xg for 3 mins.

3.2.3 Transfection and selection of HT-1080 cells

Confluent cells (80%) were harvested from a 25 cm^2 flask and diluted (1:8) 24 hrs before transfection. Cells were transfected with 1 µg DNA using “Effectene transfection reagent” (Qiagen) according to the manufacturer's instructions. For cotransfection studies, however, 2 μg DNA was used. The efficacy of transient expression could be estimated under the microscope after 12-24 hrs of culture and varied between 20-90 % depending on the construct used. 24 hrs after transfection, media contained Effectene reagent were replaced by fresh media and incubated overnight. Thereafter, the cells were harvested and appropriately plated onto tissue culture dishes and stable cell clones were selected with selection medium (see 2.3.3). Stably expressing clones were expanded and maintained in selection medium.

3.2.4 Cell cycle analysis

Confluent cells (50%-60%) from a 25 cm^2 culture flask were harvested and washed once in PBS. The cells were fixed with 2 ml cold 70% ethanol (-20°C) and kept on ice for at least 30 min [the cells can be stored at this step at –20°C]. The cells were then washed once in PBS and counted. An aliquot of 1x106 cells was incubated in PBS containing 100 µg/ml RnaseA for 30 min at 37°C, washed again and resuspended in 500 µl PBS containing 50 µg/ml propidiumiodid. Samples were kept on ice for 10 min in the dark and then analyzed by FACS.

3.2.5 Cell Synchronization

3.2.5.1 Synchronization of cells by double thymidine block

Thymidine inhibits DNA synthesis in S phase of cells by depleting nucleotide precursor pools of dCTP, which cause an arrest of cells in early S phase. A cell density of 50-60% of exponentially growing cells was shown to permit active growth through the time course of the synchronisation procedure. The first thymidine block was imposed by removing the growth media and providing a serum-free fresh medium containing 2 mM thymidine for 12-16 hrs. Cells were washed twice with serum-free medium prior to replacement with normal growth medium containing 24 μM deoxycytidine for 9 hrs, following the 9 hrs release period, a second thymidine block was induced by adding media containing 2 mM thymidine and incubation of cells for 12-16 hrs.

3.2.5.2 Synchronization of cells by Mevinolin

Mevinolin is a fungal metabolite isolated from the fungus *Aspergillus sp*., which is a potent anti-hypercholesterolemic agent and a competitive inhibitor of 3-hydroxy-3-methylglutaryl coenzyme A (HMG-CoA), inhibiting cell proliferation due to cell cycle arrest. Mevinolin at concentrations of 10 μM and 50 μM causes cell arrest at G2 and the G1, respectively. In this work, incubation of cells with 50μM mevinolin for 24h was performed to cause G1 arrest in cells.

3.2.5.3 Synchronization of cells by serum starvation

Serum starvation represents an easy method to arrest cells in G0/G1 phase, with out an interference of chemical substances. Confluent cells (50-60%) were washed twice with PBS. Serum-free medium was added for 72h.

3.2.5.4 Synchronization of cells by Nocodazole

Nocodazole is an anti-neoplastic agent, which exerts its effect in cells by interfering with the polymerization of microtubules. Nocodazole-treated cells enter mitosis but cannot form metaphase spindles because microtubules (of which the spindles are made) fail to polymerize. The absence of microtubule attachment to kinetochores activates the spindle assembly checkpoint, causing the cells to arrest in prometaphase. Treatment of cells with 40 ng/ml nocodazole for 12 hrs was sufficient to cause cell arrest in metaphase.

3.3 Microscopy

3.3.1 Fluorescence microscopy

Epifluorescent images were acquired using an inverted microscope equipped with a cooled charge coupled device camera. For observation of living cells, they were grown and inspected in CO_2-independent medium (see 2.3.3) using live-cell chambers to keep the cells incubated at 37 ˚C.

3.3.2 Confocal microscopy

Confocal imaging of living cells was performed at 37 °C on a Zeiss LSM 510 inverted confocal laser scanning microscope equipped with a Zeiss incubator XL and a 40x/1.4 NA oil-immersion objective. Cells were grown in CO_2-independent medium and kept at 37 ˚C during microscopy.

3.3.3 Photobleaching

For fluorescence recovery after photobleaching (FRAP) experiments, a single optical section was acquired with 8x zoom. Images were taken before and at 1 s time intervals after bleaching of a circular area at 20 mW nominal laser power with 15 iterations. The imaging

scans were acquired with a laser power attenuated to 0.1 – 1 % of the bleach intensity. For quantitative FRAP analysis, fluorescence intensities of the bleached region, the entire cell nucleus and background were measured at each time point. Data were corrected for extracellular background intensity and for the overall loss in total intensity as a result of the bleach pulse itself and the imaging scans. Unless stated otherwise, FRAP recovery curves were generated by calculating the relative intensity of the bleached area Irel as described (Phair et al., 2000): Irel = (I bleached spot x I entire cell nucleus at time 0)/(I bleached spot at time 0 x I entire cell nucleus)

3.3.4 Immunocytochemistry

3.3.4.1 Fixation of cells by formaldehyde

Cells were grown on microscopic coverslips, washed in PBS, fixed in 4 % formaldehyde in PBS for 15 min at 37°C, and permeabilized with 0.5 % Triton X-100 in PBS for 10 min at RT. All subsequent steps were carried out at ambient temperature. After washing with PBS, cells were first blocked for 1 hr in PBS containing 2 % BSA and 5 % goat serum and then incubated for 1 hr with the primary antibody. After washing, the bound primary antibody was counterstained by incubation for 1 hr with Cy3™-conjugated goat anti-mouse secondary antibody. Coverslips were then washed three times for 5 min in PBS, whereas the first washing cycle included 80 ng/ml of 4,6-diamidino-2-phenylindole (DAPI) to counterstain the genomic DNA. Slides were finally mounted in antifade solution (PBS containing 1.5% N-propyl-galate and 60% glycerol), and immediately inspected.
The above mentioned procedure was carried out in a humidified atmosphere.

3.3.4.2 Fixation of cells by methanol/ acetone

Cells were grown on microscopic glass coverslips, washed in PBS, fixed in 100% methanol for 6 min at –20°C, and permeabilized with 100% acetone for 3 min at –20°C. All subsequent steps were carried out at room temperature. After washing with PBS, cells were incubated for 1 hr with the primary antibody.

3.3.4.3 DRT Assay

This assay was performed as previously described (Agostinho et al., 2004), in which the specific trapping of covalent Topo -DNA adducts induced by Topo poisons is quantified by

immunofluorescence microscopy after comparison with untreated control. Cells growing on cover slips were briefly exposed to ICRF-187 50 μg/ml for 5 min before harvest. Control cells were treated with the drug solvent (DMSO) for identical periods of time and processed in parallel. Cells were rinsed in PBS and subsequently incubated with HPEM buffer containing 350 mM NaCl, 0.5% Triton X-100, 1 mM PMSF and a commercially available mixture of protease inhibitors (1 mM Pefa, 5 μM Aprotinin) on ice for 1.5-2 min with gentle agitation. Finally, the cells were fixed in 3.7% formaldehyde in HPEM and directly viewed under microscope. The method was applied on cell clones co-expressing Topo-YFP and CFP-PCNA.

3.4 Proteins analysis

3.4.1 Preparation of whole cells lysates

$3x10^6$ cultured cells were pelleted washed and resuspended in 100 µl PBS. Cell lysis was performed by addition of 100 µl of 2x lysis buffer (250 mM Tris-HCl, pH 6.8, 2% glycerol, 4% SDS, 20 mM DTT, 1.4 M urea, 20 mM EDTA, 2 mM PMSF, 5 mM pefa block, 0.04% bromphenol blue) and homogenized by ultrasound for 15 s at 20% of power. Samples were boiled at 98°C for 5 min. Aliquots equivalent to 3 x 10^5 cells were then loaded onto SDS-polyacrylamide gels.

3.4.2 Chromatine fractionation

2.5 x 10^7 cells were harvested, and two aliquots (3,5 x 10^6 cells) were saved for later Western and FACS-analyses. The remainder was spun down and resuspended (4 x 10^7 cells/ml) in ice-cold buffer A (10 mM Hepes pH 7.9, 10 mM KCl, 1.5 mM $MgCl_2$, 0.34 M sucrose, 10% glycerol, 1 mM DTT, 5 mg/ml aprotinin, 5 mg/ml leupeptin, 0.5 mg/ml pepstatin, 0.1 mM PMSF). All subsequent steps were carried out at 4°C. 0.1% Triton X-100 was added, and the cells were incubated for 5 min. Nuclei were collected by low-speed centrifugation (4 min, 1,300 x g) to yield pellet P1 and the supernatant S1. Nuclei were washed once in buffer A, and then lysed in buffer B (3 mM EDTA, 0.2 mM EGTA, 1 mM DTT, protease inhibitors). Insoluble chromatin was separated from the supernatant S3 by centrifugation (4 min, 1,700 x g), washed once in buffer B, and centrifuged again to yield the final chromatin pellet P3. The final pellet was resuspended in Western lysis buffer, and

subjected to Western blotting together with equivalent amounts of supernatants S1 and S3, and untreated cells.

3.4.3 Polyacrylamide gel electrophoresis

3.4.3.1 Gel run

Electrophoresis was performed in 1X TGS buffer or in 1X MOPS SDS running buffer as in the case of NuPAGE gels at 50-150 V.

3.4.3.2 Western blotting

After separation, proteins were electrophoretically transferred from the gel to a PVDF membrane by the semi-dry method. Briefly, five 3MM paper filters soaked in K-buffer (70 mM CAPS-NaOH pH 10.5, 10% MeOH) were stacked on the cathode side of the gel, while the PVDF membrane soaked in MeOH, one 3 MM paper filter soaked in A2-buffer (25 mM Tris-HCl pH 10.4, 20% MeOH), and two paper filters soaked in A1-buffer (300 mM Tris-HCl pH 10.4, 20 % MeOH) were stacked on the anode side of the gel. Subsequently, the stack was placed between two graphite plates and the protein transfer was carried out at 0.8 mA/cm2 for 1-4 hrs depending on the size of the protein of interest. After transfer, the PVDF membrane was soaked in PBS containing 0.05% Tween 20 and 5% milk powder and incubated overnight at 4°C. After blocking, the membrane was briefly washed with PBS containing, 0.05% Tween 20 and incubated for 1 hr with the primary antibody diluted in PBS containing, 0.05% Tween 20 and 1% BSA and washed four times (1 x 5 min, 3 x 10 min). The membrane was then incubated for 1 hr with the secondary peroxidase conjugated antibody diluted in PBS containing, 0.05% Tween 20 and 1% BSA. The membrane was again washed and the protein bands were visualized by chemiluminescence using the ECL Plus system (Amersham).

3.4.4 Catalytic activity of topoisomerase

3.4.4.1 Relaxation assay of topoisomerase

DNA relax-cleavage reactions were carried out by modifying the procedure described by (Boege et al., 1996).

Reaction mixtures contained 10 ng human Topo I, 50 ng Topo IIα or Topo II β, and 400 ng negatively supercoiled pUC18 DNA in a total volume of 40 μl of relaxation buffer. The buffer was composed of 100 mM KCl, 10 mM Tris-HCl, pH 8, 1 mM ATP 10 mM $MgCl_2$, 0.5 mM DTT, 0.5 mM EDTA, 30 μg/ml BSA for Topo IIα, Topo IIβ, 80 mM KCl, 70 mM NaCl, 10 mM Tris-HCl, pH 7.6, 10 mM $MgCl_2$, 0.5 mM DTT, 0.5 mM EDTA, 30 μg/ml BSA for Topo I. Samples were incubated at 37 °C for 30 min. DNA relaxation was stopped by the addition of 5 μl of 5% SDS and the samples were exposed to 5 μl of 1 mg/ml proteinase K for 1 hr at 50°C. The samples were then mixed with 10 μl of agarose gel loading buffer for gel electrophoresis.

All gels were stained with 1 μg/ml EtBr, and DNA bands were visualized with ultraviolet light. The relaxations were performed in presence of different concentrations of Topo toxins as listed in Table 2.1.

3.4.4.2 Cleavage assay

Reaction mixtures contained 100 ng Topo IIα or 200 ng Topo IIβ, and 400 ng negatively supercoiled pUC18 plasmid in a total volume of 40 μl of cleavage buffer containing 10 mM Tris-HCl (pH 7.9), 10 mM $MgCl_2$, 100 mM KCl and 0.1 mM EDTA. Assays were carried out in the presence of 0-100 μM etoposide, ICRF-187, Xk469, alternariol, or at concentration of 0-200 μM for genistein, lycobetaine, amsacrine, doxorubicin and quercetine. 0-20 μM camptothecin for TopoI. Topo I DNA cleavage assays contained 160 ng human Topo I and 400 ng negatively supercoiled pUC18 DNA in a total of 40 μl of buffer containing 10 mM Tris-HCl (pH 7.5), 10 mM $MgCl_2$, 70mM KCl, 80 mM NaCl, 0.5 mM EDTA, 0.5 mM DTT and 30 μg/ml BSA. Mixtures were incubated at 37 °C for 30 min and enzyme-DNA cleavage complexes were trapped by the addition of 5 μl 5% SDS. Proteinase K (5 μl of 1 mg/ml) was added and samples were incubated at 50 °C for 1 hr. The samples were mixed with 10 μl of agarose gel loading buffer and subjected to electrophoresis in 0.8-1% agarose gels containing 0.5 μg/ml EtBr. DNA bands were visualized and cleavage was monitored by the conversion of supercoiled plasmid DNA to linear molecules.

4. Results

The primary aim of this work was to investigate the function of eukaryotic Topo I, IIα, and IIβ in cell culture systems and monitor their response to pharmacological, environmental and xenobiotic Topo inhibitors in the living cell. For this purpose, it is essential to distinguish between different cell cycle phases, i.e. not only between mitosis and interphase, but also between sub-stages of interphase, because those also are accompanied by various topological problems that are to be solved by Topos. In order to specify cell cycle stages in a given cell, I used two markers. One was Proliferating Cell Nuclear Antigen (PCNA), a well-established S-phase marker allowing the discrimination of S-Phase from G1- or G2-phases. A similar marker allowing discrimination of G1- and G2-phase was not available. I decided to use the replication-initiating factor Cdc6 expected to be active in the nucleus in G1- but not G2-phase. Unexpectedly, I discovered that Cdc6 also inhibited novel features of activity in G2-phase and mitosis, which made it necessary first to clarify the cell cycle-dependent regulation of Cdc6. In the following (section 4.1), I will thus first introduce the basic properties of Cdc6 during DNA replication, and then describe my novel findings about Cdc6 regulation, which turned out to be more dynamic as thought before. After having established this set of cell cycle markers, I will then (section 4.2) describe my findings from the co-expression of fluorescent PCNA and Cdc6 with Topo I, IIα, and IIβ, which revealed fine-tuned differences between these Topos in sub-stages of interphase. Finally (section 4.3), I used the cell lines thus characterized to characterize and compare the efficiency of Topo-inhibitory drugs and natural compounds in a native environment i.e. in living cultured cells.

4.1 Human Cdc6 and PCNA as versatile markers for cell cycle stages

4.1.1 The replication initiation protein Cdc6

During the DNA replication process, eukaryotes duplicate their genomes with a remarkable fidelity, due in large part to strict regulatory mechanisms that occur primarily at the initiation stage. Once replication is initiated, DNA chains are elongated at a relatively constant rate until the entire genome is replicated (Masai et al., 1999). Eukaryotic genomes are large and organized into multiple chromosomes. To duplicate these large genomes

efficiently, eukaryotes have evolved a mechanism in which initiation of DNA replication takes place at multiple sites along the chromosomal DNA (Diffley, 2004). Several tightly regulated mechanisms during this replication initiation process are crucial to the maintenance of the genetic integrity. First, initiation must be carefully controlled so that each segment of DNA is replicated specifically at the appropriate time in the cell cycle. Second, re-replication must be prevented from occurring again at the same sites, because re-replication of a previously fired origin would lead to the duplication of a chromosome segment and thus to genome instability (Bell and Dutta, 2002). Prevention of further rounds of replication initiated after the beginning of S phase is achieved by the strict temporal separation of the "licensing" process in G1 phase, which primes origins of replication (oris) competent for replication, and the actual initiation of replication at the beginning of S phase.

Origin licensing takes place in a sequential manner by the formation of pre-replication complexes (PreRCs): The origin recognition complex (ORC) binds first to an ori, which then recruits the loading factors Cdt1 and Cdc6. Both proteins are required for the stable loading of the minichromosome maintenance complex (MCM), which provides the helicase activity required for DNA strand separation during S phase (Bell and Dutta, 2002) (Fig. 4.1.1).

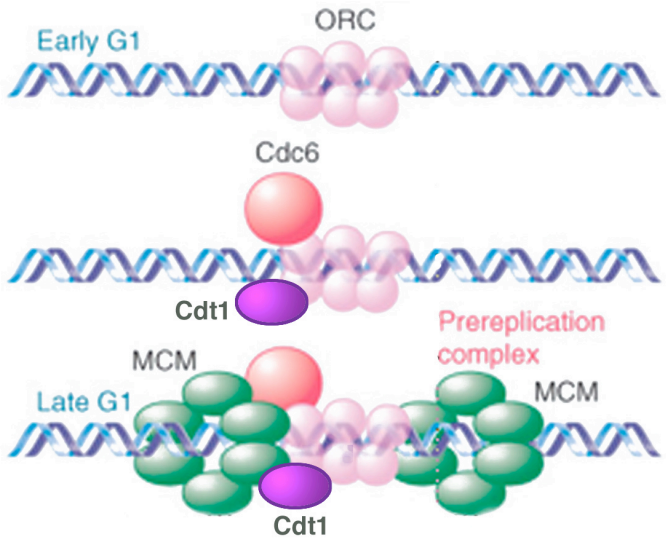

Fig. 4.1.1: **Assembly of pre-replication complex**. The replication process is first controlled by the origin recognition complex (ORC), which binds to the origin DNA and then recruits the loading factors Cdc6 and Cdt1. These cooperate to load MCM complex that unwinds the DNA.

Restriction of the licensing process to G1-phase is mainly achieved by the regulation of the two loading factors Cdt1 and Cdc6. While it is clear, that Cdt1 protein is stable only in G1-phase, regulation of Cdc6 is less well understood. In quiescent mammalian cells, an active anaphase promoting complex (APC) ubiquitin ligase provides for constant proteasomal

degradation of Cdc6. Degradation is prevented by Cdk2/cyclin-E-dependent phosphorylation when such cells re-enter the cell cycle (Mailand and Diffley, 2005).

In proliferating cells, Cdc6 is similarly phosphorylated by CDK2/cyclin A at the transition from G1- to S-phase, and it has been suggested that phosphorylated Cdc6 is readily degraded after initiation of replication (Mendez and Stillman, 2000; Petersen et al., 2000). However, in seemingly direct contradiction are results demonstrating that phosphorylation of Cdc6 translocates the protein to the cytoplasm at the beginning of S phase (Delmolino et al., 2001; Jiang et al., 1999; Petersen et al., 1999; Saha et al., 1998), and some authors suggested that Cdc6 might first be exported to the cytoplasm, and then degraded in an APC-dependent manner (Alexandrow and Hamlin, 2004; Lau et al., 2006). The picture becomes even more heterogeneous by reports demonstrating that a part of Cdc6 remains nuclear and chromatin-bound even in S-phase (Alexandrow and Hamlin, 2004; Coverley et al., 2000; Mendez and Stillman, 2000; Okuno et al., 2001). Current belief holds that one reason for these discrepancies might be that the investigations favoring the nuclear export model utilized transient heterogonous over-expression of tagged Cdc6, and that simply the excess of soluble Cdc6 is exported thereby masking the remaining nuclear pool of endogenous Cdc6 (Alexandrow and Hamlin, 2004; Arias and Walter, 2006; Borlado and Mendez, 2008; DePamphilis et al., 2006; Diffley, 2004).

4.1.2 The Polymerase anchorning factor PCNA

PCNA is a homotrimer protein that acts as a processivity factor for DNA polymerase δ in eukaryotic cells. It achieves this by encircling the DNA, thus creating a topological link to the genome. The protein encoded by this gene is found in the nucleus and is a cofactor of polymerase δ. The two DNA strands are synthesized by different mechanisms. The leading strand can be replicated continuously through the 5´-to-3´-polymerase activity of DNA polymerases (Leonhardt et al., 2000; Moldovan et al., 2007). The lagging strand, however, is replicated in a discontinuous fashion, each (Okazaki) fragment being smaller than the stretch unwound in the replication fork structure. Most DNA polymerases can synthesize a short string of nucleotides before falling off the DNA template. The tendency to dissociate quickly from DNA allows a DNA polymerase that has just finished an Okazaki fragment to be recycled quickly. This rapid dissociation would make it difficult for the polymerase to synthesize a long DNA strand produced at replication forks. This requires the presence of an accessory protein (PCNA) that functions as regulating clamp. PCNA keeps the polymerase firmly bound to the DNA when it is moving but releases it as soon as the polymerase runs into

a double-stranded region (Fig. 4.1.2). The three dimension structure of PCNA reveals that it forms a large ring around the DNA, preventing the dissociation of polymerase from DNA without affecting its speed (Moldovan et al., 2007). Since PCNA associates with replication sites in characteristic patterns (Celis and Celis, 1985), it can be used as a marker for S phase progression in living cells (Leonhardt et al., 2000).

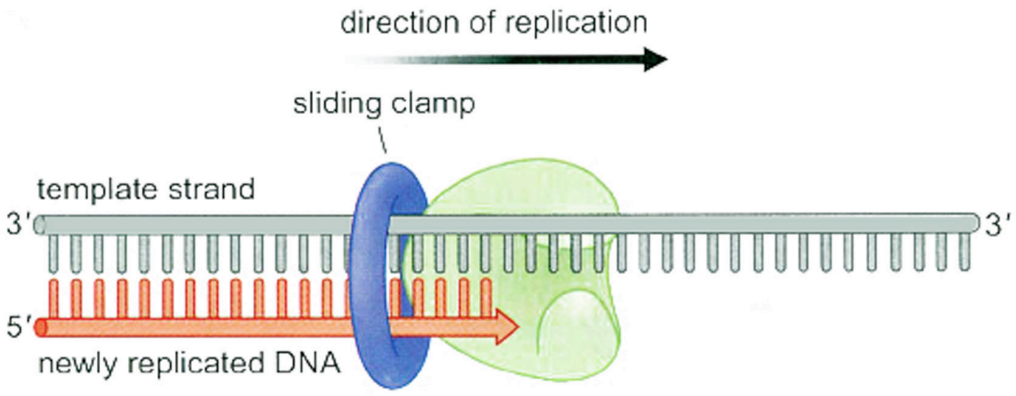

Fig. 4.1.2: **Role of PCNA at the replication fork**.

4.1.3 Production of stable cell lines expressing Cdc6 tagged YFP

To monitor Cdc6 in living and actively dividing cells, a plasmid (pMC-Cdc6-YFP-P) was constructed that enabled the co-expression of Cdc6 fused at its C-terminus to the fluorescent protein YFP and the selection marker puromycin from one bicistronic RNA. YFP was fused to the C-terminus of Cdc6, since previous experiences have suggested that YFP at this position would less likely disrupt the enzymatic function of the protein and phosphorylation of putative cyclin-dependent kinase sites in the N-terminal region of Cdc6 that are responsible for its localization (Petersen et al., 1999). Transfection of human HT-1080 cells and human embryonal kidney cells 293 (HEK-293) with this construct and subsequent puromycin selection resulted in clones, which showed morphology and growth rates similar to their parental cell lines. Six puromycin-resistant clones, termed C1-C6, were selected, and Western analysis revealed expression levels of Cdc6-YFP ranging between 1-fold (clones C1 and C3) to 10-fold (C6) excess over the endogenous Cdc6 level in untransfected HT-1080 cells (Fig. 4.1.3 A and B). In addition, to gain fluorescence-microscopic control over different sub-stages of S-phase, a plasmid (pMC-CFP-PCNA-H) was constructed that enabled the co-expression of PCNA fused at its N-terminus to CFP and the selection marker hygromycine respectively, from one bicistronic RNA. CFP was fused to

the N-terminal region of PCNA since this part is freely exposed at the outer surface of the trimeric PCNA ring wrapped around the DNA (Leonhardt et al., 2000).

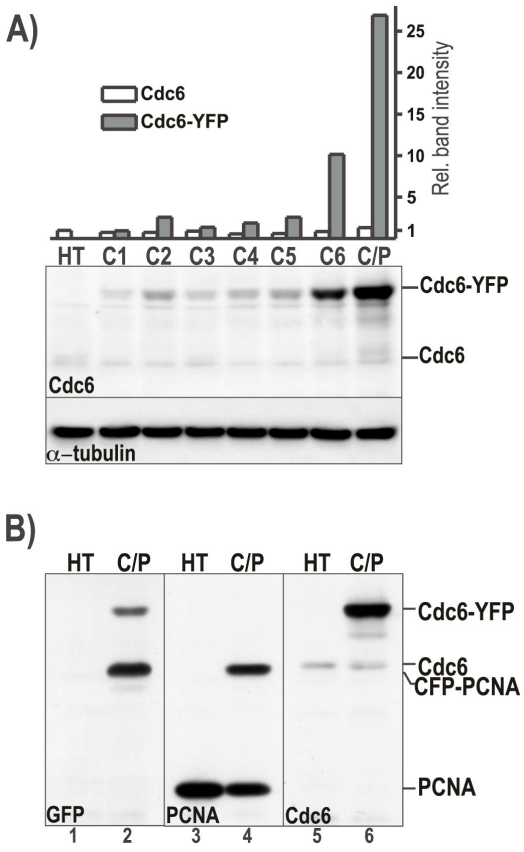

Fig. 4.1.3: **Expression of Cdc6-YFP.** (A) Whole cell lysates of untransfected HT-1080 cells (HT), cell clones expressing varying levels of Cdc6-YFP alone (C1-C6), and a cell clone co-expressing CFP-PCNA and Cdc6-YFP (C/P) were separated by SDS-PAGE and subjected to Western blotting using specific antibodies for human Cdc6 (top) or α-tubulin (bottom), the latter serving as control for equal loading. Positions of endogenous and YFP-fused Cdc6 is indicated on the right. The diagram on top shows relative band intensities of Cdc6 and Cdc6-YFP. All bars are normalized to the intensity of the Cdc6 band in untransfected HT-1080 cells, which was arbitrarily set to 1.0. (B) Further Western analysis of untransfected HT-1080 cells (HT) and the clone co-expressing CFP-PCNA and Cdc6-YFP (C/P) using anti-GFP, -PCNA, and -Cdc6 antibodies, respectively.

HT-1080 cells, and HEK-293 cells were co-transfected with pMC-Cdc6-YFP-P and pMC-CFP-PCNA-H and subsequently selected with 0.4 μg/ml puromycine and 100 μg/ml hygromycine. A clone was isolated termed C/P, which simultaneously expressed Cdc6-YFP and CFP-PCNA. Immunoblotting revealed that this clone expressed a 27-fold excess of Cdc6-YFP over the endogenous Cdc6 level in untransfected HT-1080 cells Furthermore, Cdc6-YFP and CFP-PCNA were expressed at similar levels in the clone C/P. However, the amount of heterologously expressed CFP-PCNA did not represent an over-expression compared to the endogenous PCNA level (compare lanes 3 and 4 in Fig. 4.1.3 B), because CFP-PCNA expression apparently resulted in a down-regulation of endogenous PCNA yielding an un-altered net level of the protein. On the other hand, the substantial over-expression of Cdc6-YFP in clone C/P had no impact on endogenous Cdc6 (compare lanes 5 and 6 in Fig. 4.1.3 B).

4.1.4 Normal cell cycle-dependent regulation of over-expressed Cdc6-YFP

Next, the concern was addressed that either the high quantity of Cdc6 or its fusion to YFP may perturb normal cellular regulation of Cdc6-YFP. Previous reports showed that human Cdc6 is targeted for ubiquitin-mediated proteolysis during G1, but its steady-state level increases during the following S- and G2/M-phases in synchronized cultured cells (Mendez and Stillman, 2000; Petersen et al., 2000). Here, a similar cell cycle-specific regulation of Cdc6 stability in the cell lines used in this study was observed. As shown in Figure 4.1.4 (left panel) untransfected HT-1080 cells enriched in M phase by nocodazole blockade contained a significant amount of Cdc6 (0 hr). After release from the drug, the cells entered G1 and proceeded to S phase in a time frame of one to six hours. This was accompanied by a decrease in Cdc6 expression after one to two hours and reappearance of the protein after six hours.

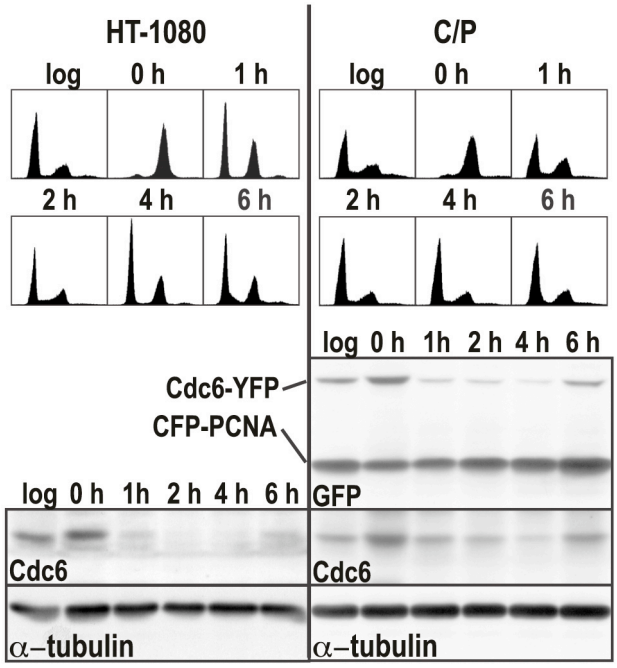

Fig. 4.1.4: **Regulation of Cdc6-YFP.** Cultures of untransfected HT-1080 and clone C/P were synchronized in metaphase by nocodazole block followed by reseeding in fresh medium. At the indicated time points after nocodazole withdrawel, samples were harvested for flow-cytometric determination of their cell cycle distribution *(top)*, and immunoblotting (bottom). log: Asynchronous, logarithmically growing cultures. The Western blots of both untransfected (left) and clone C/P (right) were probed with anti-Cdc6 and anti-α-tubulin antibodies. A blot of clone C/P was in addition probed with anti-GFP antibody, and bands

Virtually, a similar regulation of Cdc6 was observed in the clone C/P expressing the highest level of Cdc6-YFP of all clones (Fig. 4.1.4, right panel). Both endogenous and over-expressed, YFP-tagged Cdc6 was degraded and re-synthesized in the same time frame in transfected as native Cdc6 in untransfected HT-1080 cells. This indicates that cell cycle-

dependent regulation of hetrologously expressed Cdc6-YFP is unaffected by its fusion to the fluorophor or by its high abundance.

4.1.5 Degradation and nuclear export of Cdc6 are temporally separated

To visualize the consequences of the observed destruction and reappearance of Cdc6-YFP as cells proceed from mitosis to interphase, the protein was imaged in living cells over time. Figure 4.1.5 A shows an example of the clone C1, which expressed almost physiological levels of Cdc6-YFP. Noteworthy, all other clones displayed a similar regulation of this protein (data not shown). In metaphase, Cdc6-YFP was associated almost exclusively with condensed chromosomes. Association persisted from anaphase (15 min) to telophase (30 min), where the nuclear membrane reforms, and, consequently, Cdc6-YFP was nuclear during the following G1 phase (1 hr). After three hours, however, the fluorescent signal disappeared which was likely due to the expected proteasomal destruction during G1. About five hours after cell division, Cdc6 became detectable again and gradually increased in intensity in the following, but now Cdc6-YFP-specific signal was exclusively cytoplasmic.

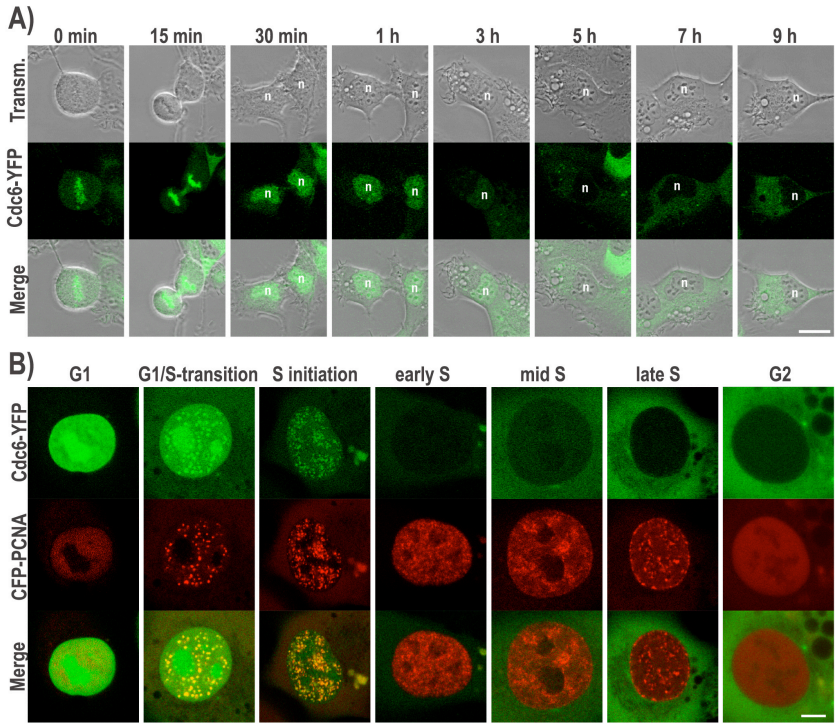

Fig. 4.1.5: **Distribution of Cdc6-YFP at distinct stages of interphase.** (**A**) Selected confocal images from a series of consecutive images taken every 15 min for 9 hours on a confocal microscope of a single cell of clone C1. The sub-optimal image quality is due to its low expression level of this clone and the need for short exposure times to reduce irradiation-mediated cell damage. n marks the position of the nucleus. Bar, 10 μm. (**B**) High resolution confocal images of different cells of clone C/P co-expressing Cdc6-YFP (pseudo-colored green) and CFP-PCNA (pseudo-colored red) at selected cell cycle phases. Bar, 5 μm.

These observations indicate that the reported proteasomal degradation of Cdc6 (Mendez and Stillman, 2000; Petersen et al., 2000) and its active export from the nucleus (Delmolino et al., 2001; Jiang et al., 1999; Petersen et al., 1999; Saha et al., 1998) do not exclude each other but are rather events separated in time during the cell cycle. I next determined in greater detail the cellular distribution of Cdc6-YFP with respect to the exact cell cycle phase spanning from G1- to G2-phase by use of clone C/P coexpressing Cdc6-YFP and CFP-PCNA, the latter serving as marker for the precise identification of S phase onset and progression. Single cells were imaged in numerous time frames at different cell cycle stages. A selection of representative high-resolution confocal images is shown in Figure 4.1.5 B. In G1-phase (first column), Cdc6-YFP was exclusively nuclear and enriched to some extent in the nucleoli, whereas fluorescence of CFP-PCNA was weak, also nuclear, but mostly excluded from nucleoli. The onset of S-phase was characterized by the expected accumulation of CFP-PCNA in so-called replication foci (Celis and Celis, 1985; Leonhardt et al., 2000). Surprisingly, Cdc6-YFP as well concentrated in each of these foci, indicating that Cdc6 has a high affinity to replicating chromatin, which arises after Cdc6 has exerted its actual function in replication licensing. This observation is in line with an investigation on *Xenopus* egg extracts, which reported that Cdc6 is reloaded onto replicating DNA as soon as replication forks were progressed a few hundred bases away from the replication origin (Oehlmann et al., 2004). However, association of Cdc6-YFP with replicating chromatin observed here did not persist. Cdc6 concentration decreased in the course of S-phase initiation (third column) until it was entirely lost from the cell in early stages of DNA replication where CFP-PCNA was distributed in numerous small foci (fourth column).

Figure 4.1.6 A demonstrates the exact time course and mechanism of Cdc6 destruction. Imaging of a single cell during S-phase initiation revealed that the first appearance of CFP-PCNA labeled replication foci directly accompanies the onset of Cdc6-YFP degradation. Quantification of fluorescence intensities corroborated the exact concurrence of with the increase of nuclear CFP-PCNA, which is a hallmark of the beginning of S phase. Direct evidence that Cdc6-YFP destruction was due to proteasomal degradation comes from an experiment where the specific proteasome inhibitor MG132 was added to the culture medium at a time point, where Cdc6 degradation has just started (bottom row). Cdc6-YFP degradation was prevented by this treatment, and Cdc6-YFP signal intensity rose again as a consequence of ongoing protein expression. Of interest, proteasome inhibition also prevented further progression into S-phase, because CFP-PCNA did not accumulate further in numerous nuclear replication foci as observed above in untreated cells. Although this could be a rather

unrelated side effect of MG132 treatment, it is tempting to speculate that Cdc6 destruction might be a prerequisite for a scheduled entry into S-phase.

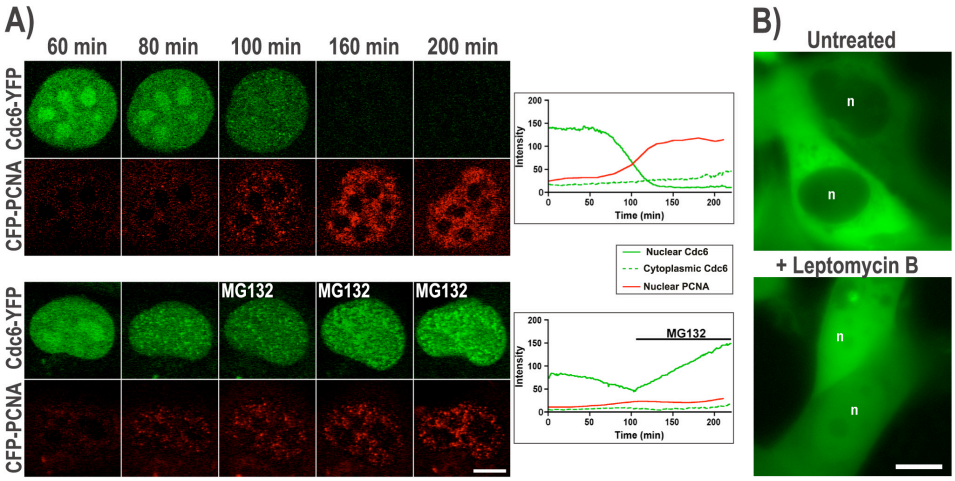

Fig. 4.1.6: **Degradation and nuclar export of Cdc6-YFP.** (A) Confocal images of single cells of clone C/P starting at G1 were taken every minute. The upper row shows a cell left untreated as it proceeds into S phase, whereas the cell shown in the lower row was exposed to the proteasome inhibitor MG132 (50 μM) at the onset of S phase. The right panel shows a plot of fluorescence intensities of nuclear and cytoplasmic Cdc6-YFP, and of nuclear CFP-PCNA as they change over the time period of image acquisition. Bar, 5 μm. (B) Epifluorescent images of cells in S/G2 phase of clone C1 either left untreated (top) or treated for 4h with 20 nM Leptomycin B. *n*, nucleus. Bar, 10 µm.

In the course of the subsequent S phase (Fig. 4.1.5, early to late S), the Cdc6-YFP protein level gradually increased again until it peaked at a maximum in G2-phase. This type of regulation of heterlogously expressed Cdc6-YFP matches that of endogenous protein levels shown previously in e.g. (Mendez, J et al., 2000). However, the protein was now mainly detected in the cytoplasm, and it has been suggested that cytoplasmic localization is due to an active nuclear export mediated by the nuclear transport receptor Crm1 (also referred to as Exportin1 or Xpo1) (Jiang et al., 1999). I confirmed this suggestion because, in our hands as well, exclusive cytosolic localization of Cdc6-YFP during late stages of the cell cycle could be reverted into a more nuclear localization by specific Crm1 inhibition by Leptomycin B (Fig. 4.1.6 B).

4.1.6 Relocalization of Cdc6 to the nucleus due to treatment of cells with hypotonic buffer

The nuclear export of Cdc6 during S/G2 phase demonstrated here in stable cell clones is in accordance with all other investigations that employed transient expression of tagged Cdc6

(Delmolino et al., 2001; Jiang et al., 1999; Petersen et al., 1999; Saha et al., 1998). However, most other approaches that studied endogenous Cdc6 demonstrated that substantial amounts remain nuclear throughout S phase (Alexandrow and Hamlin, 2004; Coverley et al., 2000; Jiang et al., 1999; Mendez and Stillman, 2000; Okuno et al., 2001). The latter reports employed biochemical fractionation procedures to show chromatin binding of endogenous Cdc6 throughout S phase, whereas the cytoplasmic localization of heterologously expressed tagged Cdc6 in S/G2 phase was detected by fluorescence microscopy. Thus, I wanted to analyze how stably expressed Cdc6-YFP behaves in a biochemical cell fractionation and chromatin extraction procedure. Cells of a low and a high expressing clone (C1 and C/P) were synchronized in early S phase by a double thymidine block, and then released from the block for 4 hours to yield a culture of predominantly S-phase cells. These cells were harvested and chromatin was extracted as described in (3.4.2). Figure 4.1.7 A demonstrates that, also in our hands, endogenous Cdc6 was significantly enriched in the fraction P3 representing proteins bound to nuclear chromatin.

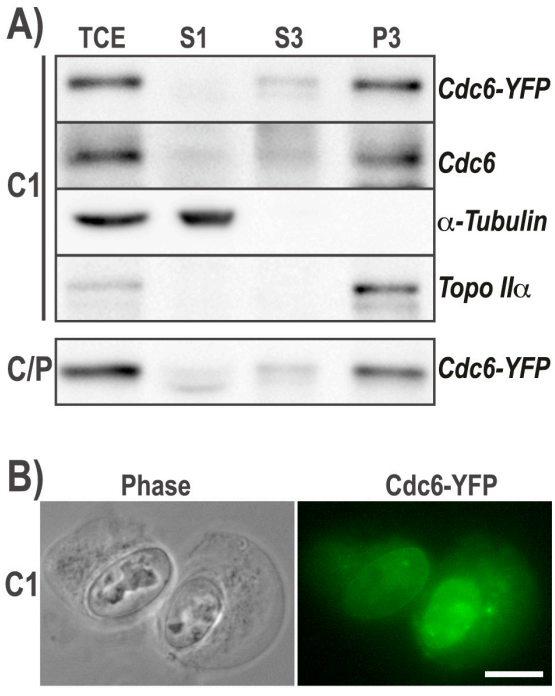

Fig. 4.1.7: **Cdc6-YFP resides in fractionated chromatin preparations of S-phase cells.** Clones C1 and C/P were synchronized in early S phase by a double thymidine block, and released from the block for 4 h. Efficient synchronization in S/G2 was confirmed by flow cytometry (not shown), and fluoresence-microscopic visual inspection revealed more than 95 % cells with cytoplasmic Cdc6-YFP. (**A**) Synchronized cell clones were subjected to the biochemical fractionation protocol for chromatin isolation. In a first step, cells were trypsin-harvested and suspended on ice in a hypotonic sucrose-containing buffer. They were then lysed by addition of a non-ionic detergent, and nuclei were separated from the cytosolic supernatant (*S1*) by centrifugation. Nuclei were then lysed in no-salt buffer and solubilized nuclear proteins (*S3*) were separated by centrifugation from the chromatin-enriched fraction (*P3*). Presence of Cdc6-YFP and endogenous Cdc6 in the total cell extract (*TCE*), cytoplasmic fraction (*S1*), soluble nuclear fraction (*S3*), or the chromatin-enriched fraction (*P3*) was determined by Western blotting. Probing against cytoplasmic α-tubulin and nuclear topoisomerase IIα confirmed the efficiency of the biochemical fractionation procedure. The lowest panel shows the result for overexpressed Cdc6-YFP from clone C/P (**B**) Aliquots of the first hypotonic suspension step described above were placed on glass slides and inspected by epifluorescence microscopy. Shown are representative phase-contrast and Cdc6-YFP-fluorescence images of clone C1. Note that upon hypotonic swelling almost all cells of both clones C1 and C/P displayed the same nuclear enrichment of Cdc6-YFP.

Importantly, Cdc6-YFP was detected to the same extent in the chromatin fraction although, in the living cells before treatment, it was mostly excluded from the nuclei. Even manifold over-expressed YFP-tagged Cdc6 of clone C/P was enriched in the nuclear fraction of S-phase cells. Fluorescence-microscopic observation of the fractionation procedure revealed the reason for this apparent re-localization of Cdc6-YFP to the nucleus. Already at the first step of the fractionation procedure hypotonic swelling of harvested cells on ice normally cytosolic S-phase Cdc6-YFP was found to be nuclear (Fig. 4.1.7 B). The fact that it remained chromatin bound during all subsequent extraction procedures (Fig. 4.1.7 A) further suggests that Cdc6 retains a strong chromatin affinity while localized in the cytosol of S-/G2 phase cells. These data indicate that the assumed difference between endogenous and exogenous Cdc6 was mainly due to different methods of detection, and they suggest that endogenous Cdc6 may undergo the same fate during extraction as Cdc6-YFP, and thus likely resides in the cytoplasm as well in unperturbed S-phase cells.

4.1.7 Crm1-controlled association of Cdc6-YFP with centrosomes and microtubuli

In the image of Cdc-YFP distribution in G2-phase (Figure 4.1.5 B, right most image), a point-shaped structure of high fluorescence intensity close to the nucleus stands out. Since I observed this in all cells having enriched the protein at the end of G2, it was obvious to assume that this could reflect an association with the centrosome. Immunohistochemical detection of a centrosomal marker, γ-tubulin, (Fig. 4.1.8 A) confirmed that a subpopulation of Cdc6-YFP indeed associated with the centrosome. Because an involvement of Cdc6-YFP in the process of cell division has been shown previously (Lau et al., 2006), I investigated the behavior of the protein in cells progressing from G2 through mitosis (Fig. 4.1.8 B). Confocal microscopy revealed that the prominent association of Cdc6-YFP persisted during prophase when the duplicated centrosomes separate and move to opposite sides of the nucleus (1:53 – 2:30 hr). It became also obvious that association of Cdc6-YFP was not restricted to the centrosomes but extended markedly to the microtubules extending from them. At prometaphase (2:30 hr), when the nuclear envelop breaks down, almost all cytoplasmic Cdc6-YFP immediately bound to the condensing chromosomes, but a clearly detectable fraction continued to stain centrosomes and microtubules until anaphase (2:57 hr), albeit to a much reduced extent. In telophase (3:02 hr), however, I was no longer able to detect centrosomal Cdc6-YFP, but the appearance of YFP-labeled fibrous structures adjacent to the forming

cleavage furrow of the daughter cells, which is typical for overlap microtubules, indicates that Cdc6-YFP remained associated with microtubules until cells were finally separated. Finally, in late telophase/G1, when the nuclear envelope has reformed, all Cdc6-YFP was nuclear, and no residual staining of centrosomes or microtubules was detectable anymore.

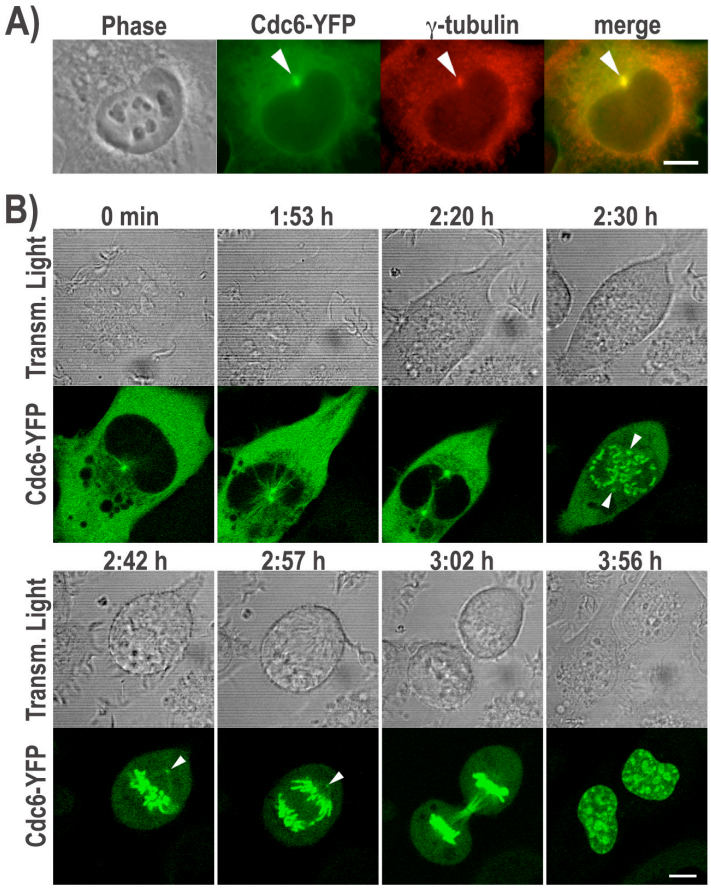

Fig. 4.1.8: **Distribution of Cdc6-YFP during late G2 and M phase.** (**A**) Cell clone C1 expressing low levels of Cdc6-YFP (green) was fixed and stained with antibodies recognizing the centrosomal marker γ-tubulin (red). Bar, 5 µm. (**B**) Clone C6 expressing high levels of Cdc6-YFP was cultured under a confocal microscope, and images of a single cell were taken either every minute or, during fast mitotic events, every 30 seconds. Selected images of the transmitted light and YFP fluorescence are shown. Acquisition of yellow fluorescence was intentionally overexposed to reveal the weak centrosome staining (arrowheads) from pro- to anaphase. Bar, 5 µm.

4.1.8 A model for Cdc6 regulation during the cell cyle

These experiments make a major contribution to an ongoing debate as to whether Cdc6 is degraded, exported to the cytoplam, or remains nuclear during S phase (Kim and Kipreos, 2008). With respect to a potential degradation, earlier work did not detect fluctuations of the Cdc6 expression level during the cell cycle (Jiang et al., 1999; Saha et al., 1998). Later on, it was demonstrated Cdc6 degradation in G1 in synchronized cells (Mendez and Stillman, 2000; Petersen et al., 2000). My results clearly support the latter hypothesis, and the time point of proteasomal destruction was specified precisely to the very beginning of DNA replication at the end of G1.

The probably biggest uncertainty concerned the question whether vertebrate Cdc6 during the S phase is exported from the nucleus or whether a substantial fraction remains nuclear. This debate obviously stems from different experimental systems for the detection of endogenous versus heterologously expressed, tagged Cdc6 (Arias and Walter, 2006; Borlado and Mendez, 2008; Kim and Kipreos, 2008). Here, I demonstrate that cytoplasmic YFP-tagged Cdc6 binds to chromatin preparations of S phase cells in the same way as endogenous Cdc6, and I provide evidence that the balance between actively to the cytoplasm exported Cdc6 and treating living cells with e.g. hypotonic buffers easily disturbs the nucleus. The fact that the protein stays stably bound to the chromatin during following extraction procedures further implies that cytoplasmic Cdc6 retains a high affinity for chromatin. This interpretation is supported by the observation that, later on in mitosis, Cdc6-YFP relocates immediately to chromosomes as soon as the barrier of the nuclear envelope breaks down. On the basis of these data, I would like to suggest that in unperturbed S phase cells Cdc6 (exogenous and endogenous) is virtually absent from the nucleus, although it binds to chromatin when given a chance (e.g. by inhibition of nuclear export or disruption of the nuclear envelope) due to an unaltered chromatin affinity of cytosolic Cdc6.

These findings raise the question why Cdc6 is kept in an active form out of the nucleus by an energy consuming mechanism instead of being depleted from the cell like its binding partner Cdt1. It is possible that Cdc6 serves function(s) between S- and M phase unrelated to origin licensing. One suggestion arises from our observation that the protein localizes to centrosomes and microtubules originating from them. It appears that this localization is linked to a functional role of cytoplasmic Cdc6 in the organization of the mitotic spindle, since RNAi-mediated depletion of Cdc6 resulted in abnormal spindle formation and chromosomal misalignment (Lau et al., 2006). Another putative reason for the continued presence of functional Cdc6 in the cytosol of S- and G2 phase cells could be its involvement in DNA surveillance. Increasing evidence suggests that Cdc6 is involved in the surveillance of the replication process during S phase via the checkpoint kinase Chk1 (Clay-Farrace et al., 2003; Oehlmann et al., 2004), and it was also shown, that Cdc6 is degraded in response to induced DNA damage during all cell cycle phases (Hall et al., 2007). If Cdc6 plays a role in these processes it must either remain available in the cell nucleus during S phase albeit at steady state levels too low to be detectable in this study, or relocate to the cell nucleus in response to signals induced by stalled replication forks or extrinsic DNA damage. Future work required to understand these aspects of Cdc6 regulation and their functional consequences clearly goes beyond the scope of this study.

In synopsis with the current knowledge about replication licensing and Cdc6 regulation (Arias and Walter, 2006; Borlado and Mendez, 2008; Kim and Kipreos, 2008), I suggest the following model for the chronology of regulatory events affecting Cdc6 (Fig. 4.1.9):

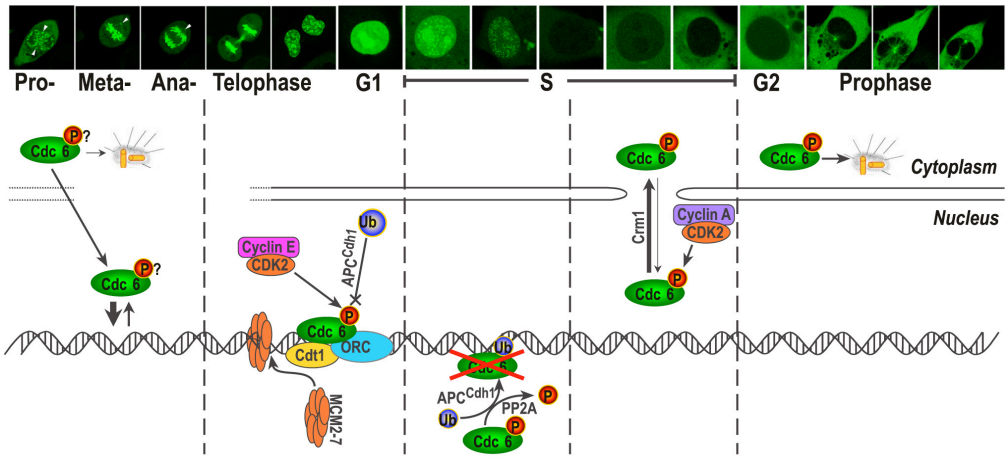

Fig. 4.1.9. **Summary of the temporal order of regulatory events affecting Cdc6 localization and stability.** The upper row is a compilation of the subcellular Cdc6 localization during the cell cycle as presented in Figures 4.1.5 and 4.1.8. Below is a sketch of the proposed regulatory mechanisms taking place in the respective cell cycle phase. The model is discussed in detail in text.

Upon breakdown of the nuclear envelope in prophase, Cdc6 gains access to condensing chromosomes. Given the high chromatin affinity of Cdc6, a dynamic binding equilibrium establishes itself throughout mitosis, where most of the protein is chromosome bound while a minor fraction binds to the centromers and microtubuli. The phosphorylation status of Cdc6 during this period is currently not clear. In the subsequent G1 phase, however, Cdc6 is phosphorylated by Cyclin E/CDK2, which protects it from ubiquitinylation by APC^{Cdh1} and subsequent degradation (Duursma and Agami, 2005; Mailand and Diffley, 2005). Cdc6 thus stabilized remains in the cell nucleus from telophase to the beginning of S phase. During this time it participates in loading the MCM2-7 helicase complex onto origins of replication with the major licensing activity taking place at telophase and in early G1. Upon initiation of replication in early S phase, Cdc6 co-localizes with early, PCNA-labeled sites of replication, and is concurrently degraded by the proteasome. Loss of protection from the APC^{Cdh1} (or other ubiquitin ligases) could involve dephosphorylation of Cdc6 – an activity that could be provided by the Protein Phosphatase 2A (PP2A), because it has recently been shown that PP2A is targeted to Cdc6 and that this is critical for proper progression from G1- to S phase. As cells proceed through S phase, Cyclin A/CDK2-dependet phosphorylation of newly synthesized Cdc6 now results in its translocation to the cytoplasm by the export receptor

Crm1 (Delmolino et al., 2001; Jiang et al., 1999; Petersen et al., 1999; Saha et al., 1998) thus contributing to the prevention of multiple rounds of replication. Finally, exported Cdc6 binds to the spindle apparatus in late G2 and throughout mitosis, where it carries out a second functional role in regulating microtubule dynamics and chromosomal alignment (Lau et al., 2006).

4.1.9 Dissecting the cell cycle using PCNA and Cdc6 as markers

The data described so far suggest that PCNA and Cdc6 are well suited for discrimination between cell cycle stages. To investigate their distribution in detail, cells co-expressing CFP-PCNA and Cdc6-YFP were first synchonized in early S phase by double thymidine and then imaged after medium exchange. Imaging of these cells revealed that PCNA accumulates at replication foci and Cdc6-YFP was at this time cytoplasmic, after that a complete image about the localization of both protein in different cell cycle stages was provided by continouse imaging of the same cell every 1 hr. I can clearly show in Figure 4.1.10, that Cdc6 is nuclear during G1, and is re-synthesized and exported to the cytoplasm during the following S phase until its concentration peaks in G2 while PCNA accumulates at the replication spots differentiating between early S Med S and late S phase cells. In early S, PCNA appears as hundred of small foci distributed throughout the nucleoplasm. During Mid S phase, foci are concentrated around the nucleoli and in the nuclear periphery. In late S phase replication foci decrease in number but increase in size.

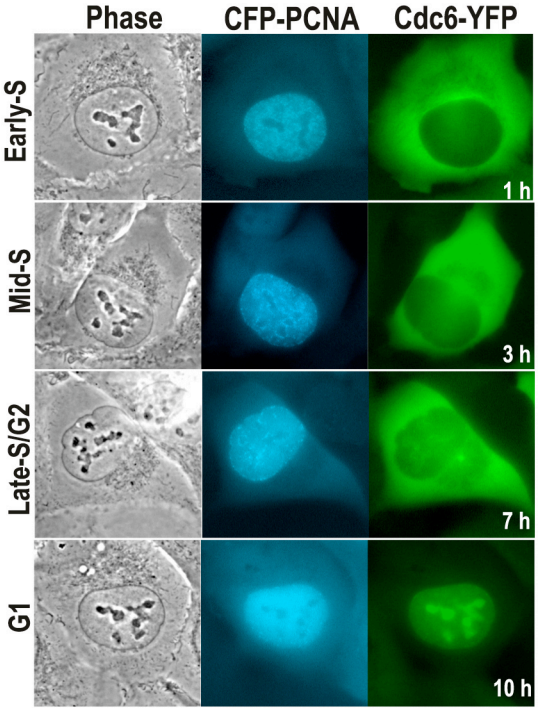

Fig. 4.1.10: **Distribution of Cdc6-YFP and CFP-PCNA during cell cycle.** Cell clone C/P was synchronized in early S phase by a double thymidine block, and released from the block at time point 0. Selected confocal images of CFP-PCNA (cyan) and Cdc6-YFP (green) from a series of consecutive images taken every hour for a period of 12 hours (1, 3, 7, and 10 h) are

As demonstrated in Fig. 4.1.5 B, PCNA is relatively uniformely distributed in the cell nucleus during most of the cell cycle, whereas at the beginning of S-phase it appears as hundreds of small foci distributed throughout the nucleoplasm. Later on, at mid S phase, these foci become concentrated around the nucleoli and in the nuclear periphery, whereas in late S phase replication foci decrease in number but increase in size. These characteristic patterns of PCNA allow to clearly identify S-phase, and, moreover, to discriminate early late, middle and late stages of S-phase. However, PCNA is a relatively indiscriminate marker for G1 and G2 phases. These are only distinguished by relative differences in the nuclear expression niveau and nucleolar accumulation (which are both lower in G1-phase). This short-coming can be ideally complemented by using Cdc6 as second biomarker, which allows to clearly discriminate G1 and G2 phases, where it is localized either inside or outside of the cell nucleus, respectively. The mutual contribution of the two markers to the identification of the precise position in cell cycle is best demonstrated in the synoptic overview presented in Fig. 4.1.10. Moreover, by virtue of its association with centrosomes and microtubules in prophase and its sudden association with the chrosomes upon breakdown of the nuclear envelope (Figs. 4.1.8 and 4.1.9), Cdc6 is also an ideal marker for a fine dissection of the G2/M-boundary as well as the various stages of the mitotic cycle.

4.2 *In vivo* - Disposition of topoisomerases I and II during interphase

To date, it is not completely clear how multiple functions are assigned to multiple types of Topos. It is also unknown how the two genetically distinct mammalian isoforms of type II Topo (Topo IIα and β) (Jenkins et al., 1992; Pommier, 2006) are assigned to their apparent unique cellular functions, although it is clear that the non-conserved C-terminal domain plays a crucial role in this (Linka et al., 2007). Current believe holds, that functional assignment of the various types and isoforms of Topos is acchieved in the living cell by directed accumulation at specific chromatin sites. For example Topo IIα, but not β, accumulates at sites of DNA replication in chicken cells (Niimi et al., 2001). However, the precise distribution of Topos during cell cycle, in particular, their association with the replication process are still a controversial subject. This is most likely due to the inherent variability of immunohistochemical methods, where distribution of proteins within a cell is influenced by factors like fixation methods and antibody preparation. Earlier studies carried out in our laboratory have significantly contributing to solve those problems, by expression of bio-fluorescent Topos and live cell imaging by confocal microscopy (Christensen et al., 2002a; Christensen et al., 2002b; Christensen et al., 2002c; Linka et al., 2007). The variation in cellular distribution of Topos during cell cycle stages G1, S and G2, however, were not addressed in those studies. Moreover, synchronization methods also can affect the normal distribution. In order to get a more general picture of this process and to monitor in a non-destructive manner the spatio-temporal behavior and disposition of human Topo I and Topo II isoforms during the cycle of a living cell, I expressed fluorescently labeled Topos together with the above cell cycle markers and monitored their relative disposition in living human cells.

4.2.1 Characterization of cells co-expressing YFP-fused topoisomerases I, IIα, IIβ with CFP-fused Cdc6 or PCNA

Tricistronic plasmids were constructed allowing co-expression of either Cdc6 or PCNA fused to CFP, in combination with either active Topo I or inactive Topo I^{Y723F}, or active Topo IIα and β. Based on previous experiences YFP was fused to the N-terminus of Topo I and to the C-terminus of Topo II, as the fusion at these positions did not disrupt enzymatic functions

(Christensen et al., 2002a; Christensen et al., 2002b; Christensen et al., 2002c; Linka et al., 2007; Mo et al., 2000). The third cistron of the tricistronic RNA carries the selection marker puromycin-N-acetyl transferase, (Fig. 4.2.1 A). Transfection of HT-1080 cells with these plasmids and subsequent puromycin selection gave in all cases rise to viable cell clones supporting stable co-expression of the YFP and CFP fused proteins, which showed morphology and growth rates similar to the parental cell lines. All selected clones were first screened using fluorescence microscopy, and only the clones, which showed the expected YFP and CFP fluorescence distribution, were selected for further investigation. In the following, representative clones co-expressing Topo I, Topo I^{Y723F}, Topo IIα and Topo IIβ with Cdc6 were termed CT1, $CT1^{Y723F}$, CT2a and CT2b, respectively. Clones co-expressing Topo I, Topo I^{Y723F}, Topo IIα and Topo IIβ with PCNA were termed PT1, $PT1^{Y723F}$, PT2a and PT2b, respectively. To assess the integrity of the fusion proteins and to compare their relative expression levels I subjected whole cell lysates to western blotting and probed the blots with YFP antibodies (recognizing both YFP and CFP). Bands of electrophoretic mobility corresponding to the expected protein size were detected (Fig. 4.2.1 B).

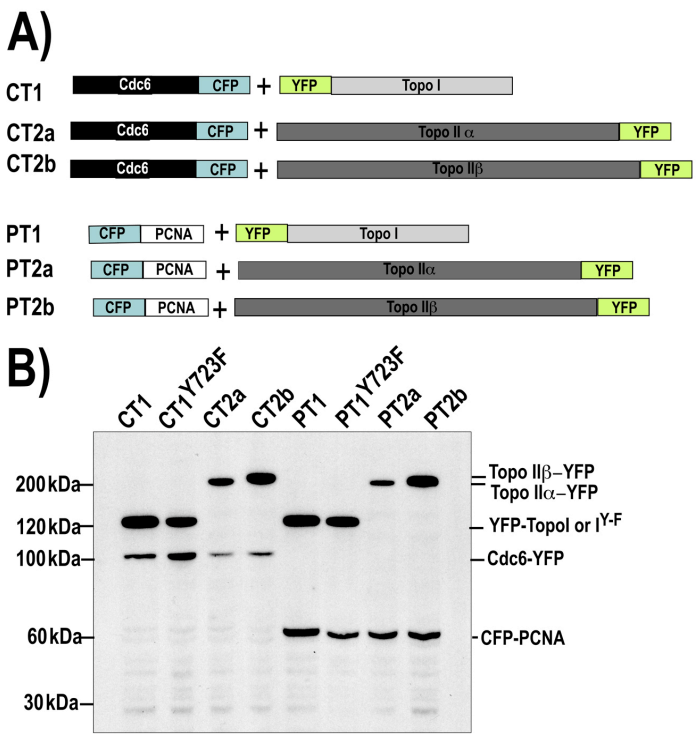

Fig. 4.2.1: **Co expression of topoisomerase enzymes with Cdc6 or PCNA in HT-1080.** (**A**) Schematic diagram of constructs: CT1, Cdc6-CFP + YFP-Top1; $CT1^{Y732F}$, Cdc6-CFP + YFP-Top1; CT2a, Cdc6-CFP + TopIIα-YFP; CT2b, Cdc6-CFP + TopIIβ-YFP; PT1, CFP-PCNA + YFP-Top1; $PT1^{Y732F}$, CFP-PCNA + YFP-Top1; PT2a, CFP-PCNA + TopIIα-YFP; PT2b, CFP-PCNA + TopIIβ-YFP. (**B**) Western blot analysis of whole cell lysates from CT1, $CT1^{Y-F}$, CT2a, CT2b, PT1, $PT1^{Y-F}$, PT2 and PT3 clones. Samples were subjected to SDS-PAGE (4-12% gradienet gel) and Westernblotting. GFP antibodies detected in all clones two bands that corresponded to protein chimeras of expected size.

In all clones, an additional band similar in size to YFP or CFP alone (~30 kDa) was observed, suggesting that the YFP/CFP fused proteins were subjected to a certain proteolytic turnover. Nevertheless, I could assume that most yellow fluorescence of the clones was due to full length Topos and most cyan fluorescence of the clones was due to the cell cycle marker.

Given the data summarized in 4.1., these cell clones appeared to be suitable models for a detailed inverstigation of the *in vivo* disposition of Topo I and II during the various stages of the cell cycle. The PT clones allowed for identification and detailed dissection of S phase stages, whereas discrimination between G1 and G2 phases was possible by comparing PT clones (exhibiting low nuclear PCNA concentration during G1-phase and a high ones during G2-phase) with CP clones (where cdc6 is nuclear in G1-phase and cytoplasmic G2- phase). The expression system allowed me to investigate the spatiotemporal disposition of Topos in the nuclear compartment and to some extent clarify the division of labor between the mammalian Topo II isoforms.

4.2.2 Nuclear distribution and mobility of topoisomerases during interphase stages

Several previous studies have investigated the gross distribution of Topos in the interphase nucleus of mammalian cells. A picture has emerged, suggesting that Topo I and II are exclusively located in the nucleus, where one portion is more or less randomly distributed in the nucleoplasm, whereas another portion is accumulated in the nucleoli (Christensen et al., 2002b; Christensen et al., 2002c). In none of these studies this pattern has been differentiated with respect to the various stages of interphase. Therefore, a host of questions has remained open. One such question regards the recruitment of Topo I and II to the replication fork (see: 1.4.2) or transcription complexes (see: 1.4.2). Another one arises from the nucleolar localization of the enzymes. At any given time, the nucleoli contain more Topos than can plausibly be required for the topological organization of the nucleolar chromatin, which is small in comparison to the entire genome. It is not clear why Topos accumulate in nucleoli to such an extent. It has been suggested (Christensen et al., 2002b; Christensen et al., 2002c) that nucleoli could serve as storage places for enzyme molecules that should not be active in the chromatin at a given time. Thus, dosage of Topos in the extra-nucleolar chromatin might be regulated by nucleolar accumulation and release. Given that gross nuclear distribution of Topos in PT and CT clones of HT-1080 cells were identical to previous published data, our model could be used to adress some of these questions. High resolution images of Topo I, IIα and IIβ assigned to various stages of the interphase cell cycle (Figs. 4.2.2 – 4.2.4) readily revealed a much more complex and dynamic distribution pattern than described previously. In the following sections, I will describe in detail the cell cycle-dependent dynamics of Topo I and Topo II in living HT-1080 cells that could be unraveled using my cell model.

4.2.2.1 Spatiotemporal distribution of topoisomerase I and II in G- and S phases

A dynamic redistribution of Topo I during the interphase cell cycle can be deduced from live cell images of the PT1 clone in G1-, S-, and G2 phase shown in (Fig. 4.2.2 A) and of the CT1 clone in G1- and G2 phases shown in (Fig. 4.2.2 B). In S phase, Topo I exhibited a mostly homogenous distrubution throughout the nucleus with a slightly spotted accentuation in the nucleoplasm (Fig. 4.2.4 A, row 2-3). I never observed such a spotted nucleoplasmic pattern of Topo I in G1- or G2 cells. A second difference between S- and G1/G2 phases became apparent when comparing nucleolar accumulation of Topo I, which was clearly detectable in G1/G2 phase but much less so in S phase. Moreover, in the nucleoli, Topo I exhibited a grainy and inhomogenous pattern in G1/G2 phase previously shown to indicate accumulation at fibrillar centers, the sites of ribosomal RNA synthesis (Christensen et al., 2004). Such focal nucleolar accumulations of Topo I were not detectable during any stage of S-phase.

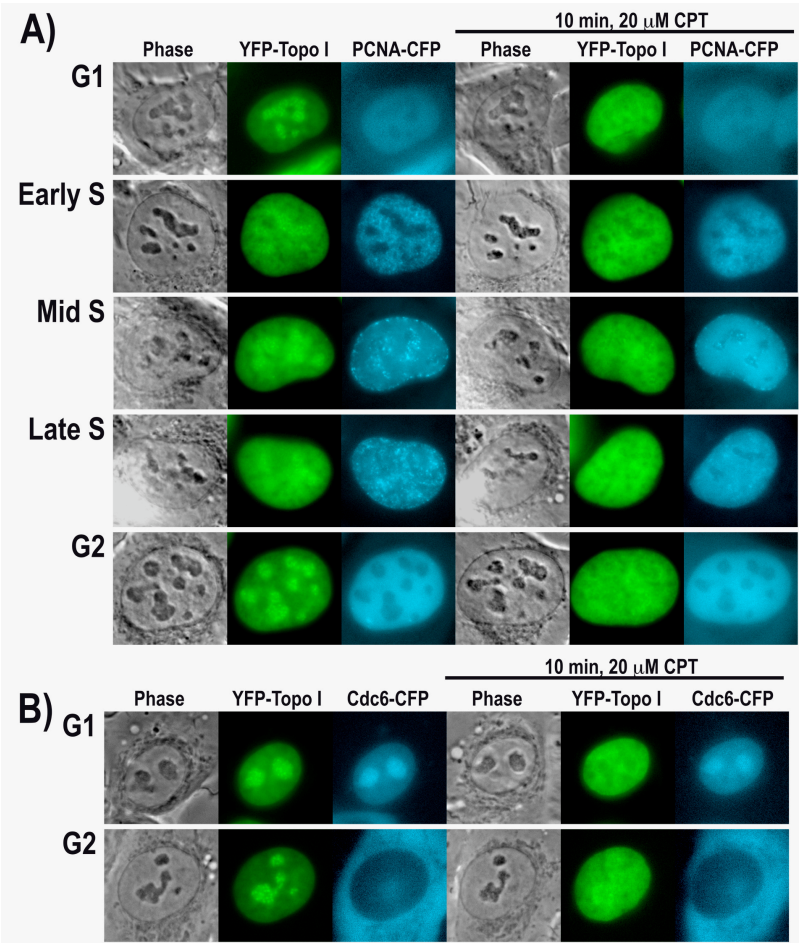

Fig.4.2.2: **Disposition of Topo I during different cell cycle stages.** Epifluorescent images of living cell clones PT1 (**A**) and CT1 (**B**). Representative images of the same cell are shown before (left) and after exposure to camptothecin (right, 20 μm CPT, 10 min). Each row shows cells at the indicated cell cycle stages, as determined by inspection of the marker proteins PCNA-CFP (**A**) or Cdc6-YFP (**B**) detected in all clones two bands that corresponded to protein chimeras of expected size.

A similar analysis carried out for Topo IIα and IIβ is summarized in Figs. 4.2.3 and 4.2.4. Interestingly, Topo IIα (Fig. 4.2.3 A, third row) behaved similar to Topo I: In S phase it concentrated in numerous nucleoplasmic spots, which became more pronounced towards mid

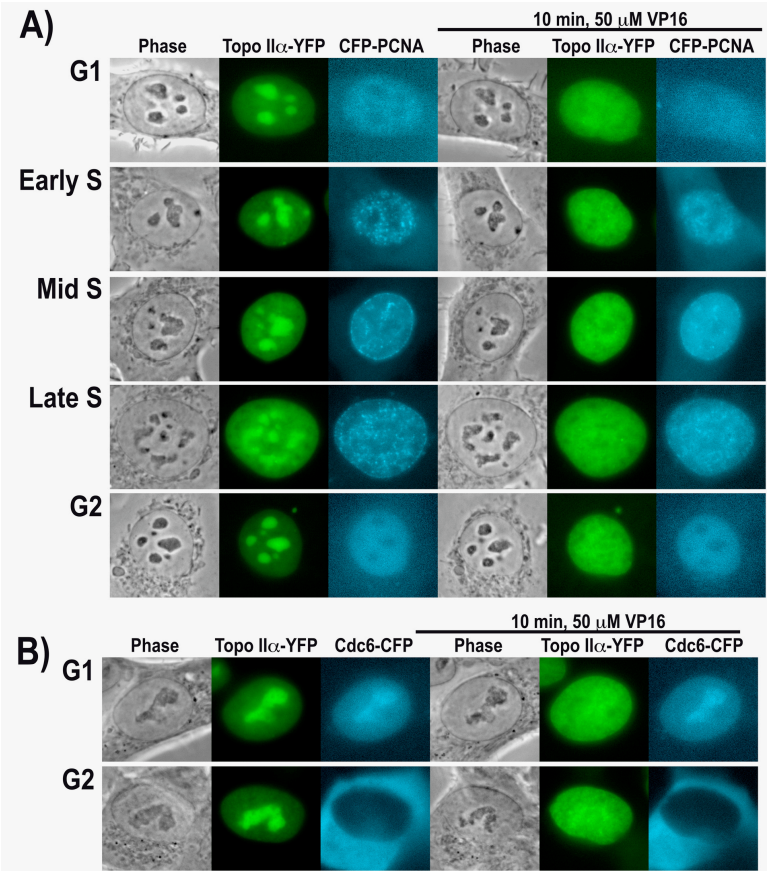

Fig.4.2.3: **Disposition of Topo IIα during different cell cycle stages.** Epifluorescent images of living cell clones PT2a (**A**) and CT2a (**B**). Representative images of the same cell are shown before (left) and after exposure to VP-16 (right, 50 μm VP-16, 10 min). Each row shows cells at the indicated cell cycle stages, as determined by inspection of the marker proteins PCNA-CFP (**A**) or Cdc6-YFP (**B**).

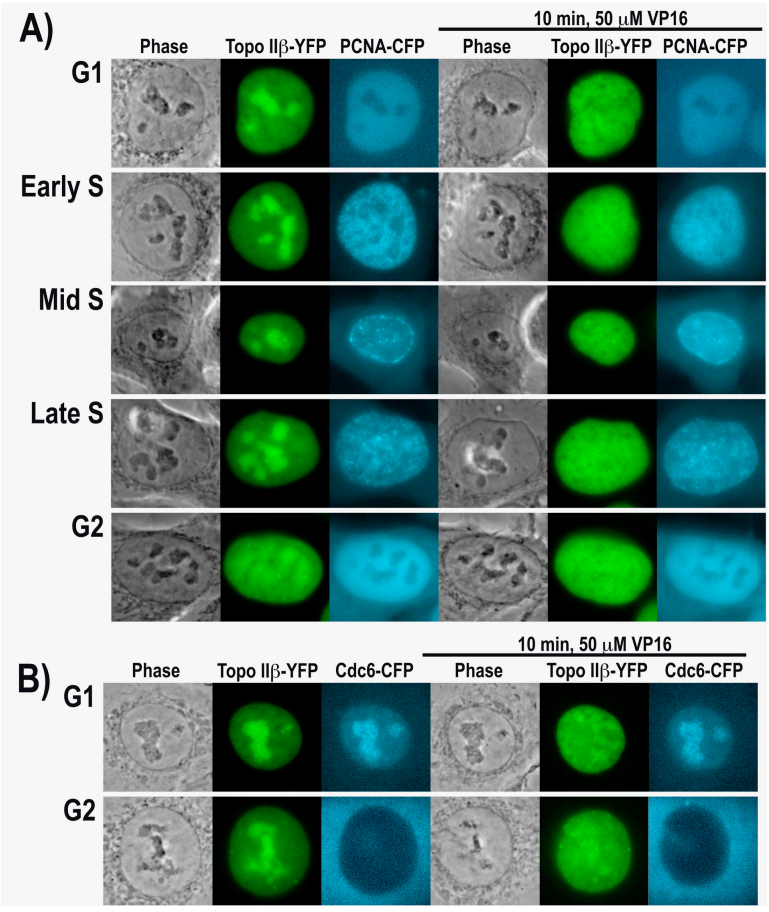

Fig.4.2.4: **Disposition of Topo II β during different cell cycle stages.** Epifluorescent images of living cell clones PT2b (**A**) and CT2b (**B**). Representative images of the same cell are shown before (left) and after exposure to VP-16 (right, 50 μm VP-16, 10 min). Each row shows cells at the indicated cell cycle stages, as determined by inspection of the marker proteins PCNA-CFP (**A**) or

to late stages of S phase, while during G1- and G2 phases it showed a homogenous nucleoplasmic distribution. Again nucleolar accumulation of Topo IIα was more pronounced

in G1- and G2 phases and hardly detectable in S phase. Topo IIβ clearly deviated from this pattern shared by Topo I and Topo IIα: Nucleolar localization of Topo IIβ was most pronounced in S-phase (Fig. 4.2.4 A, second and third rows), whereas during G1- and G2 phases it resided to a much bigger extent in the nucleoplasm (Fig. 4.2.4 B).

In summary, my data clearly are supportive of the notion that Topo IIα and IIβ play distinct roles in cellular DNA metabolism, and the established cell systems seems a suitable model for investigating these in more detail. In order to do so, I needed to establish additional tools for probing enzyme function *in vivo*.

4.2.2.2 Mobility of topoisomerase I, II α and II β in interphase cells

One such approach was to study enzyme mobility. Topos are dynamic and highly mobile enzymes. A well established concept of nuclear architecture postulates that binding of mobile proteins to immobile components of the nucleus (e.g. genomic DNA) retards their overall mobility, which can be assessed by measuring the speed of "fluorescence recovery after photobleaching" (FRAP) of GFP chimera of such proteins (Misteli et al., 2000). Recent evidence suggests that this holds true for the distribution of Topo between nucleoli and nucleoplasm, which seems governed by mobility states in such a way that the enzymes accumulate where they are least mobile (Christensen et al., 2002a; Christensen et al., 2002b; Christensen et al., 2004; Christensen et al., 2002c). Therefore, I tried to corroborate the localisation data shown in 4.2.2 with analyses of mobility. To track the mobility of different Topos in living cells, photo-bleaching techniques were employed. Images and quantitative plots in Fig. 4.2.5 show the mobility of Topo I, Topo IIα and IIβ in interphase nuclei *via* kinetics of (FRAP). Topo-tagged YFP-fluorescence was bleached irreversibly in circular areas (Ø = 1 μm) by high-powered laser pulses and fluorescence recovery in the bleached spots was recorded over time as a consequence of Topo-YFP molecules moving in from unbleached areas. It is apparent from time-lapsed fluorescent images (Fig. 4.2.5 A (top) and quantitative plots of recovery kinetics (Fig 4.2.5 A (bottom) that FRAP was fast and complete for each Topo in all cell cycle stages. This finding confirms previous findings (Christensen et al., 2002b; Christensen et al., 2002c) that completely immobile molecules are virtually absent. To address the question whether uneven distributions of the enzymes could be correlated to differences in mobility, specific areas of the nucleoplasm (e.g. replication foci and their periphery) of PT clones in S phase were bleached, and compared to nucleoplasmic sites in G phase. However, all Topos exhibited similar mobilities under all conditions.

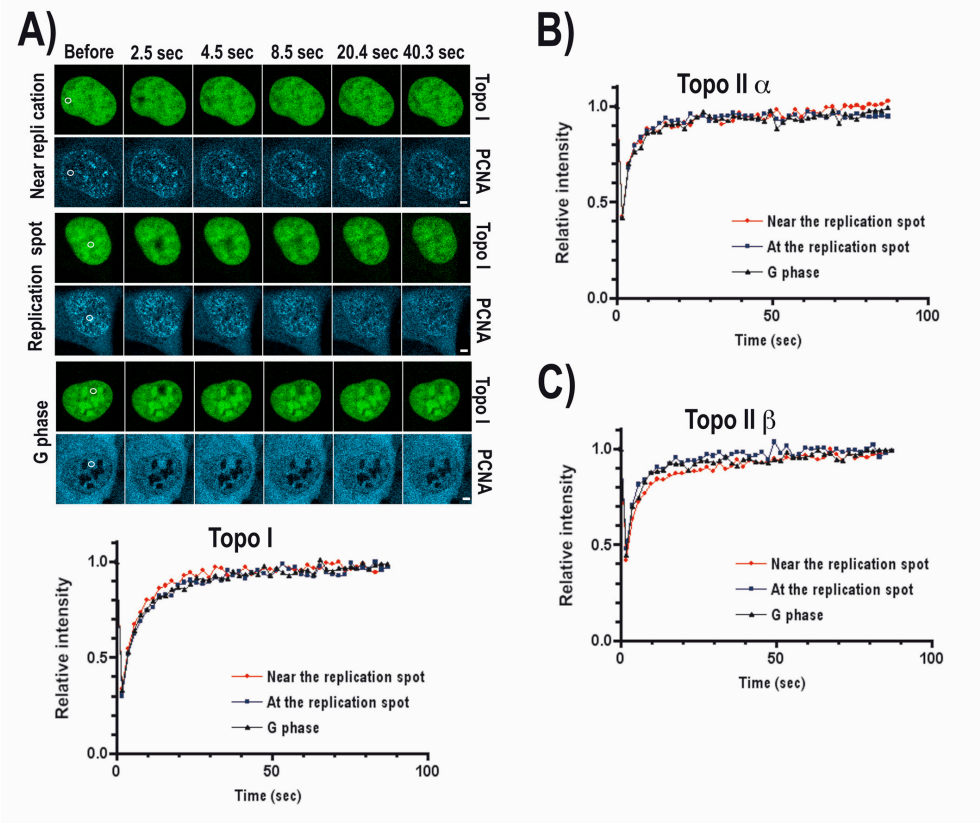

Fig.4.2.5. **FRAP analysis of Topos during different cell cycle stages.** (**A**) Confocal images of cell clone PT1 were taken before and every 2 seconds after YFP was bleached in the indicated area (white circle). S and G phase cells were discriminated by the S-phase specific marker, CFP-PCNA. This marker, also facilitated a detailed FRAP analysis of YFP-Top1 situated either next to or at replication spots. Quantitative data of fluorescence recovery kinetics are plotted below. Fluorescence intensities in the bleached region were measured and expressed as relative recovery over time. Each FRAP curve represent means of 12 FRAP measurements carried out on individual cells during three different days. (**B, C**) FRAP analysis of Topo IIα (B; cell clone PT2a) and Topo IIβ (C; clone PT2b) were performed as described in legends to Fig.

Thus, it seems that the FRAP method is not sensitive enough to detect a retardation of Topos upon their engagement in the replication process.

4.2.3 Active involvement of topoisomerases in replication factories

Taken together, the observations decribed in the previous two paragraphs seem to fit the concept that topological constraints created by the replication process are mainly removed by Topo I and Topo IIα (see: 1.4.1). The spotted pattern of these two enzymes in S-phase seems indicative of engagement in replication foci, whereas relocation to the nucleoli in G1- and G2-phase could indicate storage and/or engagement in rDNA transcription (Christensen et al., 2002a). Conversely, the pronounced nucleolar accumulation and lack of focal nucleoplasmic accumulation of Topo IIβ during S phase conforms to the hypothesis that this isoform does

not play a major role in replication (Niimi et al., 2001). Therefore it might be stored in nucleoli during this DNA-metabolic task, whereas its release from the nucleoli into the nucleoplasm during G1- and G2-phase could reflect a predominant engagement in DNA metabolic processes unrelated to replication as suggested in the literature (Ju et al., 2006; Ju and Rosenfeld, 2006; Lyu et al., 2006; Shaiu and Hsieh, 1998).

4.2.3.1 Effects of topoisomerase poisoning on the architecture of replication foci

These interpretations are further supported by the effects of Topo poisons at the various cell cycle phases demonstrated in the right half of Fig. 4.2.2-4. The same cells were visualized before (rightmost three columns) and after (leftmost three columns) exposure to saturation concentrations of a Topo poison. Thus, the maximal effect of camptothecin on the cellular distribution of Topo I and PCNA at various cell cycle stages can be judged from reading vertically across Fig. 4.2.2, whereas effects of etoposide on the disposition Topo IIα or β and PCNA can similarly deduced from Fig. 4.2.3 and 4.2.4, respectively. It is readily apparent that the drugs had two effects: Firstly, nucleolar accumulation was abolished and the entire complement of all three Topo species was relocated to the nucleoplasm. This effect occured at all cell cycle stages and my observation conforms to previous studies interpreting the phenomenon in terms of the nucleoli serving as storage pools of unused enzyme, which get depleted when all enzyme molecules are captured at nucleoplasmic sites of activity upon poisoning (Christensen et al., 2002b; Christensen et al., 2002c). The second, cell cycle specific effect of Topo poisoning was that the granular nucleoplasmic pattern of Topo I and Topo II in S-phase was abolished, and, coincidentally, replication foci delineated by PCNA disappeared. The most plausible explanation for this second observation is, that poisoning of Topo I or Topo II interrupts the replication process and leads to a dissociation of replication factories (delineated by PCNA spots). It remains unclear whether these detrimental effects are due to withdrawal of essential Topo activities from the replisome, or collapse/stalling of replication forks at Topo•DNA-compexes. To differentiate between these two possibilities and to elucidate, which Topos are actually recruited to PCNA foci, I subjected the cells to an exposure to Topo poisons short enough to not disrupt PCNA foci and to make collison of replication forks with Topo•DNA complexes unlikely, but sufficient for entrappment of active Topo I or II on DNA (Christensen et al., 2002b; Christensen et al., 2002c). Functionally meaningful colocalization of Topos acitively enganged in DNA turnover at replication foci

with PCNA should become enhanced by the treatment, whereas accidental colocalization should be decreased due to a fixation of Topo at other DNA sites.

4.2.3.2 Differential recruitment of topoisomerases to replication foci

While this experiment was carried out at all stages of S-phase, interpretable results were only obtained at late S-phase, when cells contain fewer but more prominent PCNA-positive replication spots. Fig. 4.2.6 shows a typical result obtained when cells coexpressing Topo I, IIα, or IIβ (green) and PCNA (red) had been exposed to the fitting Topo poisons (camptothecin or etoposide) for just one minute. Clearly, at this time point the spotted distribution of PCNA typical of lates S-phas is still visible. It can also be seen that all three Topos exhibit a focal accumulation in response to the drug treatment, and that these Topo foci partly overlapped with the PCNA spots. The extent of focal colocalization with PCNA however differed between the enzyme species. It was very pronounced for Topo IIα, but much less for Topo I and Topo IIβ. In quantitative terms (assessment of three representative S-phase cells of each clone) I counted in a confocal mid plane section 19 ± 2 PCNA foci, 6 ± 4 Topo I foci, 14 ± 3 Topo IIα foci and 8 ± 2 Topo IIβ foci. The overlap between these populations was 3 ± 1 foci containing Topo I and PCNA, 13 ± 3 foci containing Topo IIα and PCNA, and 3 ± 1 foci containing Topo IIβ and PCNA. In other words, more than half (62 ± 1 %) of the PCNA foci were positive for Topo IIα, whereas a significantly smaller fraction of the PCNA foci was positive for Topo I or Topo IIβ (19 ± 3 and 14 ± 2 %, respectively). Conversely, the vast majority of the Topo I and Topo IIα foci (70 ± 16 and 91 ± 4 %, respectively) but only a third of the Topo IIβ foci (37 ± 2 %) coincided with PCNA spots. In summary, these observations suggest that during S-phase the main activity focus of Topo I and Topo IIα are the replication factories, however the representation of Topo IIα in these structures is much higher than that of Topo I (62 vs. 19 %). In contrast, 63% of focal Topo IIβ activity during S-phase seems to be outside the replication fork and consequently this enzyme is very infrequently colocalized with PCNA (only in 14% of the PCNA spots).

My finding that Topo IIα is much more frequently present at replication foci than Topo IIβ is in good aggrement with evidence in non-mammalian systems (Niimi et al., 2001) and conforms to current belief of how labour is divided between the two isoforms (Nitiss, 2009a). However, my finding that Topo IIα is also much more frequent in replication foci than Topo I came as a suprise, since current belief holds that Topo I is the enzyme that releases the majority of positive supercoils ahead of the replication fork, whereas a type II enzyme is

mainly required to remove precatenanes forming behind it (Champoux, 2001; Osheroff, 1986; Wang, 1996; Wang, 2002).

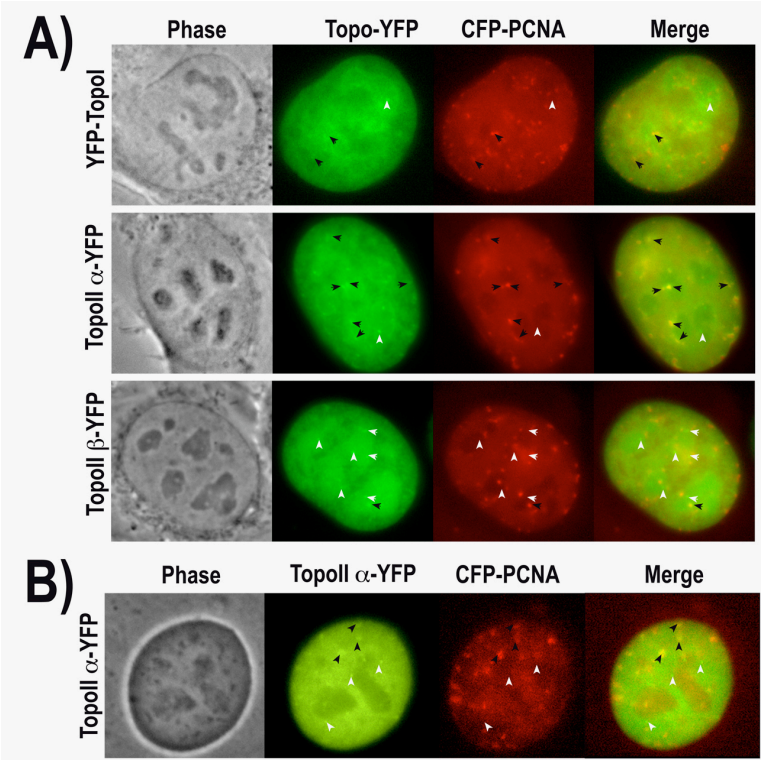

Fig. 4.2.6: **Colocalization of Topos with replication spots.** (**A**) Each row shows epifluorescent images of living cells expressing the indicated constructs. Late S phase cells were imaged 1 min after addition of specific Topo I (row 1, 20 μM CPT) or Topo II poisons (rows 2 and 3, 50 μM VP16), a time point at wich distribution of PCNA (red) is not yet influenced by the poisons. Black arrowheads indicate sites where Topos (green) colocalise with PCNA (red). White arrowheads marks Topo accumulation sites not related to replication. (**B**) Catalytic active Topo IIα-YFP is retained at replication sites by the differential retention of Topo (DRT) assay.

Cells coexpressing Topo IIα-YFP (green) and CFP-PCNA (red) were grown on glass slides, treated with the specific Topo II inhibitor ICRF-187 (50 μM, 5 min), extracted (DRT assay), fixed in formaldehyde and imaged by epifluorescent microscopy. ICRF-187 traps Topo II on the DNA subsequent to cleavage complex formation, thus only Topo IIα engaged in strand passage is retained, whereas inactive enzyme is extracted during the DRT assay. Black arrowheads indicate sites where Topo IIα-YFP colocalize with PCNA. White arrowheads indicate sites where only Topo IIα accumulated.

Moreover, studies with temperature sensitive Topo I- and Topo II mutants of yeast suggest that the two enzymes are completely interchangeable at the replication fork since only loss of both stops DNA synthesis (Kim and Wang, 1989). Given this, it is puzzling that Topo IIα seems to be the major topoisomerase present at replication sites, whereas Topo I seems to be much less represented there. On the other hand, recent biochemical studies demonstrate that Topo IIα (in contrast to Topo IIβ) is able to recognize the handedness of DNA-superhelices and thereby preferentially relaxes positive supercoils (McClendon et al., 2008; McClendon et al., 2005). On the basis of this it has been suggested that Topo IIα could play a role ahead and behind the replication fork, and thus may be the main Topo in DNA replication. My above observations seem to support this alternative hypothesis. However, the

use of Topo poisons in demonstrating this enhanced accumulation could have led to artefacts resulting from the onset of dissociation of replication forks shown in Fig. 4.2.3. and 4.2.4. to occur upon longer exposure. Therefore, I corroborated my finding by using an assay allowing discriminating between catalytically active and inert pools of the enzyme without disrupting DNA systhesis. The "differential retention of Topo" (DRT) assay introduced by Agostinho (Agostinho et al., 2004) is based on the fact that catalytic Topo II inhibitors such as ICRF-187 (see chapter 1.5.2.2) retain Topo II molecules subsequent to strand passage on the resealed DNA strand in the closed clamp conformation, which does not interfere with completion of replication. Topo II molecules thus captured in closed clamp conformation resist subsequent salt extraction, whereas temporary inactive enzyme molecules are removed. Fig. 4.2.6 B shows a typical result obtained in cells coexpressing Topo IIα and PCNA and subjected to the DRT procedure. It can clearly be seen that most (more than two thirds) of the PCNA foci were associated with Topo IIα molecules having completed strand passage (examples marked by black arrowheads). However, there were also some PCNA foci not coincident with Topo IIα activity foci (example marked by white arrowheads in third column) and some Topo IIα activity foci not coincident with PCNA foci (examples marked by white arrowheads in second column). The fact that most but not all replication foci at late S phase where associated with focal activity of Topo IIα could reflect a division of labour between Topo IIα and Topo I. This is also supported by most recent evidence that the main function of Topo I in replication could actually be disentanglement of DNA-/RNA-intermediates rather then release of positive supercoils (Tuduri et al., 2009). The additional observation that not all foci of Topo IIα coincided with PCNA-postive replication foci could moreover indicate that DNA decatenation and -synthesis may under certain conditions become separated in space and time. It is for instance feasible that the process of decatenation behind the fork could actually continue on its own for some time after replication has moved on. Thus, at late S-phase, decatenation foci of Topo IIα could become uncoupled from sites of DNA synthesis demarked by PCNA. As that may be, my observations give a strong indication that Topo IIα is not only essential for mitosis (Carpenter and Porter, 2004; Grue et al., 1998; Linka et al., 2007) but also the main Topo supporting the other major DNA metabolic tasks during cell proliferation, namely DNA replication.

4.3 Monitoring Topoisomerases-directed effects of drugs, toxins, and micro nutrients in living cells

In this third part of my thesis, I will use a new approach to assess the effects of poisons and catalytic inhibitors on the disposition of Topo IIα and IIβ in the living human cell. As elaborated in the introduction, Topo II poisons interrupt the catalytic cycle after DNA cleavage and thus stabilize the "cleavage complexes" in which Topo II is covalently bound to a DNA double-stranded break (Kaufmann et al., 1998; Pommier et al., 2003; Pourquier and Pommier, 2001). Given that DNA is an immobile component of the nucleus (Misteli et al., 2000) while Topo IIα and β are highly mobile (Christensen et al., 2002c), Topo II poisoning should result in an immobilization of the enzymes. This has indeed been previously demonstrated by confocal microscopy and photobleaching techniques in cells expressing biofluorescent Topo IIα or IIβ. It could be shown that recovery of Topo II-associated fluorescence after photobleaching (FRAP) was much slower in the presence of the strong Topo II poison VM26 and that at high doses of this drug the enzymes became virtually immobile (similar to histones) (Christensen et al., 2002c). In a similar such study, it could be shown that the time constants (forward rates) of fluorescence recovery of biofluorescent Topo I were stringently correlated to the dose of the Topo I poison camptothecin applied to the cells (Christensen et al., 2002b). Thus, FRAP can apparently be used to quantify Topo poisoning in the living cell in a non-destructive manner. The latter point seemed particularly important, because conditions of cell lysis are known to affect the cleavage/ligation equilibria of Topo II in a significant manner and this is suspected to have had a rather unpredictable influence on the available data regarding *in vivo* effects of Topo II poisons (Nitiss, 1998) which are all based on “bioassays” involving cell lysis and subsequent immunbiochemical or immunhistochemical analysis (i.e. “ICE bioassay” (Bandele and Osheroff, 2008; Bender et al., 2008), “TARDIS bioassay” (Padget et al., 2000; Willmore et al., 1998) and alkaline elution (Kohn et al., 1981)). The new approach termed TIPP bioassay (**T**opo **i**mmobilization in the **p**resence of **p**oisons) was also applied to catalytic inhibitors of Topo II such as ICRF-187 that stabilize the closed clamp formation of Topo II (Roca et al., 1994) which is also expected to be significantly less mobile than the free enzyme.

The first chapter of part three will be dedicated to the characterization of the assay system consisting of human HT-1080 cells expressing GFP-fused Topo IIα or IIβ at near physiological levels and *in vitro* assays of DNA cleavage and –decatenation employed to

compare drug efficacy *in vitro* and *in vivo*. In the second chapter I will address the issue of isoform selectivity of Topo II poisons and catalytic inhibitors established in clinical use. In the third chapter I will analyze the *in vivo* efficacy and isoform selectivity of various experimental substances and toxins recently published to poison Topo II in a isoform-specific manner (Barthelmes et al., 2001; Fehr et al., 2008; Gao et al., 1999). In the fourth chapter, I will try to elucidate whether genistein has indeed an effect on the cellular disposition of Topo II comparable to Topo II poisons used in cancer therapy.

4.3.1 *In vitro* and *in vivo* models for Topo II targeted subtances.

To calibrate my assays I measured **stimulation of Topo II-mediated DNA cleavage *in vitro*.** For this I used purified recombinant human Topo IIα or IIβ and supercoiled plasmid DNA (pUC18). Separation of the plasmid by agarose gel electrophoresis in the presence of the DNA intercalator ethidiumbromide allowed discriminating supercoiled, linear, nicked, and relaxed topological states of the plasmid by electrophoretic mobility. The controls shown in Fig.4.3.1 A comprising supercoiled pUC18, relaxed pUC18 (treated with Topo II in the absence of drugs), linear pUC18 (generated by cleavage of a single *EcoR I* site) and nicked pUC18 (produced by limited digestion with DNase) were included in each run, but are not shown in each subsequent presentation of such data. To calibrate the effects of pure catalytic inhibitors on **overall catalytic activity *in vitro***, I also measured decatenation of *crithidia fasciculata* kinteoplast DNA (kDNA) by Topo IIα and IIβ. A typical readout of this assay is demonstrated in Fig. 4.3.1 B showing Topo II-catalysed release of electrophoretically mobile DNA circles form the electrophoretically immobile catenated network of the kDNA, which remains in the application slot of the agarose gel. It should be noted that both these *in vitro* assays were not applicable to the study of anthracyclines (e.g. DOX), whose strong DNA intercalation influences the electrophoretic migration pattern of the plasmid DNA to an extent precluding interpretations of Topo II dependent effects 4.3.1 C.

For the **analysis of *in vivo* mobility of Topo II** by confocal microscopy and photo bleaching techniques (Christensen et al., 2002a; Christensen et al., 2003; Christensen et al., 2002b; Christensen et al., 2004; Christensen et al., 2002c) (TIPP-bioassay), I established several cell clones stably expressing Topo IIα-GFP or Topo IIβ-GFP at moderate levels. Immunoblotting of representative samples of these cell clones is shown in Figure 4.3.1 D. Untransfected cells (lane 1) served as control. In blots probed with GFP antibodies (Top panel), chimeric Topo IIα or IIβ (lanes 2 and 3) were detected as single protein bands of the expected size (arrow),

which were absent in untransfected HT-1080 (lane 1). To compare expression levels of GFP-fused Topo II isozymes with the endogenous enzymes, blots were probed with isoform-specific antibodies against Topo IIα (second panel) or Topo IIβ (third panel).

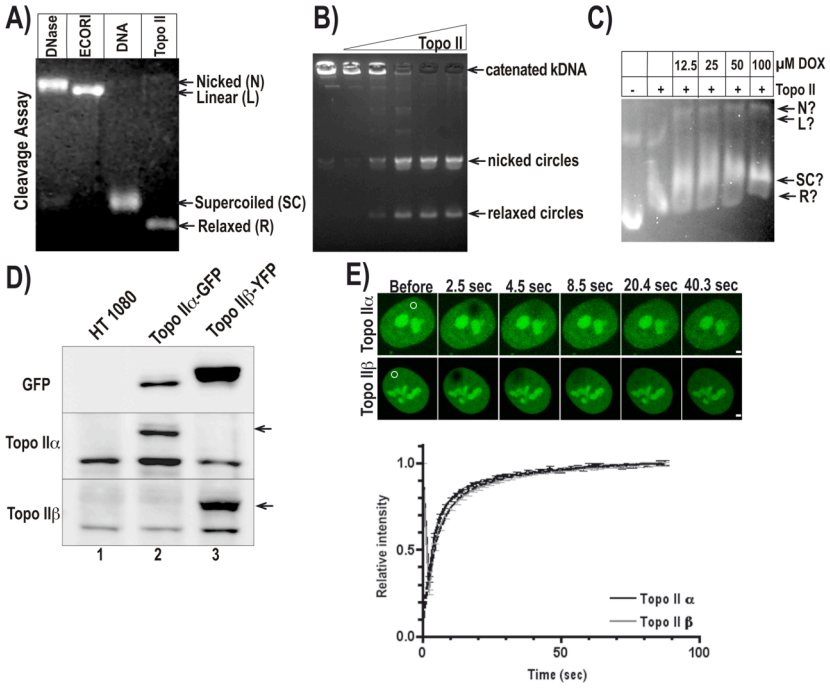

Fig. 4.3.1: **Experimental setup to evaluate different Topo drugs *in vitro* and *in vivo*. (A)** Illustration of the nicked (N), linear (L), supercoiled (SC) and Relaxed (R) topological forms of DNA detectable in the cleavage assay. Nicked pUC18 DNA was obtained by digestion the DNA with DNase I in the presence of 0.25 mg/ml ethidium bromide, 20 mM $MgCl_2$, 0.2 mM DTT, 10 mM BisTris-propane, pH 7.9, at 37 °C (according to (Boege et al., 1996) Linear pUC18 was obtained by digestion the DNA with *Eco*RI endonuclease. Topo II was used to relax pUC18 plasmid i.e. to convert the supercoiled (SC) form of DNA to a relaxed form (R). DNA products were separated by agarose gel electrophoresis in the presence of 0.25 mg/ml ethidium bromide in order to separate closed (SC and R) from open (N and L) plasmid forms. (**B**) In the decatenation assay active Topo II releases free circles (nicked and relaxed) from catenated kDNA. In the catenated form kDNA (lane 1) cannot enter an agarose gel. The wedge indicates that increasing amounts of Topo II (5, 10, 20, 40, 80 ng) was added to the kDNA. DNA-reaction products were separated by agarose gel electrophoresis in the presence of 0.25 mg/ml ethidium bromide. Positions of catenated DNA network and free DNA circles are indicated on the right margin. (**C**) Cleavage assay in presence of DOX. The first lane on the left is pUC18 DNA without Topo II. The strong DNA intercalation of DOX caused a smeared band pattern, and, thus prevented a meaningful data interpretation. (**D**) Expression of fluorescent 'drug sensors' in human HT-1080 cells. Total cell lysates of untransfected HT-1080, cell clones expressing Topo IIα-GFP or Topo IIβ-GFP were subjected to western blotting using specific antibodies against GFP (top), Topo IIα (middle) or Topo IIβ (bottom). Position of Topo IIα-GFP and Topo IIβ-GFP bands are indicated by arrows. (**E**) In the FRAP assay, the potential of drugs to influence Topo II's interaction with genomic DNA can be measured quantitatively. Confocal images of cells expressing Topo IIα-GFP (top) and Topo IIβ-GFP (bottom) were taken before and every 2.5 seconds after GFP was bleached in the indicated area (white circles). Fluorescence intensities

The GFP chimera could clearly be discriminated from the corresponding endogenous enzymes as slower migrating bands (arrows). From comparison within each lane, it became evident that Topo IIα-GFP was expressed at alower level than the endogenous protein,

whereas Topo IIβ-GFP was slightly over-expressed. Most likely, the lower expression of Topo IIα-GFP is due to its known cytotoxic effect upon over-expression (McPherson and Goldenberg, 1998). In keeping with this, a much lower number of cell clones were obtained after selection of HT-1080 cells for expression of Topo IIα-GFP. However, morphology and cell cycle distribution of the cell clones thus obtained were the same as in untransfected HT-1080 cells. Finally, I tested the mobility of the enzymes in the cell clones to be used in my study by FRAP. Time courses of fluorecsent recovery of Topo IIβ-GFP and Topo IIα-GFP (Fig.4.3.1 E) were similar to those previously observed in mixed HEK-293 cell populations expressing Topo IIβ-GFP or Topo IIα-GFP (Christensen et al., 2002c). Non-linear regression analysis of recovery kinetics was carried out as described in (Christensen et al., 2002b) using the computer software Prism (GraphPad Software Inc., San Diegeo, CA). Kinetic models assuming the coexistence of one, two, or three individual enzyme fractions with different mobility were tested. Best fits (according to R2-values > 0.9 and F-test significances < 0.001) were obtained assuming the coexistence of two enzyme fractions with different mobility. The major component was a fast moving enzyme population with a recovery rate constant (K_{fast}) of 0.247 ± 0.038 and 0.205 ± 0.036 sec^{-1} for Topo IIβ-GFP and Topo IIα-GFP, respectively. This fast population constituted about three quarters of the observed enzyme molecules (78 ± 8 of Topo IIβ-GFP and 76 ± 10 % of Topo IIα-GFP), whereas the remaining quarter had a 10-fold slower mobility (K_{slow} = 0.032 ± 0.020 and 0.031 ± 0.021 sec^{-1} for Topo IIα-GFP and Topo IIβ-GFP, respectively). The distribution into fast and slow populations has previously also been observed for Topo I (Christensen et al., 2002b) and a variety of other proteins that transiently interact with DNA (Misteli et al., 2000; Phair and Misteli, 2000). Current belief holds that the slow populations represent protein molecules actively engaged with the DNA, whereas the fast populations represents proteins currently not recruited to DNA metabolic processes and therefore more free to roam the nuclear space (Schmiedeberg et al., 2004). For both isoforms, values of maximal recovery derived from nonlinear regression of the two enzyme fractions with different mobility added up to 100 %, excluding the existence of a third, immobile enzyme fraction. In a similar study on the mobility of biofluorescent Topo I (Christensen et al., 2002b) a comparable distribution of fast and slow moving enzyme fractions was observed and attributed to enzyme fractions either engaged in catalytic DNA metabolism (slow) or not (fast). It should finally be noted that nuclear localization and distribution of the two biuofluoerecent Topo II species confirmed to previous observations made in other human cells by immunohistochemistry (Meyer et al., 1997) or GFP-tagged human enzymes (Christensen et al., 2002c). Thus, I could draw the conclusion that my cell

models were suitable for the proposed purpose, since they expressed moderate levels of correctly localized, normally mobile, GFP-tagged Topo II isoforms and exhibited a normal morphology and cell cycle progression.

4.3.2 Efficacy and isoform selectivity of clinical Topo II drugs

In the next step I used my model to investigate Topo II poisons that are established and widely used in cancer therapy to date (Nitiss, 2009b). This series included (i) the non-intercalative Topo II poison etoposide (VP16), (ii) the DNA intercalative Topo II poisons Amsacrine (m-AMSA), Doxorubicin (DOX) and Mitoxantrone (MITOX), and (iii) the catalytic Topo II inhibitor Dexrazoxane (ICRF-187) currently used as a clinical antracyclin antidote.

The synthetic podophyllotoxin derviavtive VP16 (Fig. 4.3.2 A) is the prototypic non-DNA intercalative Topo II poison (Baldwin and Osheroff, 2005). Current belief holds that the drug targets Topo IIα and Topo IIβ in a similar fashion *in vitro* (Byl et al., 2001; Cornarotti et al., 1996; Drake et al., 1989) and that both iso-enzymes contribute equally to its clinical efficacy (Nitiss, 2009b). My own observations argue against this belief. When studying the stimulation of Topo II DNA cleavage *in vitro* Fig. 4.3.2 B, I found that Topo IIα was at least 4-fold more sensitive to VP 16 (EC_{50} = 12.5 μM) than Topo IIβ (EC_{50} = 50 μM). This is consistent with older studies reporting that the drug *in vitro* has some preference for the α isoform (Drake et al., 1989). Exposure of cells expressing GFP-linked Topo IIα or Topo IIβ to 50 μM VP16 both enzymes showed a rapid nucleolar depletion Fig. 4.3.2 C,D which recently has been attributed to immobilization of the enzymes at nucleoplasmic DNA sites (Christensen et al., 2002b; Christensen et al., 2002c). Consequently, I used fluorescence recovery after photobleaching (FRAP) to measure alterations in the mobility Topo IIα and Topo IIβ in response to VP16 to adress the question of a selective targeting of the two isoforms by the drug *in vivo*. Typical examples and mean quantitative results obtained after exposure to 25 and 50 μM VP16 for 10 min are shown in (Fig. 4.3.2 E,F). It can be seen that fluorescence recovery of both enzyme forms was notably slowed down as compared to without drug (comp. red and blue to grey curve). Moreover it appeared that the attenuating effect of VP16 on fluorescence recovery was more pronounced in Topo IIα, whose FRAP curves appeared flatter than those of Topo IIβ (Fig. 4.3.2, comp. E to F). Serial recordings of FRAP-curves confirmed that for all concentrations tested, the immobilizing effect of VP16

attained equilibrium after 10 min of drug exposure (as will be demonstrated later on, see Fig. 4.3.5 F).

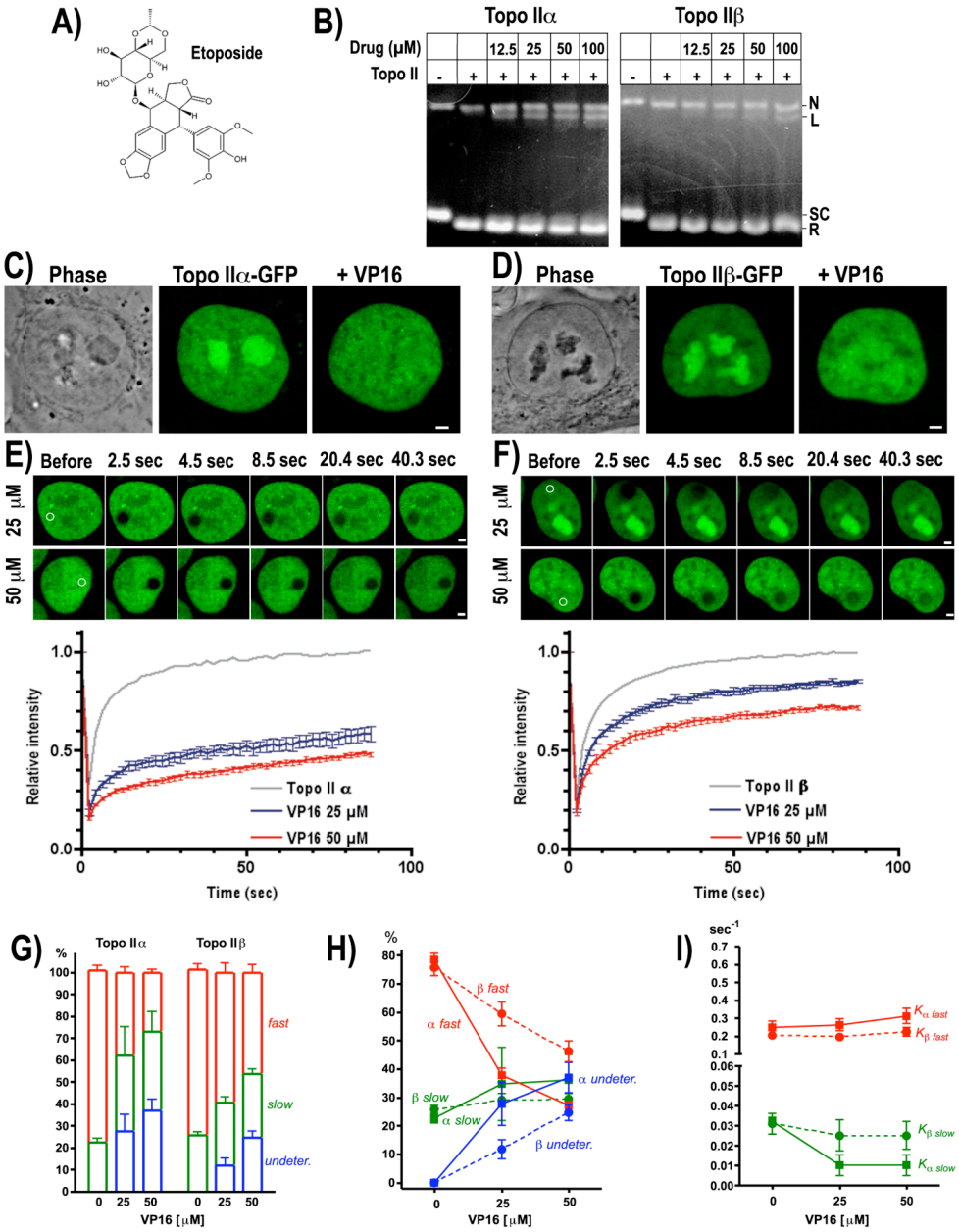

Fig. 4.3.2. **VP16 preferentially targets the α isoform both *in vitro* and *in vivo*.** (**A**) Structure of VP16. (**B**) VP-16 induces linearization of pUC18 plasmid. Supercoiled pUC18-DNA (400 ng) was either reacted with recombinant Topo IIα (left) or Topo IIβ (right) in the absence or presence of increasing concentrations of VP16. (**C and D**) VP16 induces relocalization of Topo IIα (C) and Topo IIβ (D) from nucleoli to the nucleoplasm. Confocal images are shown before (middle) and after (right) exposure to VP16 (50 μM, 10 min). (**E and F**) FRAP curves determined in the nucleoplasm of cells expressing Topo IIα-GFP (E) or Topo IIβ-GFP (F) treated with 25 (blue) or 50 μM VP16 for 20 min (red) or not (grey). Each curve is the mean of at least 10 FRAP measurements. Images of one representative example for each drug concentration is shown at the top of the curves. (**G and H**) The percentage of slow, fast and undetermined fractions of Topo IIα and Topo IIβ derived from non linear regression of the data in F and E are plotted over the molar concentration of VP16. (**I**) The mobility ($1/t_{1/2}$) of fast and slow fractions derived from non linear regression of the data in F and E plotted over the molar concentrations of VP16.

Given this, the FRAP curves shown in Fig. 4.3.2 E,F could be subjected to nonlinear regression analysis and the resulting parametric data could be interpreted in quantitative terms with regards to *in vivo*-mobility of Topo IIα and Topo IIβ as desribed in (Christensen et al., 2002b). These results are summarized in Fig. 4.3.2 G-I. Best fits (according to R2-values > 0.9 and F-test significances < 0.001) were in all cases obtained assuming the coexistence of two enzyme fractions with different mobility. Normally (without drug) nucleoplasmic Topo IIα and IIβ were entirely constituted by two populations: A fast moving population (recovery rate constants $K_{\alpha\ fast} = 0.205 \pm 0.036\ sec^{-1}$ and $K_{\beta\ fast} = 0.247 \pm 0.038\ sec^{-1}$) accounting for about two thirds of the enzyme and a slow population with 10-fold lesser mobility (recovery rate constants $K_{\alpha\ slow} = 0.032 \pm 0.020\ sec^{-1}$ and $K_{\beta\ slow} = 0.031 \pm 0.021\ sec^{-1}$) accounting for the rest. When cells were exposed to increasing concentrations of VP16, these two normal populations did not add up to 100% any more, suggesting that the drug induced a third ultra-slow population. Mobility of this drug-induced population was at least 100-fold slower than the slowest population in untreated cells. Therefore, it does not significantly contribute to fluorescence recovery during the 1.5 min window of observation addressable by FRAP in a living (and moving) cell. As a consequence, recovery rate constants could not be precisely quantified for this fraction, which will subsequently be addressed as "undetermined". However, as shown in the stacked presentation of Fig. 4.3.2 G, the relative proportion of the undetermined (ultraslow) population could be gauged with sufficient precision from the gap between 100% and the percentage constituted by the two other populations. The dose-response curves shown in Fig. 4.3.2 H, demonstrate that induction of ultraslow fractions of Topo IIα and IIβ by VP16 was mostly at the cost of corresponding fast moving fractions, which gradually declined with increasing drug concentrations. Moreover, it can be seen that the shift from fast to ultraslow was much more pronounced and induced at lower VP16 concentrations in Topo IIα, as compared to Topo IIβ. In addition, VP16 significantly reduced the mobility of the slow fraction of Topo IIα (i.e. decreased $K_{\alpha\ slow}$ by three-fold), whereas such an effect was not detectable for the slow fraction of Topo IIβ (Fig. 4.3.2 I).

On the basis of previous FRAP-studies of biofIuorescent Topos (Christensen et al., 2002b; Christensen et al., 2002c) it is currently assumed that the slow populations of Topo II consist of enzyme molecules actively engaged in DNA turnover at the time of observation, whereas the fast populations represent enzyme molecules currently not recruited to DNA metabolic processes and therefore more free to roam the nuclear space. Given this model in conjuction with a host of *in vitro* data on the mechanism of VP16 drug action (Kaufmann et al., 1998; Pommier et al., 2003; Pourquier and Pommier, 2001), it is reasonable to assume that

the ultraslow population of Topo II is constituted of enzyme molecules that are stalled by VP16 during the catalytic cycle. These molecules could either stay in the covalently DNA-bound form during the entire period of observation (i.e. being immobilised by VP16), or undergo a rapidly consecutive series of protracted catalytic cyles (i.e. being retarded by VP16). My experimental setup does not allow a distinction of these two conditions. However, the concomittant decrease in mobility of the slow fraction of Topo IIα seems to argue in favour of the second szenario, suggesting that VP16 induces a continuous transition from fast to slow to ultraslow populations of the enzyme. This model would also explain, why the fraction of the slow population was not significantly altered by the drug (Fig. 4.3.2 G, green symbols), as it would be simultaneously replenished at the cost of the fast population and depleted towards the ultraslow population. Whatever mechanims involved, the curves in Fig. 4.3.2 F-H clearly shown that VP16 has a much stronger immobilising or retarding effect on the α-form than on the β-form, confirming a pronounced α-form-selectivity of the drug *in vivo*. Current belief holds that Topo IIα is the primary target of Topo II-directed cancer therapy, whereas poisoning of Topo IIβ mostly contributes to the toxicity of such drugs (Austin and Marsh, 1998; Azarova et al., 2007; Gatto and Leo, 2003). Therefore, the α-form-selectivity of VP16 observed here, may account for the outstanding clinical success of VP16 over more than two decades (Bandele and Osheroff, 2008; Burden and Osheroff, 1998; Hande, 1998).

The intercalative acridine derivative m-AMSA (4'-(9-acridinylamino) methanesulfon-m-anisidide) (Fig. 4.3.3 A, left) is the prototype of a Topo II poison acting through the formation of a ternary drug-DNA-Topo II complex. This is best exemplified by the observation that the meta position of the anisidide confers Topo II specificity, whereas the ortho-anisidide (Fig. 4.3.3 A, right) is inactive against Topo II despite having a similar DNA intercalative potency (D'Arpa and Liu, 1989; Liu, 1989; Nelson et al., 1984). Moreover, it is a long-standing observation that m-AMSA has a bell shaped dose response curve with respect to the stimulation of Topo II-mediated DNA cleavage. This is attributed to the DNA intercalating properties of the drug thought to inhibit enzyme DNA binding at higher concentrations (Liu, 1989). The *in vitro* DNA cleavage assays shown in Fig. 4.3.3 B suggest that the drug acts similarly on Topo IIα and IIβ with respect to the lower effectivity threshold (around 12.5 μM for both isoforms), whereas at higher concentrations a decrease in cleavge indicative of a self inhibitory effect is detectable in Topo IIβ but not in Topo IIα. Thus, despite an unselective poisoning of both isoenzymes, β-selective autoquenching could in fact

render m-AMSA a Topo IIα-selective poison at higher concentrations. To check out this in the living cell, I studied the effct of m-AMSA on *in vivo* mobility of Topo IIα and β in a similar fashion as described for VP16 in the previous chapter. At the effective threshold concentration of 12.5 µM, m-AMSA exhibited the typical signature of a non-selective Topo II poison: After 10 min exposure it induced nucleolar depletion of Topo IIα and IIβ (Fig. 4.3.3 C, D).

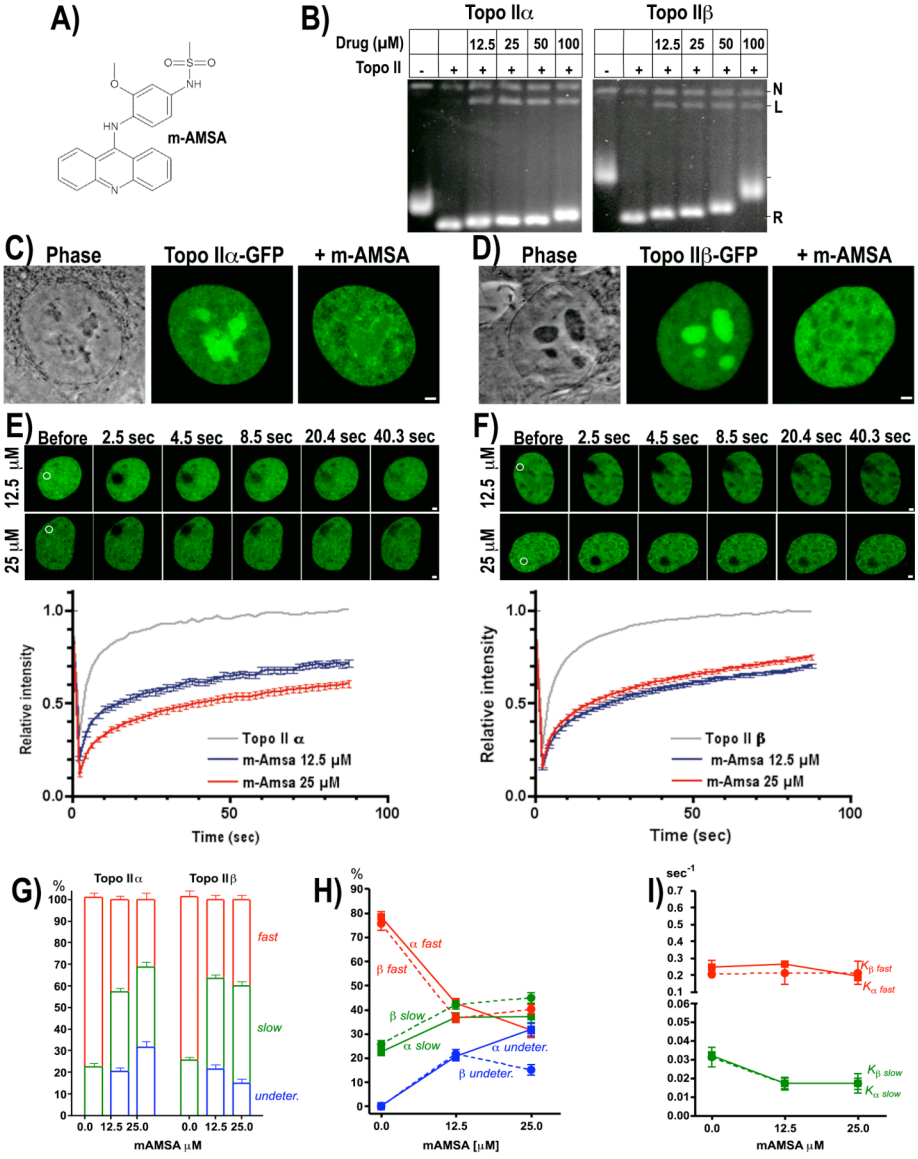

Fig. 4.3.3: **m-AMSA preferentially targets the α isoform at high concentrations. (A)** Structure of m-AMSA. (**B**) m-AMSA induces linearization of pUC18 plasmid similarly on Topo IIα and IIβ with respect to the lower effectivity threshold. (**C and D**) m-AMSA induces relocalization of Topo IIα (C) and Topo IIβ (D) from nucleoli to the nucleoplasm after exposure to (25 μM, 10 min). (**E and F**) FRAP curves determined in the nucleoplasm of cells expressing Topo IIα-GFP (E) or Topo IIβ-GFP (F) treated with 12.5 (blue) or 25 μM m-AMSA for 20 min (red) or not (grey). Each curve is the mean of at least 20 FRAP measurements. (**G and H**) The percentage of slow, fast and undetermined fractions of Topo IIα and Topo IIβ derived from non linear regression of the data in F and E are plotted over the molar concentration. (**I**) The mobility ($1/t_{1/2}$) of fast and slow fractions derived from non linear regression of the data in F and E plotted over the molar concentrations.

Fitting this observation, fluorescence recovery of both isoforms was retarded to a similar extent upon exposure to 12.5 μM m-AMSA for 10 min (Fig. 4.3.3 E,F, compare red to grey curves). These effects were in the equlibrium after 10 min as to be demonstrated later (Fig. 4.3.5 F). Interestingly, escalation of m-AMSA concentrations to 25 μM had a divergent effect on Topo IIα and β: While the FRAP curve of Topo IIα became flatter suggesting further retardation, the corresponding curve of Topo IIβ became steeper suggesting a decrease in retardation (Fig. 4.3.3 E,F, red to blue curves). Non linear regression analysis of the curves and interpretation of the data in terms of enzyme populations with different mobility (Figs. 4.3.3. G-I) revealed a profile of drug action on Topo II mobility, which in many aspects is similar to VP16: m-AMSA induced ultraslow (undetermined) populations at the cost of the fast populations and a retardation of the slow fractions (i.e. a three-fold decrease of $K_{\alpha\ slow}$ and $K_{\beta\ slow}$) (compare blue to red lines). At 12.5 μM m-AMSA these effects were quantitatively similar for Topo IIα and IIβ and the switch from fast to and ultraslow affected roughly 20% of both isoforms. In contrast, at 25 μM m-AMSA the two curves diverged: In the case of Topo IIα, the switch from fast to ultraslow fraction further increased to a value of about 30%, whereas in the case of Topo IIβ it decreased to 15%. In summary, these findings suggest that m-AMSA induces a continuous transition from fast to slow to ultraslow enzyme populations. This effect appears to be the same for Topo IIα and IIβ at concentrations up to 12.5 μM, whereas at higher concentrations it becomes α−selective, because the effect on Topo IIα further increases with dose whereas the corresponding effect on Topo IIβ gets quenched. Thus β-selective quenching (as opposed to α-selective targeting seen with VP16) renders m-AMSA a Topo IIα-selective poison at concentrations above 25 μM. It is conceivable that the different sensitivity of the two isoforms for the inhibitory effect is due to the fact that positive DNA supercoils generated by DNA-intercalation of m-AMSA at higher concentrations can still be recognized and processed by Topo IIα but not by Topo IIβ (McClendon et al., 2008).

Doxorubicine (DOX) is one of three anthracycline derivatives widely used in current clinical oncology (Fig.4.3.4 A). DOX is believed to be a Topo II poison, but it is also a strong DNA intercalator and a generator of reactive oxygen species (ROS) *via* oxidation of the quinone ring common to all anthracyclines. There is a long and still ongoing debate about how these properties contribute to antitumor activity and toxicity of the drug (Froelich-Ammon and Osheroff, 1995; Lothstein et al., 2001). Topo II isoform selectivity of DOX is unknown. It is not even clear, whether it acts indeed through Topo II poisoning (Nitiss, 2009b). This uncertainty is mostly due to the fact that an unambiguous *in vitro* assessement of

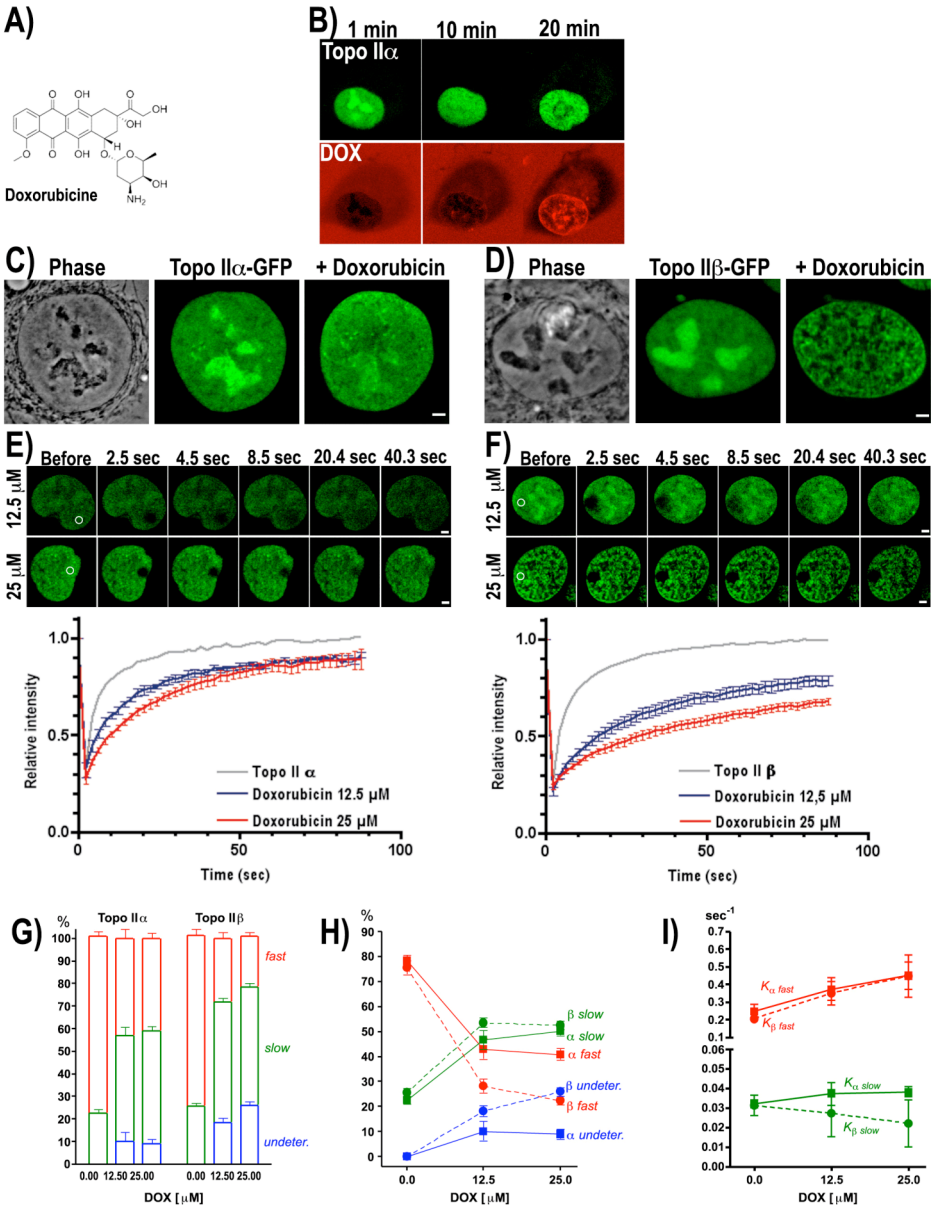

Fig. 4.3.4: **DOX preferentially targets the β isoform. (A)** Structure of DOX. (**B**) Monitoring of the cellular uptake of 25 µM DOX by its red fluorescence (bottom) after 1, 10, 20 min of exposure. (**C and D**) DOX induces relocalization of Topo IIα (C) and Topo IIβ (D) from nucleoli to the nucleoplasm after exposure to (25 μM, 20 min). (**E and F**) FRAP curves determined in the nucleoplasm of cells expressing Topo IIα-GFP (E) or Topo IIβ-GFP (F) treated with 12.5 (blue) or 25 μM DOX for 30 min (red) or not (grey). Each curve is the mean of at least 10 FRAP measurements. (**G and H**) The percentage of slow, fast and undetermined fractions of Topo IIα and Topo IIβ derived from non linear regression of the data in F and E are plotted over the molar concentration. (**I**) The mobility ($1/t_{1/2}$) of fast and slow fractions derived from non linear regression of the data in F and E plotted over the molar concentrations.

Topo II targeted effects of DOX and other anthracyclines is precluded by the strong DNA intercalation of these substances, which renders DNA based assays uninterpretable (see:

Fig. 4.3.1 C). Categorization of DOX as Topo II poison is solely based on the fact that tumors with high Topo II expression tend to be more sensitive to this drug (Gruber et al., 2007).

To readress this issue and possibly obtain new information on the isoform-preference of DOX, I analysed its effects on the *in vivo* mobility of Topo IIα and IIβ. I first monitored the cellular uptake of the drug by its red fluorescence and determined that after 20 min exposure to 25 μM concentrations a stable level accumulation in the cell nuclei was reached and, coincidentally, nuclear distribution of Topo II was altered (Fig. 4.3.4 B). A closer inspection revealed that in response to DOX (12.5 μM, 20 min) Topo IIβ was entirely depleted from nucleoli and redistributed into a reticular necloplasmic pattern, whereas Topo IIα was scarcely subjected to such alterations (Fig. 4.3.4 comp. C to D). These observations gave a first hint that DOX could possibly be a β-selective Topo II poison. To follow up on this, I measured effects of DOX on fluorescence recovery of Topo IIα and Topo IIβ (Fig. 4.3.4 E, F). I found that DOX retarded FRAP of both, but the β-form was significantly more retarded than the α-form (comp. red lines between E and F). Moreover, doubling of the dose resulted in a further retardation of Topo IIβ, whereas the effect on the α-form seemed not to increase accordingly (comp. red to blue lines). In summary, these effects (which were in the equilibrium after 20 min drug exposure, see Fig. 4.3.5 F) suggested that DOX has indeed the signature of a β–selective Topo II poison. To further elucidate the precise mode of action of DOX, I subjected FRAP curves to non-linear regression analyses. These results are summarized in Fig. 4.3.4 G-I. They suggest that DOX acts similar to VP16 and m-AMSA in as much as it increases slow and ultraslow enzyme populations at the cost of the fast ones. However in contrast to VP16 and m-AMSA, the effects of DOX on Topo IIβ were at least 2-fold stronger than on Topo IIα. Moreover, DOX did not significantly alter the mobility of the slow fractions (the downward trend in $K_{\beta\ slow}$ is not significant). Therefore, it seems unlikely that DOX induces a continuous transition from fast to slow to ultraslow enzyme populations, as assumed for m-AMSA and VP16. More likely DOX operates in two discrete steps consisting of (i) recruitment of Topo II to the DNA-catalytic cycle (resulting in an increase in slow moving population without alteration of K_{slow}) and (ii) trapping of DNA-engaged enzyme in an ultraslow state (resulting in the appearance of an undetermined fraction). This interpretation is in good agreement with biochemical data postulating that DOX inhibits Topo II religation activity through the association with the Topo II/DNA binary complex (Chen et al., 1984; Liu, 1989).

In summary, my data clearly support the notion that DOX acts as a Topo II poison in the living cell. Moreover, I find that it exhibits a clear preference for the β-isoform of Topo II.

The latter finding is unprecedented and strongly supports the hypothesis that the dose limiting side effects of DOX in non proliferative tissues (most notably the heart) are due to poisoning of the "housekeeping enzyme" Topo IIβ (Austin and Marsh, 1998; Azarova et al., 2007; Gatto and Leo, 2003) which is the only isoform expressed in such tissues (Turley et al., 1997).

The third DNA intercalating Topo II poison of clinical relevance adressed in my study was **mitoxantrone (MITOX)**, an anthracenedione derivative (Fig. 4.3.5 A) whose established activity against a number of human neoplasias is believed to be associated with stabilization of covalent DNA-Topo II reaction products (Bailly et al., 1997; Errington et al., 2004; Shenkenberg and Von Hoff, 1986). In addition to its long-standing use in cancer therapy, MITOX is recently also employed at very low dose as an immunosuppressant in the treatment of multiple sclerosis. The latter application has established clinical benefits (Komori et al., 2009) but seems to carry a significant mutagenic risk related to chromosome translocations thought to be triggered by stable Topo II-DNA intermediates (Hasan et al., 2008). Therefore, a major question in studying the *in vivo* effects of MITOX on Topo II regards the mechanism responsible for the pronounced mutagenic potential of the drug at chronic low dose administration. Similar to DOX, the strong DNA intercalative potency of MITOX precluded *in vitro* analysis of Topo II mediated DNA cleavage. Therefore, I started my investigation with the established LD_{50} of MITOX in cell culture, which is around 50 μM (Shenkenberg and Von Hoff, 1986). Exposure to 50 μM MITOX for 10 min led to a rapid redistruibution of Topo II from the nucleoli to the nucleoplasm and this effect was similar for both isoforms (Fig. 4.3.5 B,C), indicating that the drug targets both Topo IIα and IIβ. Fitting to this, I observed for both isoforms a significant attenuation of FRAP in response to MITOX. However, this effect was not in the equilibrium. Serial FRAP measurements carried out every 2 min from 10 min up to 32 min exposure to 50 μM MITOX showed that mobility of Topo IIα and Topo IIβ continously decreased over time (Fig. 4.3.5 D,E). This in clear contrast to the situation encountered in cells exposed to DOX, m-AMSA or VP16, where serial FRAP curves obtained under the same time regimen were superimposed on each other (Fig. 4.3.5 F). Non linear regression analysis of the single FRAP measurements at the various timepoints of MITOX exposure (shown in Fig. 4.3.5 D,E) was not precise enough to determine rate constants of enzyme mobility. However, it allowed with sufficient precision to quantify fractions of fast, slow and ultraslow enzyme populations. These data are plotted over time in Fig. 4.3.5 G. It becomes apparent that MITOX (like the other intercalating Topo II poisons)

increased slow and ultraslow enzyme populations at the expense of the fast population (plotted in green, blue and red, resp.).

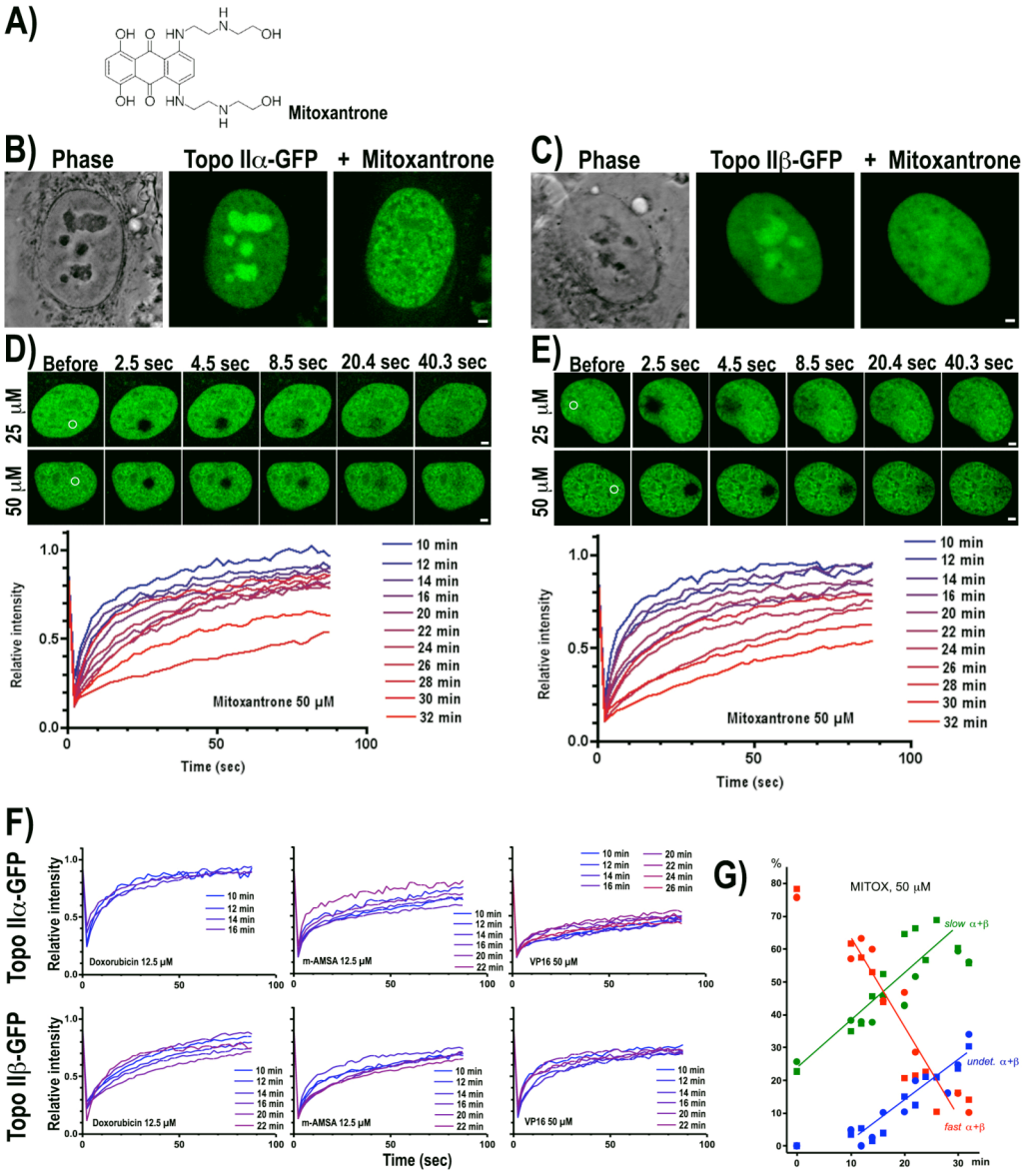

Fig. 4.3.5: **MITOX induced significant levels of long-lived Topo II-DNA complexe.** (**A**) Structure of DOX. ((**B and C**) DOX induces relocalization of Topo IIα (B) and Topo IIβ (C) from nucleoli to the nucleoplasm after exposure to (50 μM, 10 min). (**D and E**) individual FRAP curves determined in the nucleoplasm of cells expressing Topo IIα-GFP (D) or Topo IIβ-GFP (E) treated with 50 μM DOX after 10 min exposure and the FRAP measured every 2 min (from blue to red). (**F**) Individual FRAP measurements of DOX, m-AMSA, and VP16 at concentration shown in figure. (**G**) The percentage of slow, fast and undetermined fractions of Topo IIα and Topo IIβ derived from non linear regression of the data in D and E are plotted over the time (min).

It can also be seen that this effect was identical for Topo IIα and Topo IIβ (compare squares and circles) and continued over time in a linear fashion up to a hypothetical point

where all enzyme molecules are contracted to the ultraslow population. It has been proposed that Topo II-DNA complexes stabilised by Topo II poisons are readily reversible so that an equilibrium of formation and dissociation of such complexes is rapidly reached. It has furthermore been speculated that MITOX is an exception to this rule in as much as dissociation of MITOX induced complexes could be much slower than for all other Topo poisons allowing accumulation over time (Errington et al., 2004). The data presented in Fig. 4.3.5 G provide direct evidence supporting this hypothesis. Therefore it is feasible to assume that low dose, immunosuppressive MITOX treatment is capable of inducing significant levels of long-lived TOPO II-DNA complexes thought to trigger chromosome translocations (Felix et al., 2006), which are actually found in cells exposed to low dose MITOX regimen (Hasan et al., 2008).

The last substance included into my investigation of clinically relevant Topo II targeted drugs was **Dexrazoxane (ICRF-187**)(Fig. 4.3.6 A), which is not a poison but a catalytic inhibitor of Topo II. ICRF-187 belongs to a class of bis(2,6-dioxopiperazines) that all antagonize the formation of Topo II-DNA covalent cleavage complexes through inhibition of the ATPase of Topo II. In the last step of the Topo II catalytic cycle (step 5 in Fig. 1.6) the conformational change in the enzyme molecule that reopens the clamp around the resealed DNA duplex is coupled to ATP hydrolysis (Roca and Wang, 1992). By inhibiting ATP hydrolysis, ICRF-187 and other bisdioxopiperazines are thought to stabilize Topo II in the ATP bound conformation, where it it cannot open the clamp after completion of the catalytic cycle. Thus, the enzyme cannot release the resealed DNA duplex and remains tethered to it (Jensen et al., 2000; Roca et al., 1994). Under the brand name *Zinecard* ICRF-187 is used in the clinic to ameliorate the cardiotoxic side effects of anthracyclines and thus allow for dose escalation (Hellmann, 1998; Lyu et al., 2007). This effect is thought to be due to inactivation of Topo IIβ, whose poisoning is believed to confer the cardiotoxity of antracyclins (Austin and Marsh, 1998; Azarova et al., 2007; Gatto and Leo, 2003). In addition, ICRF-187 and other bisdioxopiperazines have some antitumor activity of their own believed to be effected through depletion of tumor cells from Topo II activity (Andoh, 1998; Andoh and Ishida, 1998). This effect is most likely targeted at the α-isoform, which is the one essential for cell proliferation (Carpenter and Porter, 2004; Grue et al., 1998; Linka et al., 2007). Consequently it is of interest to analyze the isoform selectivity of ICRF-187 as a starting point for developing derivatives that are either β-selective (for use as cardioprotectants) or α-selective (for use as anti cancer drugs).

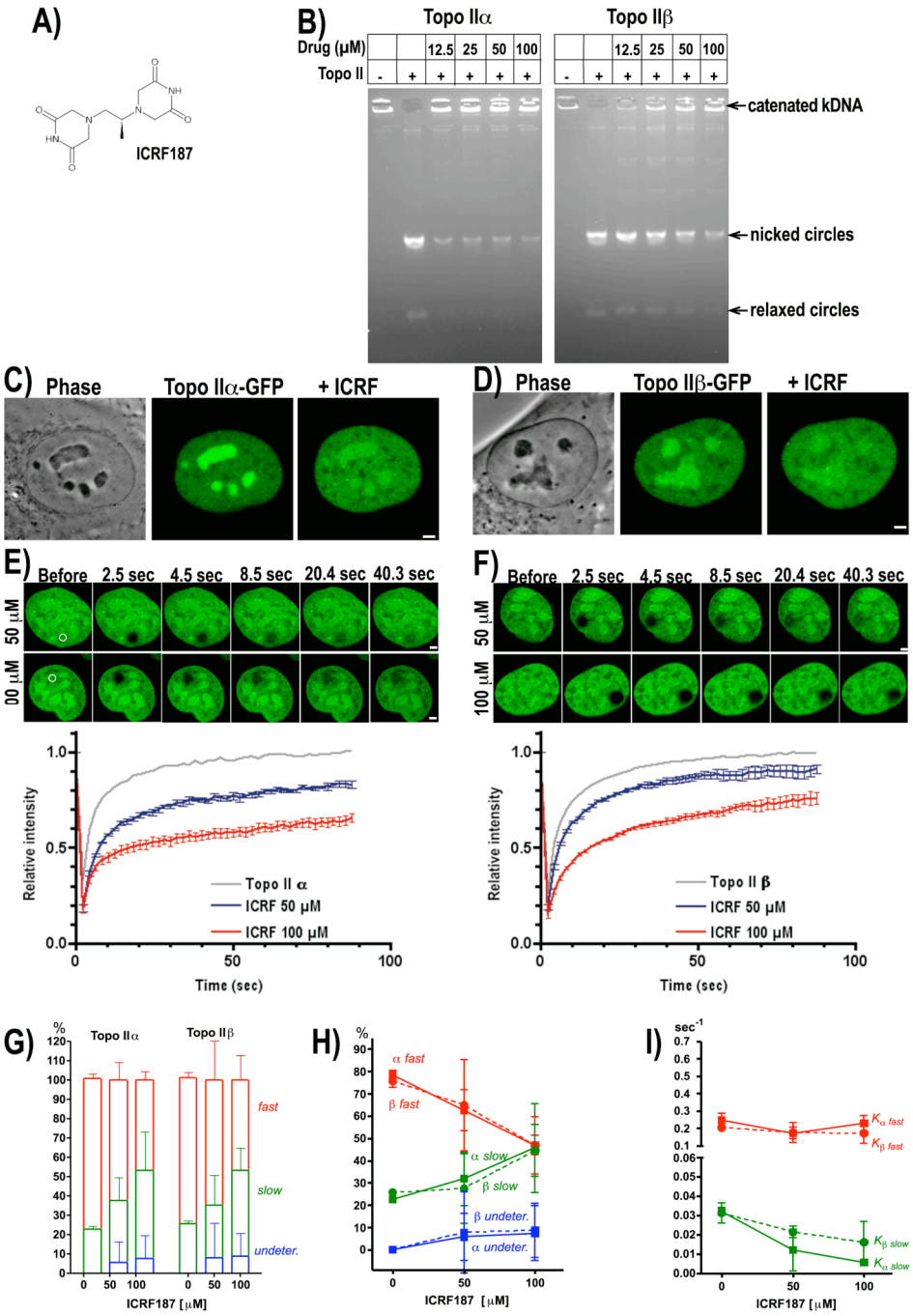

Fig. 4.3.6: **ICRF preferentially targets the α isoform. (A)** Structure of ICRF. ((**B**) The catenated form kDNA (lane 1) cannot enter an agarose gel. The α isoform was about 8 fold more effective inhibited by ICRF-187 than the β-isoform. Positions of catenated DNA network and free DNA circles are indicated on the right margin. (**C and D**) ICRF induces relocalization of Topo IIα (C) and Topo IIβ (D) from nucleoli to the nucleoplasm after exposure to (100 μM, 10 min) (**E and F**) FRAP curves determined in the nucleoplasm of cells expressing Topo IIα-GFP (C) or Topo IIβ-GFP (D) treated with 50 (blue) or 100 μM ICRF for 20 min (red) or not (grey). Each curve is the mean of at least 10 FRAP measurements. (**G and H**) The percentage of slow, fast and undetermined fractions of Topo IIα and Topo IIβ derived from non linear regression of the data in F and E are plotted over the molar concentration. (**I**) The mobility ($1/t_{1/2}$) of fast and slow fractions derived from non linear regression of the data in F and E plotted over the molar concentrations.

I used decatenation of catenated network DNA (kDNA) from the kinetoplast of *crithidia fasciculata* as a read out to compare the inhibitory effect of ICRF on catalytic activity of Topo IIα and IIβ *in vitro*. kDNA decatenation is the most specific Topo II catalytic assay, because type II Topos are the only enzymes capable of releasing single DNA circles from the catenated network (Boege et al., 1996). As shown in Fig. 4.3.6 B Topo IIα and IIβ were similarly active in kDNA decatenation, but the α isoform was inhibited about 8 fold more effective inhibited by ICRF-187 than the β-isoform (comparable inhibiory concentrations 12.5 μM (α) vs. 100 μM (β)). Thus, ICRF-187 is isoform-selective to a significant extent *in vitro*. Previous studies have shown that ICRF-187 immobilizes Topo II in the living cell (Mielke et al., 2004). Therefore I could use FRAP as a readout to adress the issue of isoform-selectivity of ICRF-187 *in vivo*. Fig. 4.3.6 C, D, demonstrate that exposure of cells to 50 μM ICRF-187 for 10 min induced some nucleolar depletion of Topo IIα and IIβ, which was less pronounced than that seen with the Topo II poisons (VP16, m-AMSA, DOX, MITOX) and similar for the two isoforms. Analysis by FRAP (Fig. 4.3.6 E, F) revealed an accompanying retardation, which was slightly more pronounced with Topo IIα (blue lines). Doubling of the dose lead to an increase in retardation, which was again more pronounced in the α-form (red lines). These retarding effects were in the equilibrium after 20 min of exposure (as determined by serial FRAP, not shown), allowing a quantitative analysis of mean equilibrium FRAP curves by non-linear regression. The parametric results are summarized in Fig. 4.3.6 G-I. Again, best fits were obtained assuming two populations with fast and slow mobility. It becomes apparent that ICRF increased the slow population and decreased the fast population correspondingly (Fig. 4.3.6 H). The stacked presentation in Fig. 4.3.6 G shows that fast and slow populations added up to a 100 % at all concentrations of ICRF, excluding significant induction of an ultraslow fraction by the drug (the blue boxes are not significant). It can also be seen that in quantitative terms the ICRF-induced shift from fast to slow population was clearly related to dose and similar for the two isoforms of Topo II.

In summary these findings are in good agreement with the proposed mechanism of action of ICRF-187, assuming that the increase in, and further retardation of, the slow fraction reflects capture of DNA-engaged enzyme molecules at the end of the catalytic cycle in a closed clamp formation. Previous observations (Mielke et al., 2004) have shown that Topo II mobility is much reduced in this state because the enzyme is tethered to the immobile DNA strand enclosed by the clamp blocked in the closed conformation (Roca and Wang, 1992). The decrease in FRAP rate constants of slow fractions (K_{slow}) thus reflects a corresponding decrease in the dissociation rate of DNA-engaged enzyme which is inversely correlated to the

increase in half-life of the closed clamp formation. On the basis of these assumptions it can be deduced from my data that Topo IIα is more sensitive to ICRF-187 than Topo IIβ, because $K_{\alpha\ slow}$ decreased about 3-fold more than $K_{\beta\ slow}$ in response to both concentrations tested Fig. 4.3.6 I. Thus, ICRF-187 seems not an isoform unselective drug as suggested in the literature (Andoh, 1998; Jensen et al., 2000; Larsen et al., 2003; Nitiss, 2009b). The drug rather holds some bias towards Topo IIα. This raises the concern that ICRF-187 might not be an optimal subtance for the protection from cardiotoxic side effects of anthracyclines, since it is expected to interfere more with the putative antiproliferative mechanism of the antracyclins (poisoning of Topo IIα) than with the mechanism believed to cause the side effects of these drugs (poisoning of Topo IIβ).

4.3.3 Validation of experimental Topo II drugs

It is still under debate how Topo IIα and IIβ individually contribute to the outcome of Topo II targeted cancer therapy. However, consense has been reached that they contribute differently (Nitiss, 2009b), and conserable efforts have been made to find subtances that selectively poison only one of the two iso-forms. As consequence, two substances have emerged that are thought to act as **α-selective Topo II poisons.** One is **NK314,** a novel synthetic benzo[c] phenanthridine alkaloid, which has been demonstrated to specifically target Topo IIα *in vitro* and in cells (Toyoda et al., 2008). NK314 is currently tested in clinical phase one trials and was not made available to me. Therefore it could not be included into this study. The other substance reported to act as an α-selective Topo II poison is **alternariol**, a mutagenic toxin of the mold fungus alternaria alternata (Fehr et al., 2008), which I have included into my study. On the other hand, a variety of substances have been identified that are thought to act as **β-selective Topo II poisons** (Gatto and Leo, 2003). From these I selected for inclusion into my study the two substances best characterized, namely the plant alkaloid **lycobetain** (Barthelmes et al., 2001) and the quinoxaline **XK469** (Snapka et al., 2001).

4.3.3.1 Putative Topo IIα – selective poisons

The mycotoxin alternariol belongs to a family of fungal polyphenols produced by *Alternaria* spp. Exposure to *Alternaria*, especially *Alternaria alternata* has been associated with adverse health effects (Brugger et al., 2006). *Alternaria* toxins are regular contaminants

of fruit and cereal products but little is known about their toxicological significance. Alternariol is one of the two major toxins *Alternaria alternata* (Fig. 4.3.7 A). It has been classified a mutagen, because it induces DNA single and double strand breaks and triggers DNA repair (Liu et al., 1992; Xu et al., 1996). More recently, it has been observed that alternariol stimulates DNA cleavage of Topo IIα but not IIβ *in vitro* (Fehr et al., 2008). My own confirmation of this finding is summarized in Fig. 4.3.7 B showing that alternariol induced Topo IIα-mediated linerization of plasmid DNA, whereas such an effect was not observed with Topo IIβ. It should be noted however that stimulation of Topo IIα DNA cleavage by alternariol was much weaker than stimulation of Topo IIα DNA cleavage by VP16 or other standard Topo II poisons. Moreover, Topo IIα–mediated DNA linearization disappeared at concentrations above 50 μM alternariol suggesting that the poisoning effect is delimited by DNA intercalative properties of the compound. In summary, these observations characterize alternariol as a weak Topo IIα selective poison *in vitro*. However, the impact of alternariol on Topo IIα and IIβ in the living cell is as yet ill defined. It has been reported that exposure of cells to high doses of alternariol (200 μM and more) depletes Topo IIα but not Topo IIβ from immublots, which was interpreted in terms of a selective poisoning of Topo IIα leading to covalent DNA-linkage of that isoform (Fehr et al., 2008). However, I observed here that exposure of cells expressing GFP-fused Topo IIα or IIβ to 200 μM alternariol had a similar effect on Topo IIα and IIβ: Both forms were subjected to nucleolar/nucleoplasmic redistribution (Fig. 4.3.7 C, D) and retardation of FRAP (Fig. 4.3.7 E, F). It should be noted that the retarding effect of alternariol on both isoforms was at least twofold enhanced, when the medium was treated with catalase prior to addition of the drug (Fig. 4.3.7 G, H). This indicates that the stability and *in vivo*-efficacy of alternariol similar to other antiproliferative plant polyphenols (Kern et al., 2007) is limited by H_2O_2 generated by the cells. Consequently, only FRAP curves obtained following catalase treatment was subjected to quantitative analysis by non linear regression. The parametric results are summarized in (Fig. 4.3.7 I - K), showing that alternariol drug induced a switch form fast to slow enzyme populations in a dose dependent manner (Fig. 4.3.7 J). At both concentrations tested, fast and slow Topo II populations added up to 100% excluding induction of an ultraslow fraction by alternariol (Fig. 4.3.7 I). Moreover, the switch from fast to slow enzyme populations induced by alternariol was not accompanied by a significant change in the FRAP rate of these populations (Fig. 4.3.7 K) indicating that the overall exchange rate of the DNA-engaged enzyme population was not significantly altered by the drug. This excludes a significant

prolongation of any step in the catalytic cyle and is best explained with a shift of the cleavage-/religation equilbrium of

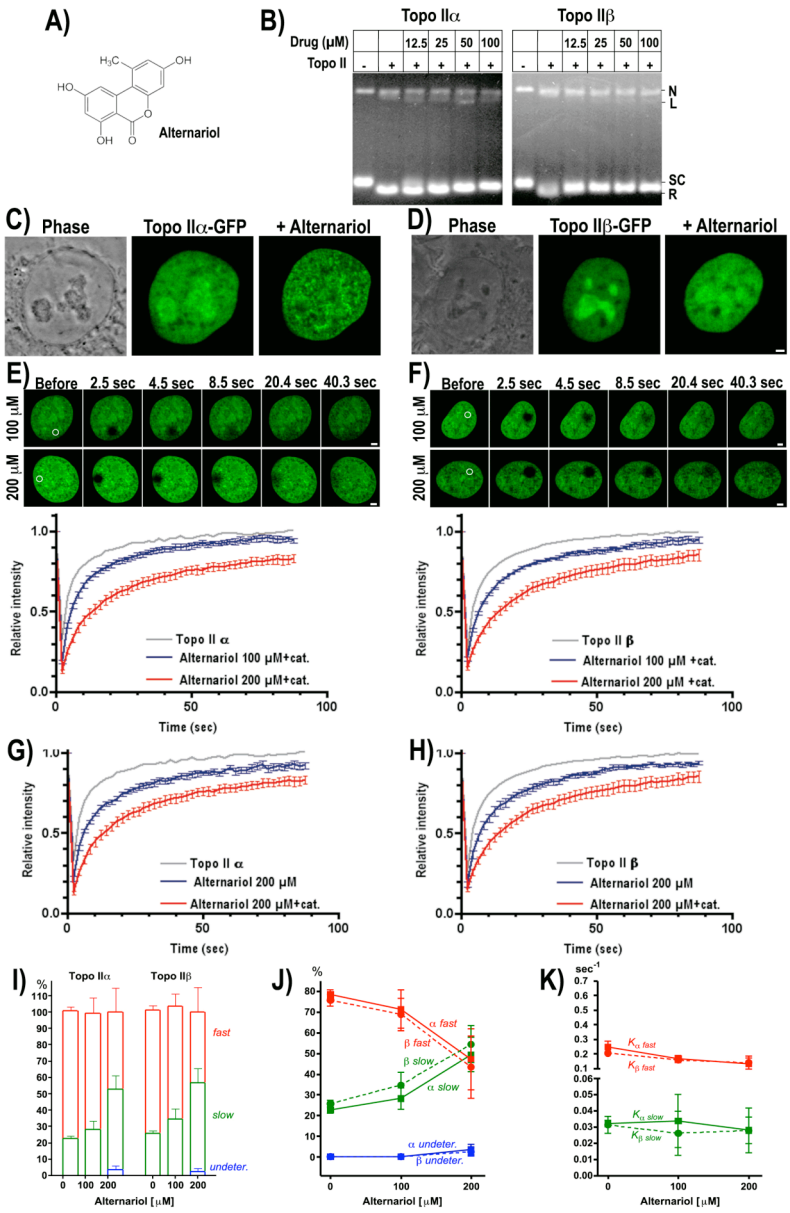

Fig. 4.3.7: **Alternariol preferentially targets the α isoform. (A)** Structure of alternariol. ((**B**) Alternariol induces linearization of pUC18 plasmid mediated by Topo IIα. Supercoiled pUC18-DNA (400 ng) was either reacted with recombinant Topo IIα (left) or Topo IIβ (right) in the absence or presence of increasing concentrations of alternariol. (**C and D**) Alternariol induces relocalization of Topo IIα (C) and to less extent of Topo IIβ (D) from nucleoli to the nucleoplasm after exposure to (200 μM, 10 min). **E and F**) FRAP curves determined in the nucleoplasm of cells expressing Topo IIα-GFP (E) or Topo IIβ-GFP (F) treated with 100 (blue) or 200 μM alternariol (in presence of 100 U/ml catalase in media) for 20 min (red) or not (grey). Each curve is the mean of at least 10 FRAP measurements.(**G and H**) FRAP curves of cell expressing Topo IIα (G) and Topo IIβ (H) treated with 200 μM alternariol (blue) or 200 μM alternariol in presence of 100 U/ml catalase. (**I, J, and K**) as disscused in (Fig. 4.3.2 G-I).

Topo II towards the cleaved state resulting in an enhanced recruitment to the DNA-engaged state without significantly altering the mobility of this state. Most notably, the effect of alternariol on *in vivo* mobility was not significantly different between Topo IIα and IIβ, despite the preference of the drug for the α-form detectable *in vitro*.

In summary, alternariol markedly differs from *bona fide* Topo II poisons by not decreasing the mobility of DNA engaged Topo II and/or inducing ultraslow populations of the enzyme. However, it stimulates Topo IIα DNA cleavage *in vitro* and induces a recruitment of Topo IIα and IIβ to the DNA engaged state *in vivo*. It seems uncertain, whether these rather discrete effects of alternariol on the cellular disposition of Topo II are indeed the molecular basis of its toxitity, especially when taking into account that these effects are much attenuated when H_2O_2 is present in the extracellular millieu.

4.3.3.2 Putative Topo IIβ – selective poisons

The **phenanthridine alkaloid lycobetaine** (Fig. 4.3.8 A) has been isolated as a minor constituent from several plant species of the family Amaryllidaceae. The anticancer properties of these plants were already known in the fourth century B. C., when Hippocrates used oil from the daffodil *Narcissus poeticus* for the treatment of uterine tumors (Evidente et al., 2009). Lycobetaine is thought to act as a specific Topo IIβ poison because *in vitro*, it stimulates DNA cleavage by recombinant human Topo IIβ but not recombinant human Topo IIα (Barthelmes et al., 2001). I could confirm this by showing that lycobetaine stimulated plasmid linearization by Topo IIβ but not Topo IIα (Fig. 4.3.8 B). In further agreement with previous studies of lycobetain (Barthelmes et al., 2001) I found that the drug shifted the electrophoretic mobility of plasmid DNA in manner dependend on the dose of the drug and the presence of Topo IIα or IIβ. It has been suggested that this could be due to lycobetain stimulating the creation of positive DNA supercoils by Topo II by its DNA intercalative properties (Barthelmes et al., 2001). However, in the living cell, the drug did not induce nucleolar depletion of either Topo II isoform (Fig. 4.3.8 C,D) nor notable alterations of the mobility of the enzymes (Fig. 4.3.8 E,F). Therefore, it seems unlikely that the established antiproliferative and genotoxic activity of lycobetaine could be due to Topo IIβ poisoning. It should, however, be mentioned that lycobetain had other dramatic effects on cellular DNA: It rapidly induced a massive disruption of chromatin architecture leading to extrusion of long DNA filaments from the cell nucleus (visible in Fig. 4.3.8 D). It is tempting to speculate that these effects are related to Topo II-mediated DNA-overwinding triggered by the drug *in vitro*.

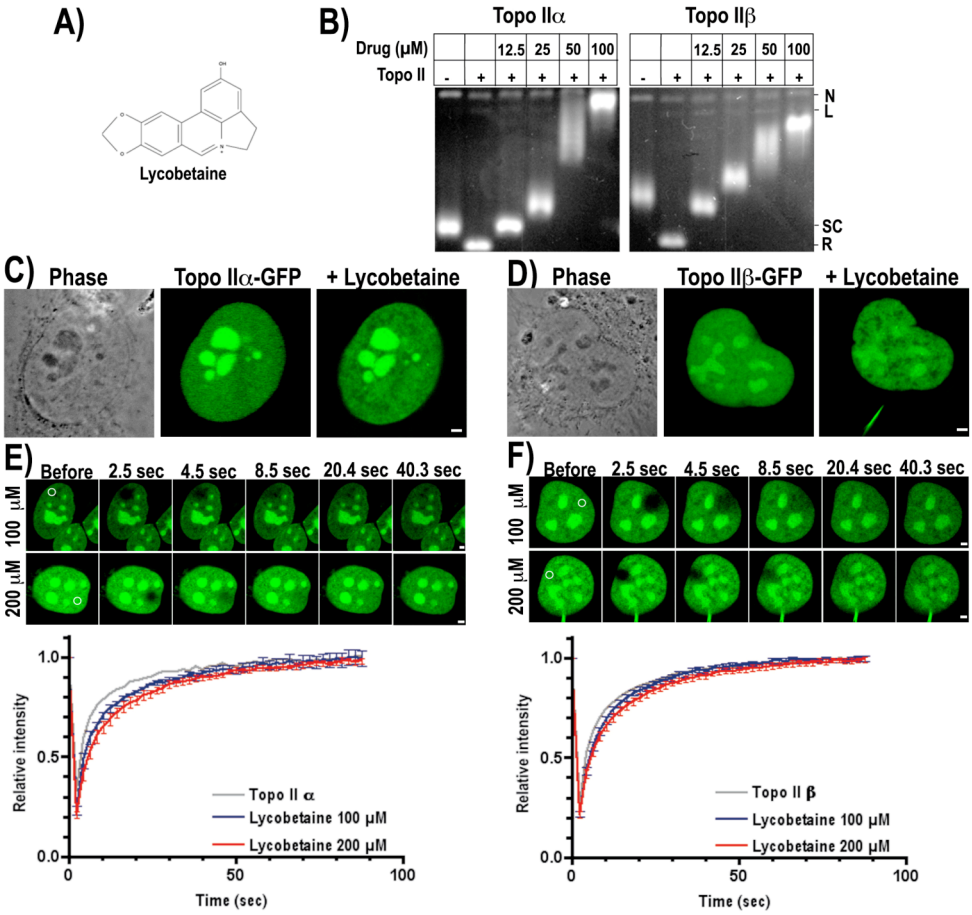

Fig. 4.3.8: **Lycobetaine preferentially targets the β isoform *in vitro*. (A)** Structure of lycobetaine. ((**B**) Lycobetaine induces linearization of pUC18 plasmid mediated by Topo IIβ. Supercoiled pUC18-DNA (400 ng) was either reacted with recombinant Topo IIα (left) or Topo IIβ (right) in the absence or presence of increasing concentrations of lycobetaine. (**C and D**) Lycobetaine did not induce relocalization of Topo IIα (C) and of Topo IIβ (D) from nucleoli to the nucleoplasm after exposure to (200 μM, 20 min). **E and F**) FRAP curves determined in the nucleoplasm of cells expressing Topo IIα-GFP (E) or Topo IIβ-GFP (F) treated with 100 (blue) or 200 μM lycobetaine for 30 min (red) or not (grey). Each curve is the mean of at least 10 FRAP measurements. over the molar concentrations.

Moreover, such a massive mobilisation of nuclear DNA could have masked retarding effects of the drug on Topo IIβ.

The quinoxaline XK469 (Fig. 4.3.9 A) was developed from the parent compound XB-947, an analog of the herbicide Assure® discovered to have anti tumor activity (Corbett et al., 1998). XK469 was the first Topo II poison reported to be β-isoform selective *in vitro* and in cultured cells and it was shown that the R-isomer was about twice as effective as the S-isomer on Topo IIβ cleavage activity (Gao et al., 1999). Studies with Topo IIβ knockout mice

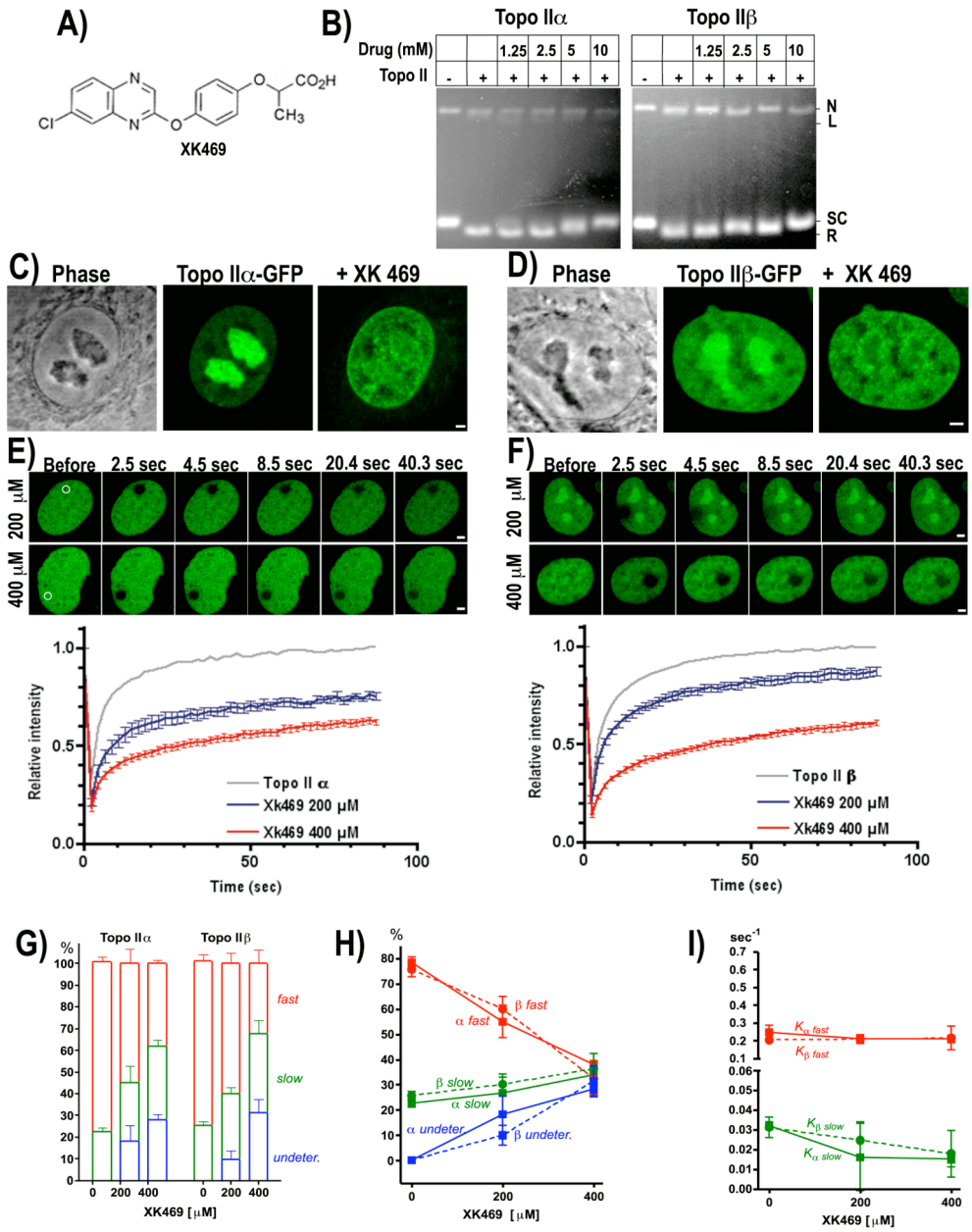

Fig. 4.3.9: **XK469 is Topo II inhibitor. (A)** Structure of XK469. (**B**) XK469 did not induce linearization of pUC18 plasmid even at very high concentrations (10 mM) but inhibits the relaxation of pUC18 mediated by α and β isoforms. (**C and D**) XK469 induced relocalization of Topo IIα (C) and of Topo IIβ (D) from nucleoli to the nucleoplasm after exposure to (200 μM, 20 min). (**E and F**) FRAP curves determined in the nucleoplasm of cells expressing Topo IIα-GFP (E) or Topo IIβ-GFP (F) treated with 200 (blue) or 400 μM XK469 for 30 min (red) or not (grey). Each curve is the mean of at least 10 FRAP measurements. (**G and H**) The percentage of slow, fast and undetermined fractions of Topo IIα and Topo IIβ derived from non linear regression of the data in F and E are plotted over the molar concentration. (**I**) The mobility ($1/t_{1/2}$) of fast and slow fractions derived from non linear regression of the data in F and E plotted over the molar concentrations.

strongly supported the notion that Topo IIβ is indeed the sole target of XK469 *in vivo* (Snapka et al., 2001). Based on encouraging pre-clinical data, a phase I trial was conducted to determine the dose limiting toxicity and maximum dose tolerated (Alousi et al., 2007). I was

not able to confirm the *in vitro* activity of XK469 as a selective Topo IIβ poison discribed in (Gao et al., 1999), rather XK469 was a very strong inhibitor of DNA relaxation (Fig. 4.3.9 B). However, the effects of XK469 on the *in vivo* disposition of Topo IIα and β exhibited the signature of a non-selective Topo II poison. The drug induced nucleolar depletion (Fig. 4.3.9 C,D) and massive retradation of both Topo II isoforms (Fig. 4.3.9 E,F). Non-linear regression analysis of FRAP curves obtained at 200 and 400 μM concentrations of XK469 revealed that the drug had an effect similar to VP16 in as much as it induced an almost quantitative switch from fast to ultraslow enzyme populations and a moderate increase and retardation of the slow population (Fig. 4.3.9 G-I). However, these effects were not notably different between Topo IIα and Topo IIβ. In fact, with respect to its impact on enzyme mobility, XK469 could be classified as the *bona fide* Topo II poison with the most equal effect on the two isoforms.

4.3.4 *In vivo* targeting of Topo IIα and IIβ by plant Polyphenols.

In the fourth part of this section, I addressed an issue that might be called the "genistein paradox". **Genistein** belongs to a familiy of plant polyphenols also comprising quercetin and a number of other flavonoids, flavones and flavanols, which have in commen that, they are quite potent poisons of Topo I (Boege et al., 1996) and/or Topo II (Bandele and Osheroff, 2007; Bandele and Osheroff, 2008; Lopez-Lazaro et al., 2007; Markovits et al., 1995; Taylor et al., 2009). Most recent studies have come to the conclusion that e.g. genistein has a potency to stimulate Topo II DNA *in vitro* and *in vivo* that is almost similar to VP16. Given the high genistein content of soy products, this would entail that asian populations are subjected to continuous Topo II poisoning equivalent to a cancer chemotherapy with etoposide. This is obviously not the case, because asian diets do not give rise to the severe side effects obligatory in cancer therapy with VP16 (nausea, lack of appetite, myelodepression, alopezia, &c.). This paradoxical situation is also given for the flavonoids prominent in western diets such as quercetin (Neukam et al., 2008). It raises the question of whether genistein and related flavone compounds indeed act as strong Topo II poisons *in vivo*. To address this question, I have measured the impact of genistein, quercetin, and epicatechin (Fig. 4.3.10 A) on the mobility of Topo IIα and IIβ in the living cell. I will present detailed data on genistein and refer related observations made with quercetin and epicatechin without showing the actual data.

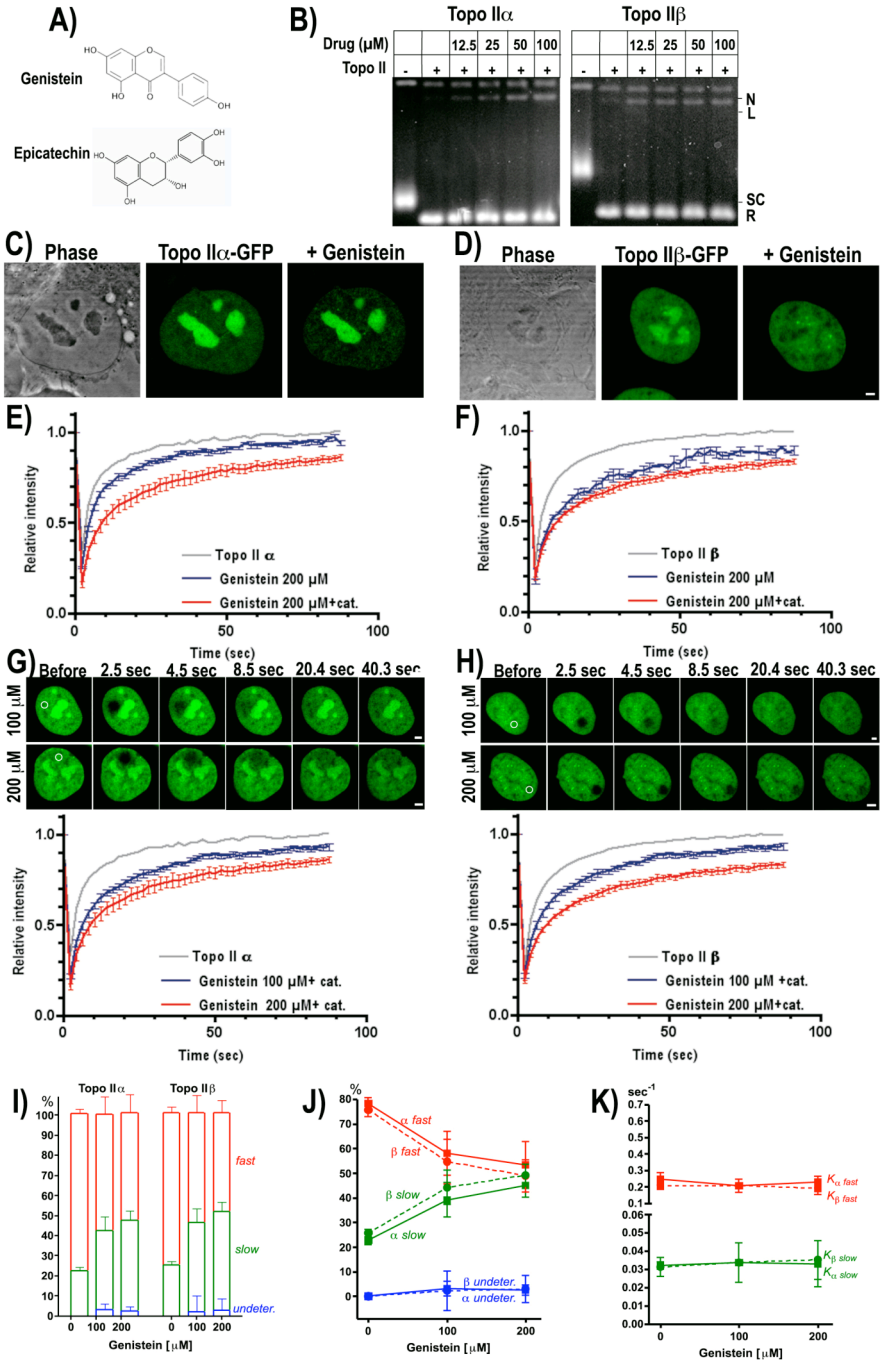

Fig. 4.3.10: **Genistein is Topo II Poison *in vitro*. (A)** Structure of genistein and epicatechin ((**B**) Genistein induces linearization of pUC18 plasmid. Supercoiled pUC18-DNA (400 ng) was either reacted with recombinant Topo IIα (left) or Topo IIβ (right) in the absence or presence of increasing concentrations of genistein. (**C and D**) Genistein induces relocalization of Topo IIα (C) and to higher extent of Topo IIβ (D) from nucleoli to the nucleoplasm after exposure to (200 μM, 20 min). **E and F**) FRAP curves determined in the nucleoplasm of cells expressing Topo IIα-GFP (E) or Topo IIβ-GFP (F) treated with 100 (blue) or 200 μM genistein (in presence of 100 U/ml catalase in media) for 20 min (red) or not (grey). Each curve is the mean of at least 10 FRAP measurements. (**G and H**) FRAP curves of cell expressing Topo IIα (G) and Topo IIβ (H) treated with 200 μM genistein (blue) or 200 μM genistein in presence of 100 U/ml catalase. (**I, J, and K**) as disscused in (Fig. 4.3.2 G-I).

In confirmation of a most recent study (Bandele and Osheroff, 2007), I found that genistein stimulated DNA cleavage by purified human Topo IIα and IIβ with an efficiency similar to VP16, and that in contrast to VP16, it induced DNA cleavage by Topo IIβ slightly more than Topo IIα (Fig 4.3.10 B). Maximal effects of genistein were observed at concentrations of 50 μM and higher. The effect of quercetin on DNA cleavage by Topo IIα and IIβ was similar to genistein albeit weaker. In contrast, epicatechin hat no such effects although it differs from quercetin only in one ketone moiety (see: Fig. 4.3.10 A). Therefore, epicatechin seemed an ideal negative control. Treatment of HT-1080 clones expressing GFP-tagged Topo II with 200 μM of genistein had no effect on the subcellular localization of Topo IIα and only a marginal effect on the localization of Topo IIβ (Fig. 4.3.10 C,D). Fitting this observation, 200 μM genistein hat no effect at all on FRAP of Topo IIα and only an insignificanat effect on FRAP of Topo IIβ (Fig. 4.3.10 E, F). However, a significant and dose dependent retardating effect of 200 μM genistein on both Topo II isoforms was observed when the medium was first treated with catalase (Fig. 4.3.10 G,H), suggesting that genstein just like alternariol (see: 4.3.7 H,I) and various other antiproliferative plant polyphenols (Kern et al., 2007) is rapidly inactivated by cell generated H_2O_2. Attenuation of FRAP kinetics by genistein following catalase treatment was analysed by non linear regression. The parametric results are summarized in (Fig. 4.3.10 I-K). Similar to alternariol, genistein induced a switch form fast to slow enzyme populations in a dose dependent manner (Fig. 4.3.10 J). At both concentrations tested, fast and slow Topo II populations added up to 100% excluding significant induction of an ultraslow fraction (Fig. 4.3.10 I). Moreover, FRAP rates of fast and slow populations were not signifcantly altered (Fig. 4.3.10 K) indicating that the drug did not significantly influence overall exchange rates of the DNA-engaged enzyme population, which excludes a significant prolongation of any step in the catalytic cyle. It should be noted that the Topo II retarding effects of genistein has no isoform preference. Similar although even less pronounced effects on the mobility of Topo IIα and IIβ were seen with quercetin, whereas epicatechin had no effect at all (not shown).

In summary, these findings suggest that stimulation of Topo II DNA cleavage by genistein, quercetin and related plant polyphenols seen *in vitro* and with cell destructive assays (Bandele and Osheroff, 2007) is due to a discrete shift of the cleavage-/religation equilbria of Topo IIα and IIβ towards the cleaved state resulting in an enhanced recruitment to the DNA-engaged state without significantly altering the mobility of this state. This effect of genistein is in clear contrast to Topo II poisons with established anti tumor activity, which

all significantly decrease the mobility of DNA-engaged Topo II and/or induce ultraslow populations of the enzyme.

5. Discussion

Inhibitors of Topo I and II are the most potent and widely used cancer drugs. Topo directed effects are thought to also contribute to environmental and food toxicity. Polyphenols, the most abundant antioxidants in our diet, benzene, an important industrial solvent and precursor for the production of drugs, plastics, synthetic rubber, and dyes, and paracetamol metabolite, the widely used over the counter analgesic, were considered as Topo targeting agents (Bender et al., 2004; Fehr et al., 2008; Lindsey et al., 2005a; Lindsey et al., 2005b). Due to the wide distribution of Topo targeting substances in nature, they should be equivalent to a daily dose of cancer chemotherapeutic agents. However, this obviously is not the case because we do not have the side effects of Topo cancer drugs. This discrepancy might be due to *in vivo* factors, which process these agents like bioavailability or metabolic turnover. Therefore, I conducted an efficient *in vivo* and *in vitro* comparison between standard Topo II drugs (used for long time as anticancer) and certain environmental substances using an experimental model enabling the study of Topo in living cells (Christensen et al., 2002b; Christensen et al., 2002c).

Piloting studies indicated that activity and drug-susceptibility of Topos is significantly influenced by the cell cycle. Therefore, Topo-directed effects must be correlated to the cell cycle stage. To distinguish in a given cell between sub-stages of interphase, I used PCNA and the transcription-initiating factor Cdc6. Several unexpected behaviors of Cdc6 were noticed, making Cdc6 localization and dynamics one part of the results mentioned in this work. By co-expression of these markers and Topos as differently coloured biofluorescent protein chimera, we will provide a cell-based assay for monitoring Topo-directed effects that are biologically relevant.

5.1 Disposition and function of topoisomerase during interphase

5.1.1 Our model is suitable and adequate

To evaluate the effect of various Topo drugs during different cell cycle stages on living cells, biomarkers were first established that allow distinguishing in a given cell between mitosis and interphase, and between sub-stages of interphase. In the first part of my thesis I

presented demonstrate the validity of Cdc6-YFP and CFP-PCNA proteins as cell cycle markers. The specific association of PCNA with the replication machinery enables differentiation between S phase stages, whereas localization of Cdc6 were used to distinguish G1 phase and G2/S phases. Separated co-expression of PCNA or Cdc6 with Topo I, IIα or IIβ, as differently coloured bio-fluorescent proteins allowed the detailed microscopic analysis of the cell cycle-specific behaviour and response to drug-inhibition of the Topos. Observed effects could then be correlated to *in vitro* effects by means of conventional relaxation and cleavage assays. We have thus established a system to monitor Topo directed effects of small molecules in living cells in conjunction with their cell cycle position. To date, this bioassay is the closest available approximation to the *in vivo* situation. We are now in a position to monitor the *in vivo* response of Topo to environmental noxae and food constituents in toxicological studies and to screen chemical libraries for new candidate cancer drugs.

The growth and morphology of cell clones expressing Topo I, IIα, or IIβ tagged YFP together with cell cycle marker did not differ from transfected cells only expressing Topo-tagged fluorescent protein investigated before (Christensen et al., 2002b; Christensen et al., 2002c; Linka et al., 2007). In addition, localization, mobility and relocalizaton upon Topo poison treatment were identical to previous findings. Thus, co-expression of Topos with PCNA or Cdc6 seemed well suited to resolve long-standing questions about the spatiotemporal distribution of Topos during interphase in living cells. In addition, western blotting showed that only full-length proteins were expressed at near physiological levels.

5.1.2 Specific functions of human topoisomerases *in vivo* during cell cycle

This part of my study provides a detailed description of the localization and activity of Topo I, Topo IIα, and Topo IIβ in human HT-1080 cells during each stage of interphase. On first glance, I found that all human Topos are localized in the nucleoplasm and concentrated in the nucleoli at all stages of cell cycle, in agreement with previous studies (Christensen et al., 2002c; Linka et al., 2007; Petrov et al., 1993; Zini et al., 1992; Zini et al., 1994) It has also been suggested that nuclear sites where Topos accumulates do not necessarily represent sites where the enzymes are most actively engaged in DNA catalysis. This was most evident in nucleoli, where Topo II concentration is highest and reloclized from nucleoli to the nucleoplasm upon Topo poison treatment indicating the place where enzyme stabilized at its

active state on the DNA that is why the use of DRT assay was important to test the activity of Topo at its localization area.

A more detailed observation shows that Topo I and Topo IIα concentrated in the nucleoli in G1 and G2 phases, whereas Topo IIβ is less concentrated in nucleoli in G1 and G2 phases. Our finding was not in agreement with a previous immunohistochemical study suggesting that Topo IIβ is completely excluded from the nucleoli (Meyer et al., 1997). Nevertheless, This finding shows that Topo II β have a role in transcription of nonribosomal RNA carried out in the nucleoplasm in G1/G2 phases. Consistent with the well-established role of Topo I in rDNA transcription, I found that Topo I concentrated at the fibrillar centers within nucleoli, throughout interphase, which has been postulated from the observation that Topo I co-lolocalizes with RNA polymerase I (Christensen et al., 2002a; Christensen et al., 2004).

On the other hand, the precise role of Topo II in nucleoli is unknown. Firstly it is excluded from the sites of rDNA transcription. An attempt to answer the question why Topo II accumulate in nucleoli to such an extent was previously suggested in (Christensen et al., 2002b; Christensen et al., 2002c). One possible explanation would be that nucleoli serve as storage places for enzyme molecules that should not be active in the chromatin at a given time. Thus, dosage of Topos in the extra-nucleolar chromatin might be regulated by nucleolar accumulation and release. At any given time, the nucleoli contain more Topo than can plausibly be required for the organization of the topological organization of the nucleolar chromatin (rDNA), which is small in comparison to the entire genome.

Unlike Topo IIα, which is specifically expressed only in proliferating cells where it resolves intertwined chromosome pairs during mitosis (Christensen et al., 2002c; Grue et al., 1998; Linka et al., 2007), Topo II β is apparently dispensable for cell growth (Austin and Marsh, 1998). However, targeted disruption of the mouse TOP2B gene showed that it has a critical role in neural and neuromuscular development (Lyu et al., 2007; Lyu et al., 2006; Lyu and Wang, 2003; Yang et al., 2000). The intranuclear localization of Topo IIβ shown here and the expression pattern of Topo IIβ together with its association with gene promotor regions (Ju et al., 2006; Ju and Rosenfeld, 2006) suggest that Topo IIβ is involved mainly in transcription of in the nucleoplasm in G1 and G2 phases.

Moreover, I found that Topo I and Topo IIα co-lolocalize with replication spots, whereas Topo IIβ shows only subset localization of replication spots. Consistent with this, it has recently been reported that catalytically active Topo IIα accumulates at late replicating chromatin (Agostinho et al., 2004). A role for the Topo IIα isoform in releasing the positive

supercoils infront of replication fork is also proposed recently, because Topo IIα relaxes positively supercoiled plasmids >10-fold faster than negatively supercoiled molecules. In contrast, Topo IIβ, which is not required for DNA replication to such an extent, displays no such preference (McClendon et al., 2008; McClendon et al., 2005). The association of Topo I with the replication foci shown here is supported by multiple biochemical observations (Khopde et al., 2008; Khopde and Simmons, 2008).

Thus, only Topo I and IIα have fundamental functional roles in replication. I assume that Topo I relax the positive supercoils that preceed the replication fork. Inaddition, type II Topos may also function ahead of the replication machinery and it is probably the α isoform that relaxes positive supercoils ahead of replication and removes the intertwining at the last step of replication. Thus, the localization study carried out in this study further supports that topological constraints created by the replication process is mainly removed by Topo I and Topo IIα and the strong accumulation of Topo IIβ in the nucleoli in S phase cells might indicate that this enzyme is not vital during replication.

FRAP analysis revealed that all Topos have similar mobilities in G1, G2, and S phases. Thus, it seemed likely that the FRAP method is not sensitive enough to detect a retarded mobility of Topos taking place in the replication or transcription process. Recently, it was reported that the Topo IIβ isoform is implicated in the initiation of DNA replication of Kaposi sarcoma associated herpes virus, which utilizes the host molecular machinery in order to proliferate (Wang et al., 2008). In agreement, I find that Topo IIβ possesses a weak-binding capability to human replication spots suggesting a DNA replication- specific role for this isoform (Rampakakis and Zannis-Hadjopoulos, 2009).

5.2 Topo II directed effects of cancer drugs, environmental toxins and food ingredients

5.2.1 An attempt at a new classification of Topo II targeted compounds according to their effect on enzyme mobility *in vivo*

Christensen *et al* showed that Topo poisons actually render Topos less mobile in the genome of a living cell, and that, given a sufficient dose, most if not all of the enzyme molecules present in the cell nucleus are affected (Christensen et al., 2002b; Christensen et

al., 2002c). Secondly, they showed that these drugs induce a relocation of the enzyme from the nucleolus to the nucleoplasm. Thirdly, they have proposed a model by which non-linear regression analysis of FRAP data can be used to calculated free and DNA-engaged fractions of Topo and to assess the effect of Topo poisons in quantitative terms (Christensen et al., 2002b). This approach has meanwhile been subjected to substantial biomathematical evaluation and generalisation for other nuclear proteins (Schmiedeberg et al., 2004). Thus, it can be considered as an established procedure for the quantitative assessment of the mobility of nuclear proteins. Here, I have take advantage of these models and methods to evaluate archetypical Topo II drugs *in vivo* and, most notably, to assess by this means the isoform-bias of various substances that are either clinically established Topo II poisons or xenobiotics believed to follow this mechanims of action. Based on the quantitative effects of these various Topo II targeted drugs on the mobility of Topo IIα and IIβ in the living cell summarized in Table 2, I would like to suggest the following new classification of such compounds:

Table 2 Drug effects on mobility of Topo IIα or Topo IIβ *in vivo*.

	effective dose [μM]	free (fast) fraction	DNA-bound (slow) fraction	mobility of DNA-bound (K_{slow})	stalled (undetermined) fraction	Inhibition Type Isoform bias
VP16	50	α:↓↓↓ β:↓↓	↔	α:↓↓↓ β:↔	α:↑↑↑ β:↑↑	stalling **α >> β**
XK469	400	↓↓	↔	↓↓	↑↑	stalling α = β
m-AMSA	25	↓↓↓	↑↑	↓↓	α:↑↑↑ β:↑	stalling **α > β**
DOX	25	↓↓↓	↑↑	↔	α: ↔ β:↑↑	stalling **β > α**
MITOX	50 non-equil.	↓↓↓↓	↑↑↑	N.D.	↑↑	stalling α = β
Genistein	200	↓	↑	↔	↔	recruitment β (>) α

Alternariol	200	↓↓	α:↑ β: ↑↑	↔	↔	recruitment **β (>) α**
ICRF-187	100	↓↓	↑↑(↑)	↓↓↓↓	↔	tethering β (>) α

↑, ↓: each symbol represents a 20% alteration in the direction indicated. Unless stated, effects were similar for Topo IIα and Topo IIβ.

↔: No or statistically insignificant changes

N.D.: not determined because reaction equilibria could not be established.

Symbols in brackets indicate trends that are not statistically significant

(i) Stalling Topo II poisons. This group encompasses the established cancer therapeutics VP16, m-AMSA, DOX and MITOX as well as the experimental drug XK469. Common to these compounds is that they reduce mobility of a significant portion of the cellular complement of Topo IIα and/or IIβ to such an extent that enzym fractions impose as immobile. Most of these compounds also increase and retard the normal DNA-engaged enzyme fraction in a manner increasing with dose, suggesting that they induce a stochastic spectrum of Topo II retarding events leading to virtual immobility as a cumulative endpoint. These retarding and immobilizing effects can be biased towards Topo IIα (VP16 and m-AMSA) or Topo IIβ (DOX) or be α–/β–unbiased (MITOX and XK469).

(ii) Topo II DNA tethering drugs. This group comprises ICRF-187 and probably several related compounds that also stabilize the closed clamp formation of Topo II by inhibiting the ATPase domain. These drugs progressively recruit Topo II to the DNA engaged state, by prolonging this state in a discrete manner. At the endpoint this drugs are likely recruit the entire Topo II complement to the DNA engaged state, without inducing a virtually immobile enzyme population.

(iii) Topo II DNA recruiting drugs. This group comprises alternariol, genistein, quercetin and probably most other flavonoids reported to stimulate Topo II – DNA cleavage. These drugs seem to affect a discrete shift in the cleavage-/religation equilibrium of Topo II, which produces a dramatic effect *in vitro* or destructive *in vivo* assays. However, these compounds have a very minor effect on enzyme mobility in the cell consisting of a limited

enhancement of enzyme recruitment to the DNA engaged state, without a change in mobility of this state.

5.2.2 A reappraisal of Topo II targeted cancer drugs

Inhibitors of Topos II play an important role in anticancer chemotherapy. Actually, there are only very few therapy regimens currently in use that do not employ at least one Topo II-targeted drug. Most important in this respect are those compounds that inhibit the second transesterification step of the catalytic cycle and thus prolong the half-life of the covalent catalytic DNA-intermediate. Both isoform have been implicated in *in vitro* drug action with similar cleavage site specificities for most Topo poisons (Austin and Marsh, 1998; Marsh et al., 1996). This suggests that, if Topo IIα and β differ *in vivo*, it must arise from factors other than the simple drug-DNA-Topo interactions, such as the level of cleavage complex, intracellular level of Topo IIα and β, or target accessibility, about which little is known. The data presented here allow me to address some of these issues.

The first crucial finding of my study relates to the half life of durg induced Topo II-DNA compelxes. I find that all clinical successful Topo II poisons actually induced ultraslow populations of Topo II. Thus near immobilization of the enzymes measured in a non destructive manner in the living cell by FRAP seems to be a feature more clearly related to cytotoxicity than DNA cleavage and covalent DNA-attachment of Topo II measured by cell and tissue assays involving cell lysis and subsequent immunbiochemical or immunhistochemical analysis, such as the "ICE bioassay" (Bandele and Osheroff, 2008; Bender et al., 2008), the "TARDIS bioassay" (Padget et al., 2000; Willmore et al., 1998) or alkaline elution (Kohn et al., 1981)). Interestingly, the latter class of assays as well as *in vitro* assays measuring plasmid cleavage by purified Topo II all seem unable to distinguish between stimulation of cleavage or increase in DNA-engagement of Topo II and a true stabilization of long-lived Topo II-DNA-inermediates. A recent study using these indiscriminating assays in conjunction with treatment-recovery cycles could demonstrate that Topo II-DNA-complexes induced by VP16 have a half life five times as long as the ones induced e.g. by genistein. By comparison with markers of DNA damage inflicted by the two drugs the authors concluded that the efficacy of topoisomerase II-targeted anticancer agents reflects the persistence of drug-induced cleavage complexes in cells (Bandele and Osheroff, 2008). On the basis of my own findings, I fully aggree with the latter conclusion. Moreover, my data suggest that the difference between the drugs could be even greater, since VP16 decreases the exchange rate of Topo-DNA-complexes at least 100-fold more than Genistein.

Interestingly, my data provide furthermore evidence that MITOX could have an even longer lasting effect than VP16, since the effect of this drug on Topo II mobility did not reach equilibrium. The most probable explanation for this phenomenon is that Topo II-DNA-complexes stabilized by MITOX could be near irreversible, thus precluding establishment of an equilibrium. This would also explain why MITOX has the capability to induce Topo II -mediated chromosome translocations even when administered at the very low doses used for immunosuppresive thera regimen (Hasan et al., 2008).

A second crucial finding of my study relates to the isoform-bias of Topo II poisons that are established in cancer therapy. I find that most of these drugs have a certain preference for Topo IIα or target both substances in a similar manner. This is in good agreement with some of the previous pharmacological studies (Austin and Marsh, 1998; Drake et al., 1989). It supports the notion that Topo IIα is the major target for the antiproliferative action of these drugs and improvement of the therapeutic principle could be gained by developing α-selective poisons. Interestingly, my data suggest that there could be two ways towards this goal. One is exemplified by m-AMSA, where α−selectivity is not attained through a higher affinity of the drug to Topo IIα but rather through a β-selective autolimitation of an primarily isoform-unselective poisoning effect. This mechanism seems to be employed by the new α-selective drug (NK314), which is an aminoacridine derivative just like m-AMSA and reported to act Topo II α-selective (Toyoda et al., 2008). Unfortunately, NK314 was not made available to me. Therefore I could not follow up on this hypothesis. The other way towards increasing α-selectivity could be based on VP16, whose poisoning effect seems to have a higher affinity for Topo IIα than Topo IIβ. One could use *in vivo* mobility of Topo IIα and IIβ as an experimental readout of a re-screen of podophyllotoxin derivatives and might thus find strong Topo II poisons that are even more α-selective than VP16.

The only class of Topo II poison currently in clinical which I find to have a clear bias towards the β-form are antracyclins such as DOX. β-selectivity of DOX shown here is a new finding. However, it fits to the long standing observation that antracyclins have a signature of side effects significantly diffenerent form all other Topo II poisons. Most notably, antracyclins are the only Topo II poisons that are dose limited by cardiotoxicity, and this adverse effect is believed to be mediated by poisoning of Topo IIβ (Austin and Marsh, 1998; Azarova et al., 2007; Gatto and Leo, 2003) which is the only Topo II isoform found in non-proliferating heart cells (Turley et al., 1997). Therefore, my finding provides a rational basis for developing or improving protective drugs that ameliorate the cardiotoxicity of antracyclins. Currently, the catalytic inhibitor ICRF-187 is used to counteract the

cardiotoxicity and thus allow for a dose escalation of antracyclins (Hellmann, 1998; Lyu et al., 2007). This effect is thought to be due to inactivation of Topo IIβ, whose poisoning is believed to confer the cardiotoxity of antracyclins (Austin and Marsh, 1998; Azarova et al., 2007; Gatto and Leo, 2003). However, I can show here that ICRF-187 is not selective for Topo IIβ, but rather seems to has some bias towards Topo IIα. Therefore, it is to be expected that cotherapy of ICRF178 and anthracyclins compromises the antiproliferative effect of the anthracyclines, which involves Topo IIα mediated generation of DNA-damage. In keeping with this, ICRF-187 was recently found to cause Topo IIα depletion, thereby reducing the DOX induced accumulation of DSB although this did not reduce DOX induced apoptosis (Yan et al., 2009). This may in part be due to the fact that ICRF-187 and other bisdioxopiperazines have some anti-cancer activity of their own, which is accredited to depletion of Topo IIα essential in mitosis (Huang et al., 2001; Wang and Eastmond, 2002). However, to me it seems meaningful to develope a β-selective catalytic inhibitor to be used as specific quencher for Topo IIβ-mediated side-effects of Topo II poisons.

Thirdly, I would like to comment on my striking finding that the putative β-selective poison XK469 in my hands behaved like an isoform-unselective Topo II poison. I cannot exclude that the substance commercially available to me was different from the one used in previous trials. However, it seems that the preclinical data previously obtained with XK469 would actually fit much better to an isoform-unselective Topo II poison than a β-selective one. XK469 has been found to have a very prominent activity against solid tumors and it was argued that this could be explained by the cell cycle regulation of Topo IIα and Topo IIβ (Corbett et al., 1998) and the fact that solid tumors tend to develop large G0 populations (Gao et al., 1999; Pitot, 1986). Therefore it was assumed that the selectivity of XK469 for Topo IIβ may allow selective targeting of solid tumors with significantly less toxicity for rapidly proliferating normal tissues and leukemias with high S-phase fractions and relatively high levels of Topo IIα (Gao et al., 1999; Gao et al., 2003). To explain the tumor selectivity of the drug it was argued that although both solid tumors and many normal tissues would be expected to have large G0 populations expressing only Topo IIβ, the solid tumor cells might be more likely to have defects in cell cycle checkpoints that prevent replication in the presence of DNA damage caused by drug-stabilized Topo IIβ DNA cleavage complexes. The fault with this argumentation seems to be that a number of more recent studies strongly point to Topo IIα as an essential target in cancer chemotherapy, since it is the isoform essential for DNA proliferation (Carpenter and Porter, 2004; Grue et al., 1998; Linka et al., 2007). Moreover, it has been shown that poisoning of the “housekeeping enzyme” Topo IIβ in non-

proliferative compartments and tissues, such as the heart or the skin, could mostly contribute to the dose-limiting toxicity of Topo II poisons (Austin and Marsh, 1998; Azarova et al., 2007; Gatto and Leo, 2003). Conversely, it has been argued that simultaneous formation of DNA cleavage complexes by Topo IIα and Topo IIβ is more likely to induce permanent DNA strand breaks in a given cell nucleus, since the two isoforms are involved in different DNA-metabolic processes (Austin and Marsh, 1998; Gatto and Leo, 2003). The bottom line of this that one would expect that an a-selective Topo II poison would ve more effective in killing rapidly growing tumors, whereas targeting of both isoforms is required for a drug effective against slow growing tumors. Since the latter profile is the one emerging for XK469 from recent phase I clinical trial (Alousi et al., 2007) it seems feasible that the drug could actually be an strong but isoform-unselective Topo II poison, as suggested by my findings.

5.2.3 The hazard of Topo II targeted toxins in food

Flavonoids are widely distributed in foods and beverages of plant origin, such as fruits, vegetables, tea, cacao, and wine (Ross and Kasum, 2002). A large body of literature exists regarding their content in various foods. For example, cherry tomatoes contain six times more quercetin per gram fresh weight than do normal size varieties of tomatoes. Only a few estimations of dietary intake of flavonoids are available. Hertog estimated intake of flavonols, flavones, and flavanones in the Netherland to be 23 mg/day (Hertog et al., 1993). The bioavailability of quercetin after ingestion of 139 mg polyphenols from onions resulted in an increase of the plasma concentration to 1.35 μM. The plasma concentration of epigallocatechin gallate after ingestion of 525 mg polyphenols found in green tea is 4.4-5 μM (Scalbert and Williamson, 2000). The polyphenol concentration in the gut should be much higher than in the plasma. For example, the dilution of 500 mg of polyphenols in the colon would give a local concentration of 3 mM. Such a high local concentration in the colon might contribute to anticarcinogenic effect (Scalbert and Williamson, 2000). The consumption of 300 ml of red wine containing about 500 mg of polyphenols leads to total polyphenols in plasma of 50 μM (Scalbert and Williamson, 2000). In my study the concentration of bioflavonoids ranged from 100-200 μM *in vivo* and 25-100 μM *in vitro*.

Genistein and some related compounds have been shown to induce Topo mediated DNA cleavage in mammalian cells (Bandele and Osheroff, 2007; Bandele and Osheroff, 2008; Boege et al., 1996). Thus, Topos-mediated DNA damage seems to be a candidate mechanism, by which some flavonoids may exert a cytotoxic potential believed to contribute

their protective effect against the development of carcinomas in animal models (Taylor et al., 2009). Likewise it has been argued that the mutagenic potential of the flavonoid alternariol which is a food contaminant arises form its potential to poison Topo IIα (Fehr et al., 2008). However, the cytotoxic activity of polyphenols such as genistein or alternariol differs from that of well-characterized Topo II poisons. Recent studies investigating the simultaneous treatment of cells with genistein and VP16 indicated that the differential actions of the two compounds are not related to the effects of genistein on cellular processes other than its activity against Topo II. Rather, they appear to result from a longer persistence of cleavage complexes induced by VP16 as compared to genistein (Bandele and Osheroff, 2007; Bandele and Osheroff, 2008). In support of this notion, I find here that effects of genistein and alternariol on Topo II mobility in the living cell are much less pronounced than those of therapeutic Topo II poisons. It seems that the polyphenols just induce an enhaced recruitment of the enzymes to the DNA engaged state without notably altering the mobility of this state. Moreover these effects were severly compromised by cell-generated H_2O_2 and only seen at concentrations which are 100-fold higher than the maximal bioavailability of genistein in serum of 1 μM following a meal rich in soy products (Scalbert and Williamson, 2000). Finally, it has been shown that genistein depresses the expression of its putative traget Topo IIα through regulation of specificity protein 1 and specificity protein 3 (Zhou et al., 2009). In summary, these findings make it unlikely that food constituents such as genistein or quercetin or mycotoxins such as alternariol are efficient Topo II poisons *in vivo*.

In this context it is also worth to consider that the effects of bio-flavonoids on Topo II are highly variable between species (Bandele and Osheroff, 2007), which seems to point at an evolutionary adaptation. It has been a long standing question how plants synthesizing Topo poisons are able to grow in the presence of such agents. One mechanism seems to be sequestration in vacuoles (Rea, 2007), which keeps these substances away from the gemome. In plants producing the Topo I poison camptothecin it has also been shown that evolution of the toxin has been accompanied by an evolution of mutations in the target enzyme that are similar to the ones evolving in human cancer cells upon continous exposure of camptothecin (Sirikantaramas et al., 2009). Along the same lines it seems conceivable that a coevolution is taking place that adapts the polyphenol content of (cultured) food plants and and their putative targets of cytotoxicity such as topoisomerases.

6. References

Agostinho, M., Rino, J., Braga, J., Ferreira, F., Steffensen, S. and Ferreira, J. (2004) Human topoisomerase IIalpha: targeting to subchromosomal sites of activity during interphase and mitosis. *Mol Biol Cell*, **15**, 2388-2400.

Alexandrow, M.G. and Hamlin, J.L. (2004) Cdc6 chromatin affinity is unaffected by serine-54 phosphorylation, S-phase progression, and overexpression of cyclin A. *Mol Cell Biol*, **24**, 1614-1627.

Alousi, A.M., Boinpally, R., Wiegand, R., Parchment, R., Gadgeel, S., Heilbrun, L.K., Wozniak, A.J., DeLuca, P. and LoRusso, P.M. (2007) A phase 1 trial of XK469: toxicity profile of a selective topoisomerase II beta inhibitor. *Invest New Drugs*, **25**, 147-154.

Alsner, J., Svejstrup, J.Q., Kjeldsen, E., Sorensen, B.S. and Westergaard, O. (1992) Identification of an N-terminal domain of eukaryotic DNA topoisomerase I dispensable for catalytic activity but essential for in vivo function. *J Biol Chem*, **267**, 12408-12411.

Andoh, T. (1998) Bis(2,6-dioxopiperazines), catalytic inhibitors of DNA topoisomerase II, as molecular probes, cardioprotectors and antitumor drugs. *Biochimie*, **80**, 235-246.

Andoh, T. and Ishida, R. (1998) Catalytic inhibitors of DNA topoisomerase II. *Biochim Biophys Acta*, **1400**, 155-171.

Arias, E.E. and Walter, J.C. (2006) PCNA functions as a molecular platform to trigger Cdt1 destruction and prevent re-replication. *Nat Cell Biol*, **8**, 84-90.

Attia, S.M., Al-Anteet, A.A., Al-Rasheed, N.M., Alhaider, A.A. and Al-Harbi, M.M. (2009) Protection of mouse bone marrow from etoposide-induced genomic damage by dexrazoxane. *Cancer Chemother Pharmacol*, **64**, 837-845.

Austin, C.A. and Marsh, K.L. (1998) Eukaryotic DNA topoisomerase II beta. *Bioessays*, **20**, 215-226.

Azarova, A.M., Lyu, Y.L., Lin, C.P., Tsai, Y.C., Lau, J.Y., Wang, J.C. and Liu, L.F. (2007) Roles of DNA topoisomerase II isozymes in chemotherapy and secondary malignancies. *Proc Natl Acad Sci U S A*, **104**, 11014-11019.

Bailly, J.D., Skladanowski, A., Bettaieb, A., Mansat, V., Larsen, A.K. and Laurent, G. (1997) Natural resistance of acute myeloid leukemia cell lines to mitoxantrone is associated with lack of apoptosis. *Leukemia*, **11**, 1523-1532.

Baird, C.L., Harkins, T.T., Morris, S.K. and Lindsley, J.E. (1999) Topoisomerase II drives DNA transport by hydrolyzing one ATP. *Proc Natl Acad Sci U S A*, **96**, 13685-13690.

Baker, S.D., Wadkins, R.M., Stewart, C.F., Beck, W.T. and Danks, M.K. (1995) Cell cycle analysis of amount and distribution of nuclear DNA topoisomerase I as determined by fluorescence digital imaging microscopy. *Cytometry*, **19**, 134-145.

Baldwin, E.L., Byl, J.A. and Osheroff, N. (2004) Cobalt enhances DNA cleavage mediated by human topoisomerase II alpha in vitro and in cultured cells. *Biochemistry*, **43**, 728-735.

Baldwin, E.L. and Osheroff, N. (2005) Etoposide, topoisomerase II and cancer. *Curr Med Chem Anticancer Agents*, **5**, 363-372.

Bandele, O.J. and Osheroff, N. (2007) Bioflavonoids as poisons of human topoisomerase II alpha and II beta. *Biochemistry*, **46**, 6097-6108.

Bandele, O.J. and Osheroff, N. (2008) The efficacy of topoisomerase II-targeted anticancer agents reflects the persistence of drug-induced cleavage complexes in cells. *Biochemistry*, **47**, 11900-11908.

Barthelmes, H.U., Niederberger, E., Roth, T., Schulte, K., Tang, W.C., Boege, F., Fiebig, H.H., Eisenbrand, G. and Marko, D. (2001) Lycobetaine acts as a selective topoisomerase II beta poison and inhibits the growth of human tumour cells. *Br J Cancer*, **85**, 1585-1591.

Bell, S.P. and Dutta, A. (2002) DNA replication in eukaryotic cells. *Annu Rev Biochem*, **71**, 333-374.

Bender, R.P., Jablonksy, M.J., Shadid, M., Romaine, I., Dunlap, N., Anklin, C., Graves, D.E. and Osheroff, N. (2008) Substituents on etoposide that interact with human topoisomerase IIalpha in the binary enzyme-drug complex: contributions to etoposide binding and activity. *Biochemistry*, **47**, 4501-4509.

Bender, R.P., Lindsey, R.H., Jr., Burden, D.A. and Osheroff, N. (2004) N-acetyl-p-benzoquinone imine, the toxic metabolite of acetaminophen, is a topoisomerase II poison. *Biochemistry*, **43**, 3731-3739.

Berger, J.M. (1998) Structure of DNA topoisomerases. *Biochim Biophys Acta*, **1400**, 3-18.

Berger, J.M., Gamblin, S.J., Harrison, S.C. and Wang, J.C. (1996) Structure and mechanism of DNA topoisomerase II. *Nature*, **379**, 225-232.

Berger, J.M. and Wang, J.C. (1996) Recent developments in DNA topoisomerase II structure and mechanism. *Curr Opin Struct Biol*, **6**, 84-90.

Bermejo, R., Doksani, Y., Capra, T., Katou, Y.M., Tanaka, H., Shirahige, K. and Foiani, M. (2007) Top1- and Top2-mediated topological transitions at replication forks ensure fork progression and stability and prevent DNA damage checkpoint activation. *Genes Dev*, **21**, 1921-1936.

Boege, F., Andersen, A., Jensen, S., Zeidler, R. and Kreipe, H. (1995) Proliferation-associated nuclear antigen Ki-S1 is identical with topoisomerase II alpha. Delineation of a carboxy-terminal epitope with peptide antibodies. *Am J Pathol*, **146**, 1302-1308.

Boege, F., Straub, T., Kehr, A., Boesenberg, C., Christiansen, K., Andersen, A., Jakob, F. and Kohrle, J. (1996) Selected novel flavones inhibit the DNA binding or the DNA religation step of eukaryotic topoisomerase I. *J Biol Chem*, **271**, 2262-2270.

Borlado, L.R. and Mendez, J. (2008) CDC6: from DNA replication to cell cycle checkpoints and oncogenesis. *Carcinogenesis*, **29**, 237-243.

Brill, S.J., DiNardo, S., Voelkel-Meiman, K. and Sternglanz, R. (1987) Need for DNA topoisomerase activity as a swivel for DNA replication for transcription of ribosomal RNA. *Nature*, **326**, 414-416.

Brugger, E.M., Wagner, J., Schumacher, D.M., Koch, K., Podlech, J., Metzler, M. and Lehmann, L. (2006) Mutagenicity of the mycotoxin alternariol in cultured mammalian cells. *Toxicol Lett*, **164**, 221-230.

Burden, D.A. and Osheroff, N. (1998) Mechanism of action of eukaryotic topoisomerase II and drugs targeted to the enzyme. *Biochim Biophys Acta*, **1400**, 139-154.

Byl, J.A., Cline, S.D., Utsugi, T., Kobunai, T., Yamada, Y. and Osheroff, N. (2001) DNA topoisomerase II as the target for the anticancer drug TOP-53: mechanistic basis for drug action. *Biochemistry*, **40**, 712-718.

Carey, J.F., Schultz, S.J., Sisson, L., Fazzio, T.G. and Champoux, J.J. (2003) DNA relaxation by human topoisomerase I occurs in the closed clamp conformation of the protein. *Proc Natl Acad Sci U S A*, **100**, 5640-5645.

Carpenter, A.J. and Porter, A.C. (2004) Construction, characterization, and complementation of a conditional-lethal DNA topoisomerase IIalpha mutant human cell line. *Mol Biol Cell*, **15**, 5700-5711.

Celis, J.E. and Celis, A. (1985) Cell cycle-dependent variations in the distribution of the nuclear protein cyclin proliferating cell nuclear antigen in cultured cells: subdivision of S phase. *Proc Natl Acad Sci U S A*, **82**, 3262-3266.

Chaly, N. and Brown, D.L. (1996) Is DNA topoisomerase II beta a nucleolar protein? *J Cell Biochem*, **63**, 162-173.

Champoux, J.J. (2001) DNA topoisomerases: structure, function, and mechanism. *Annu Rev Biochem*, **70**, 369-413.

Chen, G.L., Yang, L., Rowe, T.C., Halligan, B.D., Tewey, K.M. and Liu, L.F. (1984) Nonintercalative antitumor drugs interfere with the breakage-reunion reaction of mammalian DNA topoisomerase II. *J Biol Chem*, **259**, 13560-13566.

Christensen, M.O., Barthelmes, H.U., Boege, F. and Mielke, C. (2002a) The N-terminal domain anchors human topoisomerase I at fibrillar centers of nucleoli and nucleolar organizer regions of mitotic chromosomes. *J Biol Chem*, **277**, 35932-35938.

Christensen, M.O., Barthelmes, H.U., Boege, F. and Mielke, C. (2003) Residues 190-210 of human topoisomerase I are required for enzyme activity in vivo but not in vitro. *Nucleic Acids Res*, **31**, 7255-7263.

Christensen, M.O., Barthelmes, H.U., Feineis, S., Knudsen, B.R., Andersen, A.H., Boege, F. and Mielke, C. (2002b) Changes in mobility account for camptothecin-induced subnuclear relocation of topoisomerase I. *J Biol Chem*, **277**, 15661-15665.

Christensen, M.O., Krokowski, R.M., Barthelmes, H.U., Hock, R., Boege, F. and Mielke, C. (2004) Distinct effects of topoisomerase I and RNA polymerase I inhibitors suggest a dual mechanism of nucleolar/nucleoplasmic partitioning of topoisomerase I. *J Biol Chem*.

Christensen, M.O., Larsen, M.K., Barthelmes, H.U., Hock, R., Andersen, C.L., Kjeldsen, E., Knudsen, B.R., Westergaard, O., Boege, F. and Mielke, C. (2002c) Dynamics of human DNA topoisomerases IIalpha and IIbeta in living cells. *J Cell Biol*, **157**, 31-44.

Classen, S., Olland, S. and Berger, J.M. (2003) Structure of the topoisomerase II ATPase region and its mechanism of inhibition by the chemotherapeutic agent ICRF-187. *Proc Natl Acad Sci U S A*, **100**, 10629-10634.

Clay-Farrace, L., Pelizon, C., Santamaria, D., Pines, J. and Laskey, R.A. (2003) Human replication protein Cdc6 prevents mitosis through a checkpoint mechanism that implicates Chk1. *Embo J*, **22**, 704-712.

Cline, S.D. and Osheroff, N. (1999) Cytosine arabinoside lesions are position-specific topoisomerase II poisons and stimulate DNA cleavage mediated by the human type II enzymes. *J Biol Chem*, **274**, 29740-29743.

Corbett, T.H., LoRusso, P., Demchick, L., Simpson, C., Pugh, S., White, K., Kushner, J., Polin, L., Meyer, J., Czarnecki, J., Heilbrun, L., Horwitz, J.P., Gross, J.L., Behrens, C.H., Harrison, B.A., McRipley, R.J. and Trainor, G. (1998) Preclinical antitumor efficacy of analogs of XK469: sodium-(2-[4-(7-chloro-2-quinoxalinyloxy)phenoxy]propionate. *Invest New Drugs*, **16**, 129-139.

Cornarotti, M., Tinelli, S., Willmore, E., Zunino, F., Fisher, L.M., Austin, C.A. and Capranico, G. (1996) Drug sensitivity and sequence specificity of human recombinant DNA topoisomerases IIalpha (p170) and IIbeta (p180). *Mol Pharmacol*, **50**, 1463-1471.

Coutts, J., Plumb, J.A., Brown, R. and Keith, W.N. (1993) Expression of topoisomerase II alpha and beta in an adenocarcinoma cell line carrying amplified topoisomerase II alpha and retinoic acid receptor alpha genes. *Br J Cancer*, **68**, 793-800.

Coverley, D., Pelizon, C., Trewick, S. and Laskey, R.A. (2000) Chromatin-bound Cdc6 persists in S and G2 phases in human cells, while soluble Cdc6 is destroyed in a cyclin A-cdk2 dependent process. *J Cell Sci*, **113 (Pt 11)**, 1929-1938.

Cozzarelli, N.R., Cost, G.J., Nollmann, M., Viard, T. and Stray, J.E. (2006) Giant proteins that move DNA: bullies of the genomic playground. *Nat Rev Mol Cell Biol*, **7**, 580-588.

Crespi, M.D., Ivanier, S.E., Genovese, J. and Baldi, A. (1986) Mitoxantrone affects topoisomerase activities in human breast cancer cells. *Biochem Biophys Res Commun*, **136**, 521-528.

D'Arpa, P. and Liu, L.F. (1989) Topoisomerase-targeting antitumor drugs. *Biochim Biophys Acta*, **989**, 163-177.

Dalla Rosa, I., Goffart, S., Wurm, M., Wiek, C., Essmann, F., Sobek, S., Schroeder, P., Zhang, H., Krutmann, J., Hanenberg, H., Schulze-Osthoff, K., Mielke, C., Pommier, Y., Boege, F. and Christensen, M.O. (2009) Adaptation of topoisomerase I paralogs to nuclear and mitochondrial DNA. *Nucleic Acids Res*.

Danks, M.K., Schmidt, C.A., Cirtain, M.C., Suttle, D.P. and Beck, W.T. (1988) Altered catalytic activity of and DNA cleavage by DNA topoisomerase II from human leukemic cells selected for resistance to VM-26. *Biochemistry*, **27**, 8861-8869.

Delmolino, L.M., Saha, P. and Dutta, A. (2001) Multiple mechanisms regulate subcellular localization of human CDC6. *J Biol Chem*, **276**, 26947-26954.

DePamphilis, M.L., Blow, J.J., Ghosh, S., Saha, T., Noguchi, K. and Vassilev, A. (2006) Regulating the licensing of DNA replication origins in metazoa. *Curr Opin Cell Biol*, **18**, 231-239.

Diffley, J.F. (2004) Regulation of early events in chromosome replication. *Curr Biol*, **14**, R778-786.

Dong, K.C. and Berger, J.M. (2007) Structural basis for gate-DNA recognition and bending by type IIA topoisomerases. *Nature*, **450**, 1201-1205.

Drake, F.H., Hofmann, G.A., Bartus, H.F., Mattern, M.R., Crooke, S.T. and Mirabelli, C.K. (1989) Biochemical and pharmacological properties of p170 and p180 forms of topoisomerase II. *Biochemistry*, **28**, 8154-8160.

Duursma, A. and Agami, R. (2005) p53-Dependent regulation of Cdc6 protein stability controls cellular proliferation. *Mol Cell Biol*, **25**, 6937-6947.

Errington, F., Willmore, E., Leontiou, C., Tilby, M.J. and Austin, C.A. (2004) Differences in the longevity of topo IIalpha and topo IIbeta drug-stabilized cleavable complexes and the relationship to drug sensitivity. *Cancer Chemother Pharmacol*, **53**, 155-162.

Evidente, A., Kireev, A.S., Jenkins, A.R., Romero, A.E., Steelant, W.F., Van Slambrouck, S. and Kornienko, A. (2009) Biological evaluation of structurally diverse amaryllidaceae alkaloids and their synthetic derivatives: discovery of novel leads for anticancer drug design. *Planta Med*, **75**, 501-507.

Fehr, M., Pahlke, G., Fritz, J., Christensen, M.O., Boege, F., Altemoller, M., Podlech, J. and Marko, D. (2008) Alternariol acts as a topoisomerase poison, preferentially affecting the IIalpha isoform. *Mol Nutr Food Res*.

Felix, C.A. (2001) Leukemias related to treatment with DNA topoisomerase II inhibitors. *Med Pediatr Oncol*, **36**, 525-535.

Felix, C.A., Kolaris, C.P. and Osheroff, N. (2006) Topoisomerase II and the etiology of chromosomal translocations. *DNA Repair (Amst)*, **5**, 1093-1108.

Forterre, P. and Gadelle, D. (2009) Phylogenomics of DNA topoisomerases: their origin and putative roles in the emergence of modern organisms. *Nucleic Acids Res*, **37**, 679-692.

Fortune, J.M. and Osheroff, N. (1998) Merbarone inhibits the catalytic activity of human topoisomerase IIalpha by blocking DNA cleavage. *J Biol Chem*, **273**, 17643-17650.

Fortune, J.M. and Osheroff, N. (2000) Topoisomerase II as a target for anticancer drugs: when enzymes stop being nice. *Prog Nucleic Acid Res Mol Biol*, **64**, 221-253.

Frankenberg-Schwager, M., Becker, M., Garg, I., Pralle, E., Wolf, H. and Frankenberg, D. (2008) The role of nonhomologous DNA end joining, conservative homologous

recombination, and single-strand annealing in the cell cycle-dependent repair of DNA double-strand breaks induced by H(2)O(2) in mammalian cells. *Radiat Res*, **170**, 784-793.

Froelich-Ammon, S.J. and Osheroff, N. (1995) Topoisomerase poisons: harnessing the dark side of enzyme mechanism. *J Biol Chem*, **270**, 21429-21432.

Gao, H., Huang, K.C., Yamasaki, E.F., Chan, K.K., Chohan, L. and Snapka, R.M. (1999) XK469, a selective topoisomerase IIbeta poison. *Proc Natl Acad Sci U S A*, **96**, 12168-12173.

Gao, H., Yamasaki, E.F., Chan, K.K., Shen, L.L. and Snapka, R.M. (2003) DNA sequence specificity for topoisomerase II poisoning by the quinoxaline anticancer drugs XK469 and CQS. *Mol Pharmacol*, **63**, 1382-1388.

Gartenberg, M.R. and Wang, J.C. (1992) Positive supercoiling of DNA greatly diminishes mRNA synthesis in yeast. *Proc Natl Acad Sci U S A*, **89**, 11461-11465.

Gatto, B. and Leo, E. (2003) Drugs acting on the beta isoform of human topoisomerase II (p180). *Curr Med Chem Anticancer Agents*, **3**, 173-185.

Gellert, M. (1981) DNA topoisomerases. *Annu Rev Biochem*, **50**, 879-910.

Goto, T. and Wang, J.C. (1984) Yeast DNA topoisomerase II is encoded by a single-copy, essential gene. *Cell*, **36**, 1073-1080.

Graham, F.L., Smiley, J., Russell, W.C. and Nairn, R. (1977) Characteristics of a human cell line transformed by DNA from human adenovirus type 5. *J Gen Virol*, **36**, 59-74.

Gruber, B.M., Anuszewska, E.L., Bubko, I., Gozdzik, A., Fokt, I. and Priebe, W. (2007) Effect of structural modification at the 4, 3', and 2' positions of doxorubicin on topoisomerase II poisoning, apoptosis, and cytotoxicity in human melanoma cells. *Arch Immunol Ther Exp (Warsz)*, **55**, 193-198.

Grue, P., Grasser, A., Sehested, M., Jensen, P.B., Uhse, A., Straub, T., Ness, W. and Boege, F. (1998) Essential mitotic functions of DNA topoisomerase IIalpha are not adopted by topoisomerase IIbeta in human H69 cells. *J Biol Chem*, **273**, 33660-33666.

Hall, J.R., Kow, E., Nevis, K.R., Lu, C.K., Luce, K.S., Zhong, Q. and Cook, J.G. (2007) Cdc6 stability is regulated by the Huwe1 ubiquitin ligase after DNA damage. *Mol Biol Cell*, **18**, 3340-3350.

Hanahan, D. (1983) Studies on transformation of Escherichia coli with plasmids. *J Mol Biol*, **166**, 557-580.

Hande, K.R. (1998) Etoposide: four decades of development of a topoisomerase II inhibitor. *Eur J Cancer*, **34**, 1514-1521.

Hannan, K.M., Hannan, R.D. and Rothblum, L.I. (1998) Transcription by RNA polymerase I. *Front Biosci*, **3**, d376-398.

Hasan, S.K., Mays, A.N., Ottone, T., Ledda, A., La Nasa, G., Cattaneo, C., Borlenghi, E., Melillo, L., Montefusco, E., Cervera, J., Stephen, C., Satchi, G., Lennard, A., Libura, M., Byl, J.A., Osheroff, N., Amadori, S., Felix, C.A., Voso, M.T., Sperr, W.R., Esteve, J., Sanz, M.A., Grimwade, D. and Lo-Coco, F. (2008) Molecular analysis of t(15;17) genomic breakpoints in secondary acute promyelocytic leukemia arising after treatment of multiple sclerosis. *Blood*, **112**, 3383-3390.

Heck, M.M., Hittelman, W.N. and Earnshaw, W.C. (1988) Differential expression of DNA topoisomerases I and II during the eukaryotic cell cycle. *Proc Natl Acad Sci U S A*, **85**, 1086-1090.

Hellmann, K. (1998) Overview and historical development of dexrazoxane. *Semin Oncol*, **25**, 48-54.

Hertog, M.G., Hollman, P.C., Katan, M.B. and Kromhout, D. (1993) Intake of potentially anticarcinogenic flavonoids and their determinants in adults in The Netherlands. *Nutr Cancer*, **20**, 21-29.

Holm, C., Goto, T., Wang, J.C. and Botstein, D. (1985) DNA topoisomerase II is required at the time of mitosis in yeast. *Cell*, **41**, 553-563.

Huang, K.C., Gao, H., Yamasaki, E.F., Grabowski, D.R., Liu, S., Shen, L.L., Chan, K.K., Ganapathi, R. and Snapka, R.M. (2001) Topoisomerase II poisoning by ICRF-193. *J Biol Chem*, **276**, 44488-44494.

Irons, R.D. (2000) Molecular models of benzene leukemogenesis. *J Toxicol Environ Health A*, **61**, 391-397.

Jenkins, J.R., Ayton, P., Jones, T., Davies, S.L., Simmons, D.L., Harris, A.L., Sheer, D. and Hickson, I.D. (1992) Isolation of cDNA clones encoding the beta isozyme of human DNA topoisomerase II and localisation of the gene to chromosome 3p24. *Nucleic Acids Res*, **20**, 5587-5592.

Jensen, L.H., Nitiss, K.C., Rose, A., Dong, J., Zhou, J., Hu, T., Osheroff, N., Jensen, P.B., Sehested, M. and Nitiss, J.L. (2000) A novel mechanism of cell killing by anti-topoisomerase II bisdioxopiperazines. *J Biol Chem*, **275**, 2137-2146.

Jiang, W., Wells, N.J. and Hunter, T. (1999) Multistep regulation of DNA replication by Cdk phosphorylation of HsCdc6. *Proc Natl Acad Sci U S A*, **96**, 6193-6198.

Ju, B.G., Lunyak, V.V., Perissi, V., Garcia-Bassets, I., Rose, D.W., Glass, C.K. and Rosenfeld, M.G. (2006) A topoisomerase IIbeta-mediated dsDNA break required for regulated transcription. *Science*, **312**, 1798-1802.

Ju, B.G. and Rosenfeld, M.G. (2006) A breaking strategy for topoisomerase IIbeta/PARP-1-dependent regulated transcription. *Cell Cycle*, **5**, 2557-2560.

Kandaswami, C., Lee, L.T., Lee, P.P., Hwang, J.J., Ke, F.C., Huang, Y.T. and Lee, M.T. (2005) The antitumor activities of flavonoids. *In Vivo*, **19**, 895-909.

Kaufmann, S.H., Gore, S.D., Miller, C.B., Jones, R.J., Zwelling, L.A., Schneider, E., Burke, P.J. and Karp, J.E. (1998) Topoisomerase II and the response to antileukemic therapy. *Leuk Lymphoma*, **29**, 217-237.

Kern, M., Fridrich, D., Reichert, J., Skrbek, S., Nussher, A., Hofem, S., Vatter, S., Pahlke, G., Rufer, C. and Marko, D. (2007) Limited stability in cell culture medium and hydrogen peroxide formation affect the growth inhibitory properties of delphinidin and its degradation product gallic acid. *Mol Nutr Food Res*, **51**, 1163-1172.

Khan, Q.A., Kohlhagen, G., Marshall, R., Austin, C.A., Kalena, G.P., Kroth, H., Sayer, J.M., Jerina, D.M. and Pommier, Y. (2003) Position-specific trapping of topoisomerase II by benzo[a]pyrene diol epoxide adducts: implications for interactions with intercalating anticancer agents. *Proc Natl Acad Sci U S A*, **100**, 12498-12503.

Khopde, S., Roy, R. and Simmons, D.T. (2008) The binding of topoisomerase I to T antigen enhances the synthesis of RNA-DNA primers during simian virus 40 DNA replication. *Biochemistry*, **47**, 9653-9660.

Khopde, S. and Simmons, D.T. (2008) Simian virus 40 DNA replication is dependent on an interaction between topoisomerase I and the C-terminal end of T antigen. *J Virol*, **82**, 1136-1145.

Kim, J. and Kipreos, E.T. (2008) Control of the Cdc6 replication licensing factor in metazoa: the role of nuclear export and the CUL4 ubiquitin ligase. *Cell Cycle*, **7**, 146-150.

Kim, R.A. and Wang, J.C. (1989) Function of DNA topoisomerases as replication swivels in Saccharomyces cerevisiae. *J Mol Biol*, **208**, 257-267.

Kingma, P.S., Corbett, A.H., Burcham, P.C., Marnett, L.J. and Osheroff, N. (1995) Abasic sites stimulate double-stranded DNA cleavage mediated by topoisomerase II. DNA lesions as endogenous topoisomerase II poisons. *J Biol Chem*, **270**, 21441-21444.

Kingma, P.S. and Osheroff, N. (1997a) Apurinic sites are position-specific topoisomerase II poisons. *J Biol Chem*, **272**, 1148-1155.

Kingma, P.S. and Osheroff, N. (1997b) Spontaneous DNA damage stimulates topoisomerase II-mediated DNA cleavage. *J Biol Chem*, **272**, 7488-7493.

Kohn, K.W., Ewig, R.A.G., Erickson, L.C. and Zwelling, L.A. (1981) Measurement of strand breaks and cross-links by alkaline elution. In Friedberg, E.C. and Hanawalt, P.C. (eds.), *DNA Repair: A Labaratory Manual of Research Techniques*. Marcel Dekker, New York, pp. 379-401.

Komori, M., Kondo, T. and Tanaka, M. (2009) [Mitoxantrone for the treatment of patients with multiple sclerosis]. *Brain Nerve*, **61**, 575-580.

Kretzschmar, M., Meisterernst, M. and Roeder, R.G. (1993) Identification of human DNA topoisomerase I as a cofactor for activator-dependent transcription by RNA polymerase II. *Proc Natl Acad Sci U S A*, **90**, 11508-11512.

Kusumoto, H., Rodgers, Q.E., Boege, F., Raimondi, S.C. and Beck, W.T. (1996) Characterization of novel human leukemic cell lines selected for resistance to merbarone, a catalytic inhibitor of DNA topoisomerase II. *Cancer Res*, **56**, 2573-2583.

Lang, A.J., Mirski, S.E., Cummings, H.J., Yu, Q., Gerlach, J.H. and Cole, S.P. (1998) Structural organization of the human TOP2A and TOP2B genes. *Gene*, **221**, 255-266.

Larsen, A.K., Escargueil, A.E. and Skladanowski, A. (2003) Catalytic topoisomerase II inhibitors in cancer therapy. *Pharmacol Ther*, **99**, 167-181.

Lau, E., Zhu, C., Abraham, R.T. and Jiang, W. (2006) The functional role of Cdc6 in S-G2/M in mammalian cells. *EMBO Rep*, **7**, 425-430.

Lehman, I.R. (1974) DNA ligase: structure, mechanism, and function. *Science*, **186**, 790-797.

Leonhardt, H., Rahn, H.P., Weinzierl, P., Sporbert, A., Cremer, T., Zink, D. and Cardoso, M.C. (2000) Dynamics of DNA replication factories in living cells. *J Cell Biol*, **149**, 271-280.

Leppard, J.B. and Champoux, J.J. (2005) Human DNA topoisomerase I: relaxation, roles, and damage control. *Chromosoma*, **114**, 75-85.

Li, T.K. and Liu, L.F. (2001) Tumor cell death induced by topoisomerase-targeting drugs. *Annu Rev Pharmacol Toxicol*, **41**, 53-77.

Libura, J., Slater, D.J., Felix, C.A. and Richardson, C. (2005) Therapy-related acute myeloid leukemia-like MLL rearrangements are induced by etoposide in primary human CD34+ cells and remain stable after clonal expansion. *Blood*, **105**, 2124-2131.

Lindsey, R.H., Bender, R.P. and Osheroff, N. (2005a) Stimulation of topoisomerase II-mediated DNA cleavage by benzene metabolites. *Chem Biol Interact*, **153-154**, 197-205.

Lindsey, R.H., Jr., Bender, R.P. and Osheroff, N. (2005b) Effects of benzene metabolites on DNA cleavage mediated by human topoisomerase II alpha: 1,4-hydroquinone is a topoisomerase II poison. *Chem Res Toxicol*, **18**, 761-770.

Lindsley, J.E. and Wang, J.C. (1993) On the coupling between ATP usage and DNA transport by yeast DNA topoisomerase II. *J Biol Chem*, **268**, 8096-8104.

Linka, R.M., Porter, A.C., Volkov, A., Mielke, C., Boege, F. and Christensen, M.O. (2007) C-terminal regions of topoisomerase IIalpha and IIbeta determine isoform-specific functioning of the enzymes in vivo. *Nucleic Acids Res*, **35**, 3810-3822.

Liu, G.T., Qian, Y.Z., Zhang, P., Dong, W.H., Qi, Y.M. and Guo, H.T. (1992) Etiological role of Alternaria alternata in human esophageal cancer. *Chin Med J (Engl)*, **105**, 394-400.

Liu, L.F. (1989) DNA topoisomerase poisons as antitumor drugs. *Annu Rev Biochem*, **58**, 351-375.

Liu, L.F., Rowe, T.C., Yang, L., Tewey, K.M. and Chen, G.L. (1983) Cleavage of DNA by mammalian DNA topoisomerase II. *J Biol Chem*, **258**, 15365-15370.

Liu, L.F. and Wang, J.C. (1987) Supercoiling of the DNA template during transcription. *Proc Natl Acad Sci U S A*, **84**, 7024-7027.

Liu, Z., Deibler, R.W., Chan, H.S. and Zechiedrich, L. (2009) The why and how of DNA unlinking. *Nucleic Acids Res*, **37**, 661-671.

Lopez-Lazaro, M., Willmore, E. and Austin, C.A. (2007) Cells lacking DNA topoisomerase II beta are resistant to genistein. *J Nat Prod*, **70**, 763-767.

Lothstein, L., Israel, M. and Sweatman, T.W. (2001) Anthracycline drug targeting: cytoplasmic versus nuclear--a fork in the road. *Drug Resist Updat*, **4**, 169-177.

Lyu, Y.L., Kerrigan, J.E., Lin, C.P., Azarova, A.M., Tsai, Y.C., Ban, Y. and Liu, L.F. (2007) Topoisomerase IIbeta mediated DNA double-strand breaks: implications in doxorubicin cardiotoxicity and prevention by dexrazoxane. *Cancer Res*, **67**, 8839-8846.

Lyu, Y.L., Lin, C.P., Azarova, A.M., Cai, L., Wang, J.C. and Liu, L.F. (2006) Role of topoisomerase IIbeta in the expression of developmentally regulated genes. *Mol Cell Biol*, **26**, 7929-7941.

Lyu, Y.L. and Wang, J.C. (2003) Aberrant lamination in the cerebral cortex of mouse embryos lacking DNA topoisomerase IIbeta. *Proc Natl Acad Sci U S A*, **100**, 7123-7128.

Mailand, N. and Diffley, J.F. (2005) CDKs promote DNA replication origin licensing in human cells by protecting Cdc6 from APC/C-dependent proteolysis. *Cell*, **122**, 915-926.

Mao, Y., Mehl, I.R. and Muller, M.T. (2002) Subnuclear distribution of topoisomerase I is linked to ongoing transcription and p53 status. *Proc Natl Acad Sci U S A*, **99**, 1235-1240.

Markovits, J., Junqua, S., Goldwasser, F., Venuat, A.M., Luccioni, C., Beaumatin, J., Saucier, J.M., Bernheim, A. and Jacquemin-Sablon, A. (1995) Genistein resistance in human leukaemic CCRF-CEM cells: selection of a diploid cell line with reduced DNA topoisomerase II beta isoform. *Biochem Pharmacol*, **50**, 177-186.

Marsh, K.L., Willmore, E., Tinelli, S., Cornarotti, M., Meczes, E.L., Capranico, G., Fisher, L.M. and Austin, C.A. (1996) Amsacrine-promoted DNA cleavage site determinants for the two human DNA topoisomerase II isoforms alpha and beta. *Biochem Pharmacol*, **52**, 1675-1685.

Martinez, V., Mir, O., Domont, J., Bouscary, D. and Goldwasser, F. (2007) Mitoxantrone-related acute myeloblastic leukaemia in a patient with metastatic hormone-refractory prostate cancer. *Anticancer Drugs*, **18**, 233-235.

Masai, H., Sato, N., Takeda, T. and Arai, K. (1999) CDC7 kinase complex as a molecular switch for DNA replication. *Front Biosci*, **4**, D834-840.

McClendon, A.K., Gentry, A.C., Dickey, J.S., Brinch, M., Bendsen, S., Andersen, A.H. and Osheroff, N. (2008) Bimodal recognition of DNA geometry by human topoisomerase II alpha: preferential relaxation of positively supercoiled DNA requires elements in the C-terminal domain. *Biochemistry*, **47**, 13169-13178.

McClendon, A.K., Rodriguez, A.C. and Osheroff, N. (2005) Human topoisomerase IIalpha rapidly relaxes positively supercoiled DNA: implications for enzyme action ahead of replication forks. *J Biol Chem*, **280**, 39337-39345.

McPherson, J.P. and Goldenberg, G.J. (1998) Induction of apoptosis by deregulated expression of DNA topoisomerase IIα. *Cancer Res*, **58**, 4519-4524.

Meczes, E.L., Marsh, K.L., Fisher, L.M., Rogers, M.P. and Austin, C.A. (1997) Complementation of temperature-sensitive topoisomerase II mutations in Saccharomyces cerevisiae by a human TOP2 beta construct allows the study of topoisomerase II beta inhibitors in yeast. *Cancer Chemother Pharmacol*, **39**, 367-375.

Mendez, J. and Stillman, B. (2000) Chromatin association of human origin recognition complex, cdc6, and minichromosome maintenance proteins during the cell cycle: assembly of prereplication complexes in late mitosis. *Mol Cell Biol*, **20**, 8602-8612.

Merino, A., Madden, K.R., Lane, W.S., Champoux, J.J. and Reinberg, D. (1993) DNA topoisomerase I is involved in both repression and activation of transcription. *Nature*, **365**, 227-232.

Meyer, K.N., Kjeldsen, E., Straub, T., Knudsen, B.R., Hickson, I.D., Kikuchi, A., Kreipe, H. and Boege, F. (1997) Cell cycle-coupled relocation of types I and II topoisomerases and modulation of catalytic enzyme activities. *J Cell Biol*, **136**, 775-788.

Mielke, C., Christensen, M.O., Barthelmes, H.U. and Boege, F. (2004) Enhanced processing of UVA-irradiated DNA by human topoisomerase II in living cells. *J Biol Chem*, **279**, 20559-20562.

Mielke, C., Kalfalah, F.M., Christensen, M.O. and Boege, F. (2007) Rapid and prolonged stalling of human DNA topoisomerase I in UVA-irradiated genomic areas. *DNA Repair (Amst)*, **6**, 1757-1763.

Mielke, C., Tummler, M., Schubeler, D., von Hoegen, I. and Hauser, H. (2000) Stabilized, long-term expression of heterodimeric proteins from tricistronic mRNA. *Gene*, **254**, 1-8.

Misteli, T., Gunjan, A., Hock, R., Bustin, M. and Brown, D.T. (2000) Dynamic binding of histone H1 to chromatin in living cells. *Nature*, **408**, 877-881.

Mo, Y.Y., Wang, C. and Beck, W.T. (2000) A novel nuclear localization signal in human DNA topoisomerase I. *J Biol Chem*, **275**, 41107-41113.

Moldovan, G.L., Pfander, B. and Jentsch, S. (2007) PCNA, the maestro of the replication fork. *Cell*, **129**, 665-679.

Mondal, N. and Parvin, J.D. (2001) DNA topoisomerase IIalpha is required for RNA polymerase II transcription on chromatin templates. *Nature*, **413**, 435-438.

Muller, M.T., Pfund, W.P., Mehta, V.B. and Trask, D.K. (1985) Eukaryotic type I topoisomerase is enriched in the nucleolus and catalytically active on ribosomal DNA. *Embo J*, **4**, 1237-1243.

Nakanishi, M., Shimada, M. and Niida, H. (2006) Genetic instability in cancer cells by impaired cell cycle checkpoints. *Cancer Sci*, **97**, 984-989.

Nelson, E.M., Tewey, K.M. and Liu, L.F. (1984) Mechanism of antitumor drug action: poisoning of mammalian DNA topoisomerase II on DNA by 4'-(9-acridinylamino)-methanesulfon-m-anisidide. *Proc Natl Acad Sci U S A*, **81**, 1361-1365.

Neukam, K., Pastor, N. and Cortes, F. (2008) Tea flavanols inhibit cell growth and DNA topoisomerase II activity and induce endoreduplication in cultured Chinese hamster cells. *Mutat Res*, **654**, 8-12.

Niimi, A., Suka, N., Harata, M., Kikuchi, A. and Mizuno, S. (2001) Co-localization of chicken DNA topoisomerase IIalpha, but not beta, with sites of DNA replication and possible involvement of a C-terminal region of alpha through its binding to PCNA. *Chromosoma*, **110**, 102-114.

Nitiss, J.L. (1998) Investigating the biological functions of DNA topoisomerases in eukaryotic cells. *Biochim Biophys Acta*, **1400**, 63-81.

Nitiss, J.L. (2009a) DNA topoisomerase II and its growing repertoire of biological functions. *Nat Rev Cancer*, **9**, 327-337.

Nitiss, J.L. (2009b) Targeting DNA topoisomerase II in cancer chemotherapy. *Nat Rev Cancer*, **9**, 338-350.

Nitiss, J.L., Liu, Y.X., Harbury, P., Jannatipour, M., Wasserman, R. and Wang, J.C. (1992) Amsacrine and etoposide hypersensitivity of yeast cells overexpressing DNA topoisomerase II. *Cancer Res*, **52**, 4467-4472.

Oehlmann, M., Score, A.J. and Blow, J.J. (2004) The role of Cdc6 in ensuring complete genome licensing and S phase checkpoint activation. *J Cell Biol*, **165**, 181-190.

Okuno, Y., McNairn, A.J., den Elzen, N., Pines, J. and Gilbert, D.M. (2001) Stability, chromatin association and functional activity of mammalian pre-replication complex proteins during the cell cycle. *Embo J*, **20**, 4263-4277.

Osheroff, N. (1986) Eukaryotic topoisomerase II. Characterization of enzyme turnover. *J Biol Chem*, **261**, 9944-9950.

Osheroff, N. (1987) Role of the divalent cation in topoisomerase II mediated reactions. *Biochemistry*, **26**, 6402-6406.

Padget, K., Carr, R., Pearson, A.D., Tilby, M.J. and Austin, C.A. (2000) Camptothecin-stabilised topoisomerase I-DNA complexes in leukaemia cells visualised and quantified in situ by the TARDIS assay (trapped in agarose DNA immunostaining). *Biochem Pharmacol*, **59**, 629-638.

Petersen, B.O., Lukas, J., Sorensen, C.S., Bartek, J. and Helin, K. (1999) Phosphorylation of mammalian CDC6 by cyclin A/CDK2 regulates its subcellular localization. *Embo J*, **18**, 396-410.

Petersen, B.O., Wagener, C., Marinoni, F., Kramer, E.R., Melixetian, M., Lazzerini Denchi, E., Gieffers, C., Matteucci, C., Peters, J.M. and Helin, K. (2000) Cell cycle- and cell growth-regulated proteolysis of mammalian CDC6 is dependent on APC-CDH1. *Genes Dev*, **14**, 2330-2343.

Petrov, P., Drake, F.H., Loranger, A., Huang, W. and Hancock, R. (1993) Localization of DNA topoisomerase II in Chinese hamster fibroblasts by confocal and electron microscopy. *Exp Cell Res*, **204**, 73-81.

Phair, R.D. and Misteli, T. (2000) High mobility of proteins in the mammalian cell nucleus. *Nature*, **404**, 604-609.

Pitot, H.C. (1986) The molecular determinants of carcinogenesis. *Symp Fundam Cancer Res*, **39**, 187-196.

Pommier, Y. (2006) Topoisomerase I inhibitors: camptothecins and beyond. *Nat Rev Cancer*, **6**, 789-802.

Pommier, Y. (2009) DNA topoisomerase I inhibitors: chemistry, biology, and interfacial inhibition. *Chem Rev*, **109**, 2894-2902.

Pommier, Y., Pourquier, P., Fan, Y. and Strumberg, D. (1998) Mechanism of action of eukaryotic DNA topoisomerase I and drugs targeted to the enzyme. *Biochim Biophys Acta*, **1400**, 83-105.

Pommier, Y., Redon, C., Rao, V.A., Seiler, J.A., Sordet, O., Takemura, H., Antony, S., Meng, L., Liao, Z., Kohlhagen, G., Zhang, H. and Kohn, K.W. (2003) Repair of and checkpoint response to topoisomerase I-mediated DNA damage. *Mutat Res*, **532**, 173-203.

Pommier, Y., Zwelling, L.A., Mattern, M.R., Erickson, L.C., Kerrigan, D., Schwartz, R. and Kohn, K.W. (1983) Effects of dimethyl sulfoxide and thiourea upon intercalator-induced DNA single-strand breaks in mouse leukemia (L1210) cells. *Cancer Res*, **43**, 5718-5724.

Pourquier, P. and Pommier, Y. (2001) Topoisomerase I-mediated DNA damage. *Adv Cancer Res*, **80**, 189-216.

Povirk, L.F. (1996) DNA damage and mutagenesis by radiomimetic DNA-cleaving agents: bleomycin, neocarzinostatin and other enediynes. *Mutat Res*, **355**, 71-89.

Povirk, L.F. and Shuker, D.E. (1994) DNA damage and mutagenesis induced by nitrogen mustards. *Mutat Res*, **318**, 205-226.

Rampakakis, E. and Zannis-Hadjopoulos, M. (2009) Transient dsDNA breaks during pre-replication complex assembly. *Nucleic Acids Res.*

Rasheed, S., Nelson-Rees, W.A., Toth, E.M., Arnstein, P. and Gardner, M.B. (1974) Characterization of a newly derived human sarcoma cell line (HT-1080). *Cancer*, **33**, 1027-1033.

Rea, P.A. (2007) Plant ATP-binding cassette transporters. *Annu Rev Plant Biol*, **58**, 347-375.

Redinbo, M.R., Champoux, J.J. and Hol, W.G. (2000) Novel insights into catalytic mechanism from a crystal structure of human topoisomerase I in complex with DNA. *Biochemistry*, **39**, 6832-6840.

Roca, J., Ishida, R., Berger, J.M., Andoh, T. and Wang, J.C. (1994) Antitumor bisdioxopiperazines inhibit yeast DNA topoisomerase II by trapping the enzyme in the form of a closed protein clamp. *Proc Natl Acad Sci U S A*, **91**, 1781-1785.

Roca, J. and Wang, J.C. (1992) The capture of a DNA double helix by an ATP-dependent protein clamp: a key step in DNA transport by type II DNA topoisomerases. *Cell*, **71**, 833-840.

Ross, J.A. (2000) Dietary flavonoids and the MLL gene: A pathway to infant leukemia? *Proc Natl Acad Sci U S A*, **97**, 4411-4413.

Ross, J.A. and Kasum, C.M. (2002) Dietary flavonoids: bioavailability, metabolic effects, and safety. *Annu Rev Nutr*, **22**, 19-34.

Ross, J.A., Potter, J.D. and Robison, L.L. (1994) Infant leukemia, topoisomerase II inhibitors, and the MLL gene. *J Natl Cancer Inst*, **86**, 1678-1680.

Ross, W., Rowe, T., Glisson, B., Yalowich, J. and Liu, L. (1984) Role of topoisomerase II in mediating epipodophyllotoxin-induced DNA cleavage. *Cancer Res*, **44**, 5857-5860.

Ross, W.E., Glaubiger, D. and Kohn, K.W. (1979) Qualitative and quantitative aspects of intercalator-induced DNA strand breaks. *Biochim Biophys Acta*, **562**, 41-50.

Ross, W.E., Glaubiger, D.L. and Kohn, K.W. (1978) Protein-associated DNA breaks in cells treated with adriamycin or ellipticine. *Biochim Biophys Acta*, **519**, 23-30.

Rowley, J.D. (1998) The critical role of chromosome translocations in human leukemias. *Annu Rev Genet*, **32**, 495-519.

Saha, P., Chen, J., Thome, K.C., Lawlis, S.J., Hou, Z.H., Hendricks, M., Parvin, J.D. and Dutta, A. (1998) Human CDC6/Cdc18 associates with Orc1 and cyclin-cdk and is selectively eliminated from the nucleus at the onset of S phase. *Mol Cell Biol*, **18**, 2758-2767.

Sander, M., Hsieh, T., Udvardy, A. and Schedl, P. (1987) Sequence dependence of Drosophila topoisomerase II in plasmid relaxation and DNA binding. *J Mol Biol*, **194**, 219-229.

Scalbert, A. and Williamson, G. (2000) Dietary intake and bioavailability of polyphenols. *J Nutr*, **130**, 2073S-2085S.

Schilsky, R.L. (1996) Methotrexate: An Effective Agent for Treating Cancer and Building Careers. The Polyglutamate Era. *Oncologist*, **1**, 244-247.

Schmiedeberg, L., Weisshart, K., Diekmann, S., Meyer Zu Hoerste, G. and Hemmerich, P. (2004) High- and low-mobility populations of HP1 in heterochromatin of mammalian cells. *Mol Biol Cell*, **15**, 2819-2833.

Schoeffler, A.J. and Berger, J.M. (2008) DNA topoisomerases: harnessing and constraining energy to govern chromosome topology. *Q Rev Biophys*, **41**, 41-101.

Schvartzman, J.B. and Stasiak, A. (2004) A topological view of the replicon. *EMBO Rep*, **5**, 256-261.

Shaiu, W.L. and Hsieh, T.S. (1998) Targeting to transcriptionally active loci by the hydrophilic N-terminal domain of Drosophila DNA topoisomerase I. *Mol Cell Biol*, **18**, 4358-4367.

Shen, Y., Shen, H.M., Shi, C.Y. and Ong, C.N. (1996) Benzene metabolites enhance reactive oxygen species generation in HL60 human leukemia cells. *Hum Exp Toxicol*, **15**, 422-427.

Shenkenberg, T.D. and Von Hoff, D.D. (1986) Mitoxantrone: a new anticancer drug with significant clinical activity. *Ann Intern Med*, **105**, 67-81.

Sherratt, D.J., Soballe, B., Barre, F.X., Filipe, S., Lau, I., Massey, T. and Yates, J. (2004) Recombination and chromosome segregation. *Philos Trans R Soc Lond B Biol Sci*, **359**, 61-69.

Shiozaki, K. and Yanagida, M. (1992) Functional dissection of the phosphorylated termini of fission yeast DNA topoisomerase II. *J Cell Biol*, **119**, 1023-1036.

Shykind, B.M., Kim, J., Stewart, L., Champoux, J.J. and Sharp, P.A. (1997) Topoisomerase I enhances TFIID-TFIIA complex assembly during activation of transcription. *Genes Dev*, **11**, 397-407.

Siddiqui, I.A., Adhami, V.M., Saleem, M. and Mukhtar, H. (2006) Beneficial effects of tea and its polyphenols against prostate cancer. *Mol Nutr Food Res*, **50**, 130-143.

Sirikantaramas, S., Yamazaki, M. and Saito, K. (2009) A survival strategy: The coevolution of the camptothecin biosynthetic pathway and self-resistance mechanism. *Phytochemistry*.

Snapka, R.M., Gao, H., Grabowski, D.R., Brill, D., Chan, K.K., Li, L., Li, G.C. and Ganapathi, R. (2001) Cytotoxic mechanism of XK469: resistance of topoisomerase IIbeta knockout cells and inhibition of topoisomerase I. *Biochem Biophys Res Commun*, **280**, 1155-1160.

Sng, J.H., Heaton, V.J., Bell, M., Maini, P., Austin, C.A. and Fisher, L.M. (1999) Molecular cloning and characterization of the human topoisomerase IIalpha and IIbeta genes: evidence for isoform evolution through gene duplication. *Biochim Biophys Acta*, **1444**, 395-406.

Sordet, O., Khan, Q.A. and Pommier, Y. (2004) Apoptotic topoisomerase I-DNA complexes induced by oxygen radicals and mitochondrial dysfunction. *Cell Cycle*, **3**, 1095-1097.

Spector, L.G., Xie, Y., Robison, L.L., Heerema, N.A., Hilden, J.M., Lange, B., Felix, C.A., Davies, S.M., Slavin, J., Potter, J.D., Blair, C.K., Reaman, G.H. and Ross, J.A. (2005) Maternal diet and infant leukemia: the DNA topoisomerase II inhibitor hypothesis: a report from the children's oncology group. *Cancer Epidemiol Biomarkers Prev*, **14**, 651-655.

Stewart, L., Ireton, G.C. and Champoux, J.J. (1997) Reconstitution of human topoisomerase I by fragment complementation. *J Mol Biol*, **269**, 355-372.

Stewart, L., Ireton, G.C. and Champoux, J.J. (1999) A functional linker in human topoisomerase I is required for maximum sensitivity to camptothecin in a DNA relaxation assay. *J Biol Chem*, **274**, 32950-32960.

Stewart, L., Redinbo, M.R., Qiu, X., Hol, W.G. and Champoux, J.J. (1998) A model for the mechanism of human topoisomerase I. *Science*, **279**, 1534-1541.

Sugimoto, K., Yamada, K., Egashira, M., Yazaki, Y., Hirai, H., Kikuchi, A. and Oshimi, K. (1998) Temporal and spatial distribution of DNA topoisomerase II alters during proliferation, differentiation, and apoptosis in HL-60 cells. *Blood*, **91**, 1407-1417.

Taylor, C.K., Levy, R.M., Elliott, J.C. and Burnett, B.P. (2009) The effect of genistein aglycone on cancer and cancer risk: a review of in vitro, preclinical, and clinical studies. *Nutr Rev*, **67**, 398-415.

Tewey, K.M., Chen, G.L., Nelson, E.M. and Liu, L.F. (1984a) Intercalative antitumor drugs interfere with the breakage-reunion reaction of mammalian DNA topoisomerase II. *J Biol Chem*, **259**, 9182-9187.

Tewey, K.M., Rowe, T.C., Yang, L., Halligan, B.D. and Liu, L.F. (1984b) Adriamycin-induced DNA damage mediated by mammalian DNA topoisomerase II. *Science*, **226**, 466-468.

Thrash, C., Bankier, A.T., Barrell, B.G. and Sternglanz, R. (1985) Cloning, characterization, and sequence of the yeast DNA topoisomerase I gene. *Proc Natl Acad Sci U S A*, **82**, 4374-4378.

Toyoda, E., Kagaya, S., Cowell, I.G., Kurosawa, A., Kamoshita, K., Nishikawa, K., Iiizumi, S., Koyama, H., Austin, C.A. and Adachi, N. (2008) NK314, a topoisomerase II inhibitor that specifically targets the alpha isoform. *J Biol Chem*.

Tsutsui, K., Tsutsui, K., Hosoya, O., Sano, K. and Tokunaga, A. (2001) Immunohistochemical analyses of DNA topoisomerase II isoforms in developing rat cerebellum. *J Comp Neurol*, **431**, 228-239.

Tuduri, S., Crabbe, L., Conti, C., Tourriere, H., Holtgreve-Grez, H., Jauch, A., Pantesco, V., De Vos, J., Thomas, A., Theillet, C., Pommier, Y., Tazi, J., Coquelle, A. and Pasero, P. (2009) Topoisomerase I suppresses genomic instability by preventing interference between replication and transcription. *Nat Cell Biol*.

Turley, H., Comley, M., Houlbrook, S., Nozaki, N., Kikuchi, A., Hickson, I.D., Gatter, K. and Harris, A.L. (1997) The distribution and expression of the two isoforms of DNA topoisomerase II in normal and neoplastic human tissues. *Br. J. Cancer*, **75**, 1340-1346.

Wall, M.E. and Wani, M.C. (1995) Camptothecin and taxol: discovery to clinic--thirteenth Bruce F. Cain Memorial Award Lecture. *Cancer Res*, **55**, 753-760.

Wallace, L.A. (1989) Major sources of benzene exposure. *Environ Health Perspect*, **82**, 165-169.

Wang, H., Mao, Y., Chen, A.Y., Zhou, N., LaVoie, E.J. and Liu, L.F. (2001) Stimulation of topoisomerase II-mediated DNA damage via a mechanism involving protein thiolation. *Biochemistry*, **40**, 3316-3323.

Wang, J.C. (1969) Degree of superhelicity of covalently closed cyclic DNA's from Escherichia coli. *J Mol Biol*, **43**, 263-272.

Wang, J.C. (1971) Interaction between DNA and an Escherichia coli protein omega. *J Mol Biol*, **55**, 523-533.

Wang, J.C. (1991) DNA topoisomerases: why so many? *J Biol Chem*, **266**, 6659-6662.

Wang, J.C. (1996) DNA topoisomerases. *Annu Rev Biochem*, **65**, 635-692.

Wang, J.C. (2002) Cellular roles of DNA topoisomerases: a molecular perspective. *Nat Rev Mol Cell Biol*, **3**, 430-440.

Wang, J.C. (2009) A journey in the world of DNA rings and beyond. *Annu Rev Biochem*, **78**, 31-54.

Wang, J.C. and Davidson, N. (1968) Cyclization of phage DNAs. *Cold Spring Harb Symp Quant Biol*, **33**, 409-415.

Wang, L. and Eastmond, D.A. (2002) Catalytic inhibitors of topoisomerase II are DNA-damaging agents: induction of chromosomal damage by merbarone and ICRF-187. *Environ Mol Mutagen*, **39**, 348-356.

Wang, Y., Li, H., Tang, Q., Maul, G.G. and Yuan, Y. (2008) Kaposi's sarcoma-associated herpesvirus ori-Lyt-dependent DNA replication: involvement of host cellular factors. *J Virol*, **82**, 2867-2882.

Wasserman, R.A., Austin, C.A., Fisher, L.M. and Wang, J.C. (1993) Use of yeast in the study of anticancer drugs targeting DNA topoisomerases: expression of a functional recombinant human DNA topoisomerase II alpha in yeast. *Cancer Res*, **53**, 3591-3596.

Watson, J.D. and Crick, F.H. (1953a) Genetical implications of the structure of deoxyribonucleic acid. *Nature*, **171**, 964-967.

Watson, J.D. and Crick, F.H. (1953b) Molecular structure of nucleic acids; a structure for deoxyribose nucleic acid. *Nature*, **171**, 737-738.

Wei, H., Ruthenburg, A.J., Bechis, S.K. and Verdine, G.L. (2005) Nucleotide-dependent domain movement in the ATPase domain of a human type IIA DNA topoisomerase. *J Biol Chem*, **280**, 37041-37047.

Willmore, E., Frank, A.J., Padget, K., Tilby, M.J. and Austin, C.A. (1998) Etoposide targets topoisomerase IIalpha and IIbeta in leukemic cells: isoform-specific cleavable complexes visualized and quantified in situ by a novel immunofluorescence technique. *Mol Pharmacol*, **54**, 78-85.

Woessner, R.D., Mattern, M.R., Mirabelli, C.K., Johnson, R.K. and Drake, F.H. (1991) Proliferation- and cell cycle-dependent differences in expression of the 170 kilodalton and 180 kilodalton forms of topoisomerase II in NIH-3T3 cells. *Cell Growth Differ*, **2**, 209-214.

Xu, D.S., Kong, T.Q. and Ma, J.Q. (1996) The inhibitory effect of extracts from Fructus lycii and Rhizoma polygonati on in vitro DNA breakage by alternariol. *Biomed Environ Sci*, **9**, 67-70.

Yan, T., Deng, S., Metzger, A., Godtel-Armbrust, U., Porter, A.C. and Wojnowski, L. (2009) Topoisomerase II{alpha}-dependent and -independent apoptotic effects of dexrazoxane and doxorubicin. *Mol Cancer Ther*.

Yang, X., Li, W., Prescott, E.D., Burden, S.J. and Wang, J.C. (2000) DNA topoisomerase IIbeta and neural development. *Science*, **287**, 131-134.

Zechiedrich, E.L., Khodursky, A.B. and Cozzarelli, N.R. (1997) Topoisomerase IV, not gyrase, decatenates products of site-specific recombination in Escherichia coli. *Genes Dev*, **11**, 2580-2592.

Zechiedrich, E.L. and Osheroff, N. (1990) Eukaryotic topoisomerases recognize nucleic acid topology by preferentially interacting with DNA crossovers. *Embo J*, **9**, 4555-4562.

Zhang, H., Barcelo, J.M., Lee, B., Kohlhagen, G., Zimonjic, D.B., Popescu, N.C. and Pommier, Y. (2001) Human mitochondrial topoisomerase I. *Proc Natl Acad Sci U S A*, **98**, 10608-10613.

Zhou, N., Yan, Y., Li, W., Wang, Y., Zheng, L., Han, S., Yan, Y. and Li, Y. (2009) Genistein Inhibition of Topoisomerase IIalpha Expression Participated by Sp1 and Sp3 in HeLa Cell. *Int J Mol Sci*, **10**, 3255-3268.

Zini, N., Martelli, A.M., Sabatelli, P., Santi, S., Negri, C., Astaldi Ricotti, G.C. and Maraldi, N.M. (1992) The 180-kDa isoform of topoisomerase II is localized in the nucleolus and belongs to the structural elements of the nucleolar remnant. *Exp Cell Res*, **200**, 460-466.

Zini, N., Santi, S., Ognibene, A., Bavelloni, A., Neri, L.M., Valmori, A., Mariani, E., Negri, C., Astaldi-Ricotti, G.C. and Maraldi, N.M. (1994) Discrete localization of different DNA topoisomerases in HeLa and K562 cell nuclei and subnuclear fractions. *Exp Cell Res*, **210**, 336-348.

Zorbas, H. and Keppler, B.K. (2005) Cisplatin damage: are DNA repair proteins saviors or traitors to the cell? *Chembiochem*, **6**, 1157-1166.

Zwelling, L.A., Hinds, M., Chan, D., Mayes, J., Sie, K.L., Parker, E., Silberman, L., Radcliffe, A., Beran, M. and Blick, M. (1989) Characterization of an amsacrine-resistant line of human leukemia cells. Evidence for a drug-resistant form of topoisomerase II. *J Biol Chem*, **264**, 16411-16420.

7. List of abbreviations

AMLs	Amyloid leukemia
APC	Anaphase promoting complex
ATP	Adenosine triphosphate
Cdc6	Cell devision cycle 6
CFP	Cyan fluorescent protein
Cpt	Camptothecin
CTD	C-terminal domain
DMSO	Dimethylsulfoxide
Doxorubicin	DOX
DSB	DNA double strand break
EtBr	Ethidium bromide
FACS	Fluorescence activated cell sorting
FC	Fibrillar center
FCS	Foetal bovine serum
Fig.	Figure
FRAP	Fluorescence recovery after photobleaching
GFP	Green fluorescent protein
hr	Hour
i.e.	Id est
ICE	Isolating *in vivo* complexes of enzyme to DNA
ICRF-187	Dexrasoxane
IRES	Internal ribosome entry site
kDa	kilodaltons
kDNA	Catenated DNA
m-AMSA	amsacrine
Mcm	Mini chromosome maintenance complex
min	Minute
Mitoxantrone	MITOX
MLL	mixed lineage leukemia
Nocodazole	Methyl-(5-(2-thienylcarbnyl)-1H-benzimidazo-2-yl) carbamate
NTD	N-terminal domain

Orc	Origin recognition complex
Ori	Origin of replication
pac	Pyromycin-N-acetyltransferase
PBS	Phosphate buffer saline
PCNA	Proliferating cell nuclear antigen
PCR	Polymerase chain reaction
PP2A	Protein phosphatase 2A
preRCs	pre-replication complex
TOP	Topoisomerase gene
Topo	Topoisomerase
Topo I	Human nuclear topoissomerase I
Topo IIα	Human nuclear topoisomerase IIα
Topo IIβ	Human nuclear topoisomerase IIβ
Topos	DNA topoisomerases
VP16	Etoposide
X gal	5-Brom-4-chlor-3-indoxyl-β-D-galactopyranosid
YFP	Yellow fluorescent protein

8. Appendix

8.1 Plasmid maps

8.1.A pMC-2PS-delta HindIII-P

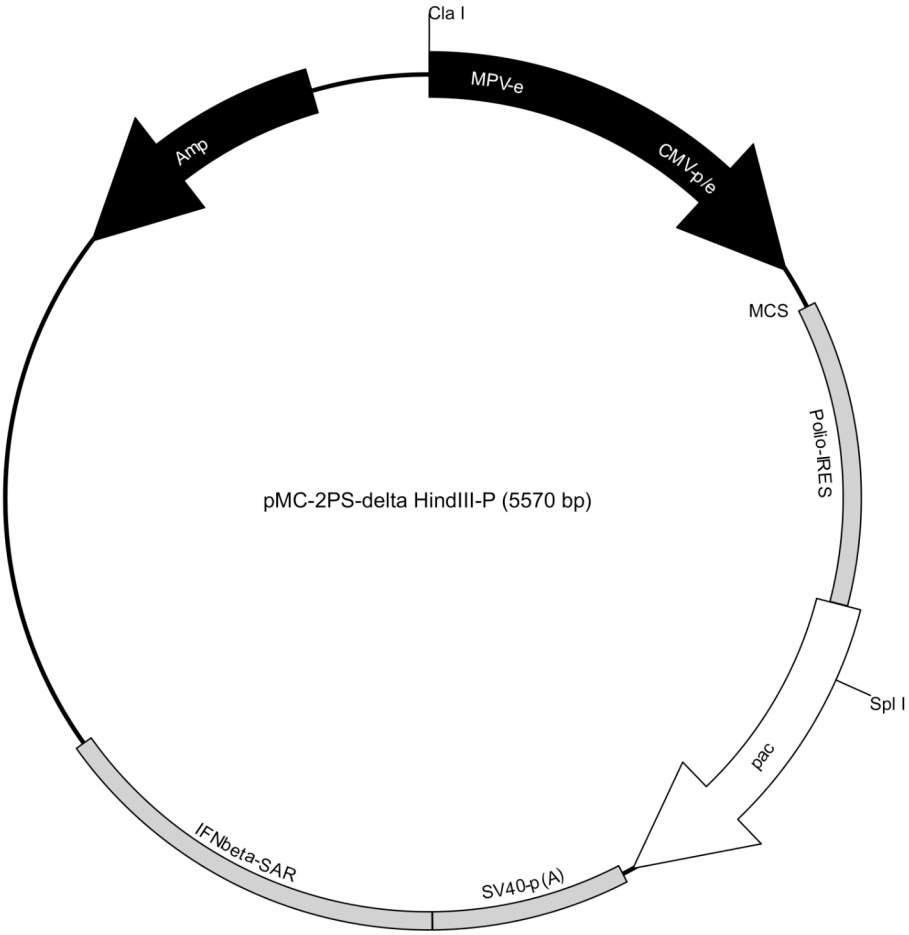

Fig. 8.1**: Basic bicistronic expression plasmid pMC-2PS-delta HindIII-P. (Mielke et al; 2000)**

8.1.B pMC-EYFP-P-N

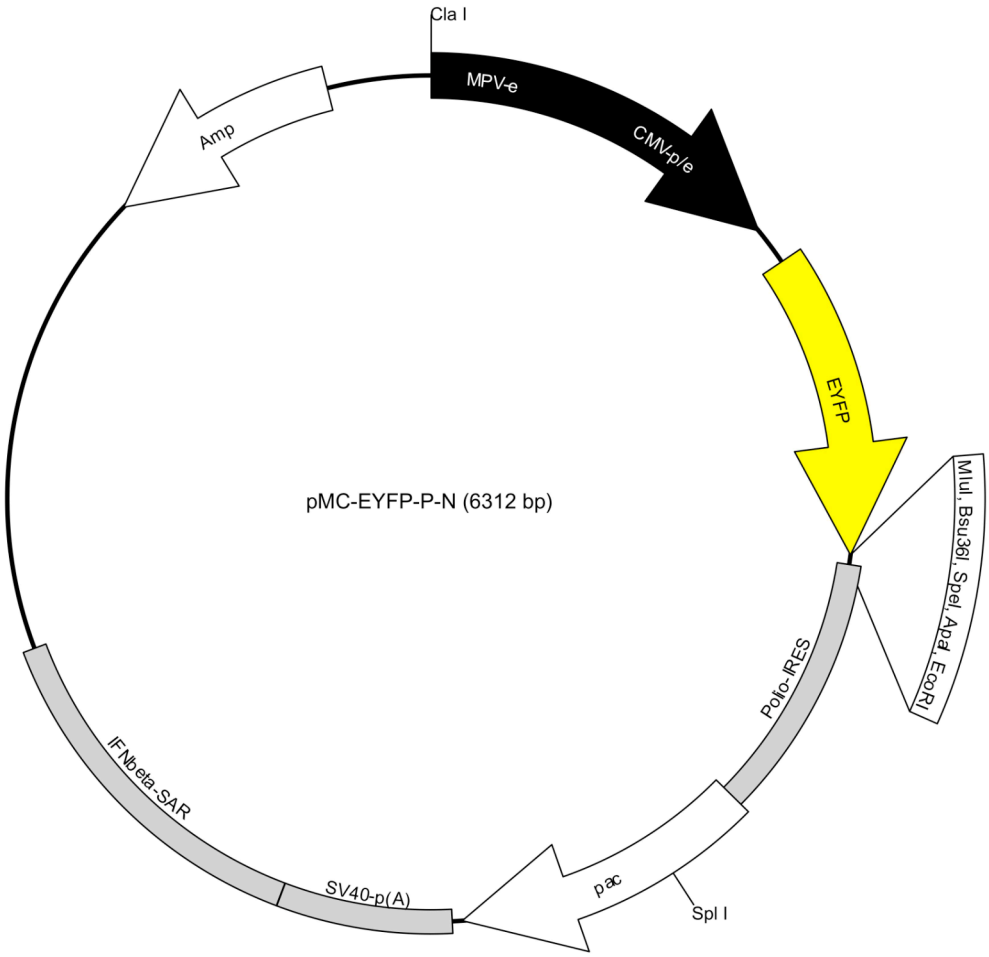

Fig. 8.2: Bicistronic expression plasmid pMC-EYFP-P-N.

8.1.C pMC- EYFP-P

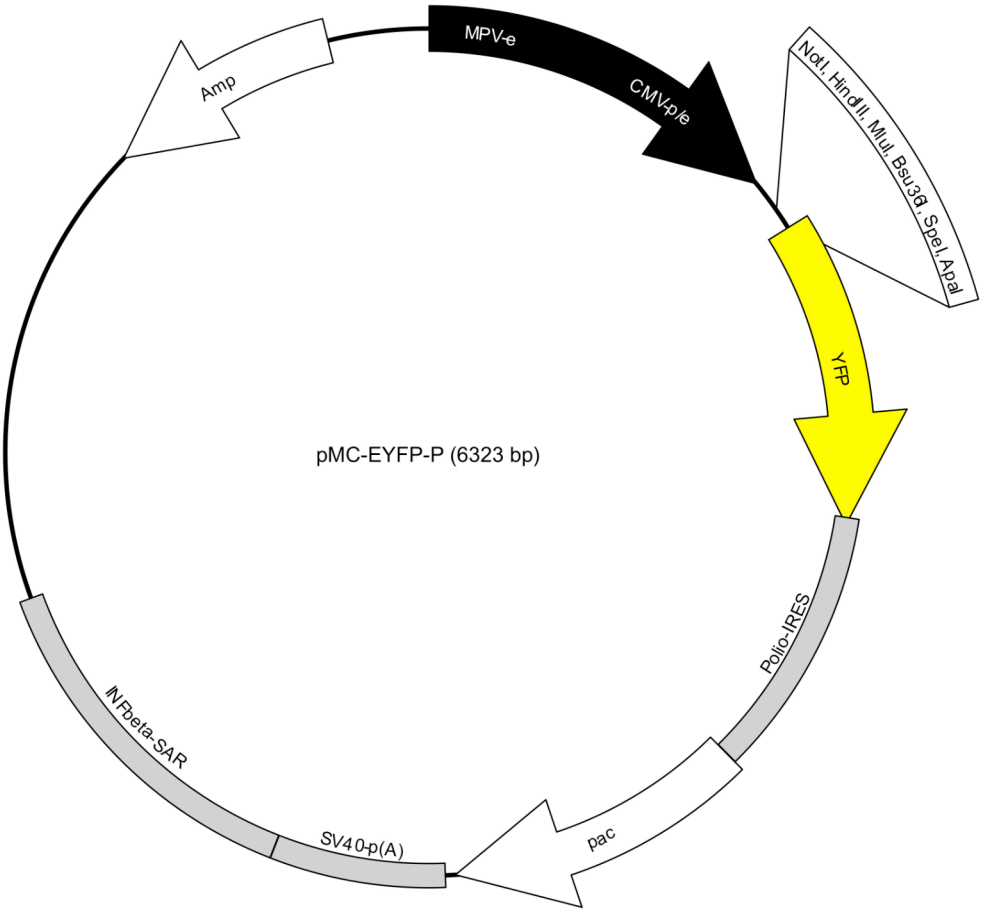

Fig. 8.3**: Bicistronic expression plasmid pMC-EYFP-P.**

9. Acknowledgments

First of all, I would like to express my gratitude to Prof. Fritz Boege for giving me the opportunity to work in his laboratory and for supervising my PhD project. A special thanks goes to Dr. Christian Mielke who was a great supervisor that provided me with independence. He gave me the time that I needed to do my experiments properly without looking over my shoulder all the time. He treated me like a colleague from the onset and I appreciate that. I also would like to thank Dr. Morten Christensen for listening and providing all helpful advice in work and by writing!

During my years working I have had the pleasure to work with several friendly and supportive people in the lab; Beatrice, Björn, Birgit, Christoph, Elke, Ellen, Ilaria, Rene, Said and Stefan (rigorously in alphabetical order). To Ellen you were my teacher and my friend when I first came into the lab - thanks a lot!. To Beatrice and Ilaria you are two of the kindest, most considerate people I have ever known. Stefan and Björn for the kind and entertaining atmosphere that you guys brought. To Birgit and Elke, thanks for your kind conversation and your help. I would also like to thank Steffi Schmittmeier for being my friend and for correction of my English.

I would like to thank Frank Essmann from the Institute of Molecular Medicine of the University of Düsseldorf who assisted me with the FACS analysis. I would like to thank Prof. Peter Proksch for being my co-referee. Many thanks to the Graduiertenkolleg 1033 “Molekulare Ziele von Alterungsprozessen und Ansatzpunkte der Alterungsprävention“

I would like to thank my friends Hind and Laila for sharing problems during our time here in Germany and I will never miss the time we spent together!

Without my family this accomplishment would have been extremely difficult if not impossible. To my parents, thank you for providing endless encouragement.

To Hazem, thank you so much for all of the love, laughs and understanding. Thank you for telling me over and over again that I could do this.

10. Erklärung

Hiermit erkläre ich, dass ich die vorliegende Dissertation eigenständig und ohne unerlaubte Hilfe angefertigt habe. Ich habe diese Dissertation in der vorgelegten oder in ähnlicher Form noch bei keiner anderen Institution eingereicht. Ich habe bisher keine erfolglosen Promotionsversuche unternommen.

Düsseldorf, den

Faiza Kalfalah